Modelling snow dynamics and groundwater-surface water interactions in mountainous, foothill and plain regions in North Saskatchewan River Basin, Canada

by

Majid Zaremehrjardy

A thesis submitted in partial fulfillment of the requirements for the degree of

Master of Science

Department of Earth and Atmospheric Sciences
University of Alberta

ABSTRACT

Snowmelt and groundwater-surface water (GW-SW) interactions are dominant controllers of hydrological cycles and water availability in northern latitudes that are characterized with 'cold region hydrology'. Snowmelt is the main source of groundwater recharge and surface runoff, as snow accumulation holds the largest share of water resources in cold regions. However, reliability of snow depth and snowmelt modelling and projections of GW-SW response to snow dynamics under climate change are subjected to debate. To fill this gap, this study has been undertaken with the main objectives of (1) revisiting and characterizing the performance and uncertainty of using two commonly-used approaches for snowmelt modelling, namely Energy-Balance Modules (EBMs) and Temperature-Index Modules (TIMs), as well as two common Snow Density formulations (SNDs) that map snow water equivalent (SWE) to snow depth; and (2) assessing the response of GW-SW interactions to snowmelt dynamics under future climate change scenarios. For snowmelt analysis, we coupled the Soil and Water Assessment Tool (SWAT) model with EBM and TIM modules along with two SND formulations, by modifying its source code, in order to examine model representation of snow depth simulation. The Analysis of Variance (ANOVA) was used to assess spatio-temporal variation of uncertainty by decomposition of the total projected snow depth uncertainty to its generating sources due to the use of EBM, TIM, five Global Climate Models (GCMs), two emission scenarios (RCP2.6 and RCP8.5), and two downscaling methods (DS1 and DS2). The analyses were implemented in mountainous, foothills and plains regions of the North Saskatchewan River Basin (NSRB) as a large, snow-dominated watershed with high variability of climate, vegetation, and topography. Results showed that regardless of snowmelt approaches, i.e., EBMs, TIMs, and SND selection, modelling performance in mountainous regions is poor

due to low quality of input climate data. However SND selection plays an important part in performance and uncertainty of snow depth in foothills and plains regions, where more accurate and high resolution climate data are available to setup the initial models. The uncertainty decomposition results showed that model parameter uncertainty, due to the use of EBM or TIM, dominantly controlled snow depth projections, particularly in mountainous and foothills regions. However, in plains regions, the uncertainty contribution of model parameters becomes less dominant and more variable in different months of the year, and the contribution of climate change models and scenarios becomes more important. After comparison of performance and uncertainties associated with different snowmelt modules, the most reliable module was chosen for calibrating the SWAT model. Thus, to answer the second main objective, we developed the surface water and groundwater modelling through SWAT-MODFLOW model in order to assess the inter-relation of regional snowmelt and GW-SW interactions and their changes under climate change. Results predicted that under future climate change, earlier snowmelt is expected in mountainous regions, which directly affects the GW-SW interactions mainly in mountainous and foothills catchments. On the other hand, correlation analysis of regional snowmelt and GW-SW interactions showed a higher correlation (R^2 =0.494) in mountainous regions, compared to very low correlation ($R^2 < 0.01$) in foothill and plain regions. In foothills and plains regions, higher levels of evapotranspiration (ET), and the dominant effect of rainfall on groundwater recharge and surface water availability, are introduced as possible effects of low correlations between snowmelt and GW-SW dynamics. It was also discussed that due to underground aquifer connectivity, the mountainous regions may receive less influence from any adjacent aquifers, while those in foothills and plains areas are cumulatively influenced by incoming groundwater flows from neighboring aquifers. However, this requires more research when better aquifer

boundaries are delineated and available for the modelling study. Overall, it is shown that the hydro-climate variability, topography and land-use in different regions play an important role in (1) the reliability and performance of snowmelt modules in reproducing snow depth and streamflow; (2) the cascade of uncertainty of snow depth projections; and (3) the inter-relation of snowmelt and GW-SW dynamics and governing processes that control GW-SW interactions.

PREFACE

This master's research is based on a hydrological model of North Saskatchewan River Basin (NSRB) created by Majid Zaremehrjardy. It is a paper-based master's thesis where Chapters 2 and 3 are manuscripts which are submitted (or will be submitted) to peer-reviewed journals. Majid Zaremehrjardy is the primary authors of the both manuscripts.

The first manuscript (Chapter 2) is under review by *Journal of Hydrology*. Co-authors are Dr. Monireh Faramarzi, an Assistant Professor in the Department of Earth and Atmospheric Sciences who led and supervised this study, and reviewed early and final drafts of the manuscript and Dr. Saman Razavi, an Associate Professor in the School of Environment and Sustainability of the University of Saskatchewan, who reviewed final draft of the manuscript. The second manuscript (Chapter 3) is under preparation for submission to a peer-reviewed journal in hydrology research. Co-authors are Justin Victor, Daniel Alessi, Brian Smerdon, Seonggyu Park and Monireh Faramarzi.

DEDICATION

I dedicate this thesis to my five-member family, and particularly my mother, without the support of whom it was impossible for me to continue my education abroad.

I also dedicate this work to Mohammad, Fateme, Amir B. and Amir H., who were always there to help me walk through the hardest times of my life.

ACKNOWLEDGEMENTS

I would like to express my sincere gratitude to my supervisor, Dr. Monireh Farmarzi, for offering the opportunity to start this program, which would have been impossible to succeed in without her excellent supervision and dedication to this project. She has been extremely helpful and encouraging throughout this program, resulting in novel ideas that led to interesting discussions and future insights into hydrology research. She also facilitated the connection of this research to various audiences in science and industry by supporting students and post-doctoral fellows into several meetings and conferences. I am also greatly appreciative of Dr. Daniel Alessi for providing very helpful feedbacks and suggestions, which was pivotal in preparation of this research. The invaluable feedbacks and contributions from Dr. Faramarzi and Dr. Alessi in supervisory committee meetings along with constant dedication to this project were essential to the success of this program. Moreover, I want to thank Dr. Brian Smerdon for his ongoing instructions and feedbacks on this project. In the end, I would like to acknowledge Dr. Duane Froese for agreeing to chair my master's thesis defense.

My sincere gratitude to my colleagues at the Watershed Science and Modelling Laboratory, especially Pouya Khalili, for their assistance in different stages of this research project.

Finally, I would like to thank my family and friends for their emotional and intellectual support, especially Mohammad, Fateme and Ryan for their companionship and favors, and Dr. Majid Iravani and Dr. Monireh Faramarzi for their moral and emotional support.

TABLE OF CONTENTS

LIST OF TABLES

LIST OF FIGURES

CHAPTER I – INTRODUCTION

1.1 Overview

Water is the essential and most important part of lives of every living creature. Despite the abundance of water in different forms throughout the world, the availability of freshwater to different geographical locations in different times is subject to many factors such as climate and topography, among other factors. Apart from natural factors that impact the uneven distribution of freshwater, the effect of human-induced factors such as economic expansion, population growth and industrial developments on water resources cannot be neglected (Faramarzi et al., 2017). In recent decades, the concern of negative impacts of climate change on water resources has been widely increased. It is generally agreed that increased greenhouse gas concentrations in the atmosphere, in combination with natural climate variability, are causing long-term changes in the pattern of hydrological processes such as runoff, groundwater recharge, snowmelt and evapotranspiration (Huntington and Niswonger, 2012; Intergovernamental Panel on Climate Change, 2013). These impacts are mostly due to the projected increase in global temperature and changes in precipitation patterns, which might ultimately lead to variations in the distribution of floods and droughts (Reshmidevi et al., 2018). The negative changes of water resources such as runoff decrease and increased evapotranspiration can also lead to changes in groundwater resources and their connectivity to surface water, altering groundwater recharge and water withdrawal from aquifers (Stoll et al., 2011). Such changes are, however, variable within different climate systems and geological formations throughout the world. In particular, the study of cold regions such as Canadian Prairies is of great interest in northern latitudes because of its singular properties in terms of land-cover, climate, topography and natural climate variability.

The hydrology of Canadian Prairies has been recognized as a semi-arid, cold region hydrology with different factors affecting runoff generation, water storage and the connectivity between ecosystem services (Dumanski, et al., 2015). The climate of this region has been widely variable, resulting in multiple extreme events (i.e., floods and droughts) to occur. The increase of extreme events affects the water availability and usage for different user sections such as industrial, agricultural, municipal, and environmental water users (Brimelow et al., 2014; Mahmood et al., 2017). Although snowmelt is the main contributor to both surface water flow and sub-surface flow in cold regions (Aygün et al., 2020), the changing patterns of hydrological processes in Canadian Prairies is subject to numerous factors, some of which are unique to cold regions. Apart from snowmelt, wetlands, seasonal freezing and thawing of top soils, and glaciers are among other factors that have turned Canadian Prairies hydrology into a complicated system, where identifying the sources and dynamics of related processes can be challenging (van der Kamp et al., 2003). Wetlands, which are dominant in the Prairies, significantly affect flood control, contaminant filtering and groundwater – surface water interactions (Shaw et al., 2012; Y. Liu et al., 2018). The seasonal freezing and thawing of top soils, which is a result of long-term winters, controls the water infiltration and groundwater recharge (Zhang et al., 2010) during and after melting season. The evolution and melt of mountain glaciers, which are controlled by in-situ hydro-climate processes, contribute to runoff generation in headwaters and water flow movement in downstream rivers, which are variable in time and space (Schaner et al., 2012). However as mentioned before, among all driving forces affecting Canadian Prairie hydrology, snowmelt is one of the most important hydrological processes in snow-dominated basins as it has a notable influence on total water availability in warm seasons. Although snowfall accounts for only one-third of total precipitation in Canadian Prairies, snowmelt contributes to more than 80%

of the streamflow in this area (Dumanski et al., 2015). Therefore, simulation of snowmelt is one of the key aspects of hydrological modelling, especially in order to catch the hydrological dynamics in large regions for decision making purposes.

In recent decades, hydrological models have been widely used as means to understand numerous hydrological processes and their inter-connections in large-scale (regional) studies. However, in snow-dominated areas such as Canadian Prairies, accurate simulation of snowmelt has been a major challenge in hydrological modelling. In general, two commonly-used methods of temperature index snowmelt modules (TIMs) and energy balance snowmelt modules (EBMs) are implemented in hydrological models to simulate the snowmelt processes (Debele et al., 2010). TIMs typically simulate snowmelt as a function of air temperature, snowpack surface temperature, and an empirical constant representing the rate of snowmelt. On the other hand, EBMs demonstrate the dependence of rate and quantity of snowmelt to heat and energy exchange between the snowpack, ground surface and atmosphere (Valeo and Ho, 2004). While EBMs take into account the physical aspects of snowmelt in a more accurate way, they are also data-demanding and require numerous input data for snowmelt simulation including snow surface albedo, cloud cover fraction, leaf area index, relative humidity, incoming longwave and shortwave solar radiation, dew point temperature, and other parameters and datasets (Qi et al., 2017). Acquiring a reliable set of such datasets in large regions is not feasible; therefore, some of them should be assigned to hydrological modelling as parameters, rather than input datasets. Adding numerous parameters to the hydrological models may increase the parameter uncertainty, which results in wider ranges of model responses when it comes to future projections and climate change impact assessments. Hence, it is important to quantify and assess the uncertainty

associated with TIMs and EBMs as two widely used approaches for snowmelt simulation and ultimately in water resources assessment and utilization in decision-making process.

On the other aspect of this research, the relations between snowmelt and groundwater-surface water interactions were argued in regional-scale studies, the scale of which is important for policy and planning. In general, the relation between surface water and groundwater is close and complex, which requires more assessment of both components in order to establish effective strategies for integrated water resources management (Intergovernamental Panel on Climate Change, 2013; Qi et al., 2019; Lewandowski et al., 2020). The interaction of groundwater and surface water (GW-SW) within a region governs the availability and dynamics of both groundwater and surface water (Allen et al., 2010). Also, it is argued that runoff generation is effectively controlled by hydrology connectivity of landscapes, hillslopes, or soil components (Brannen et al., 2015), and GW-SW interactions dominate the timing and magnitude of streamflow at the catchment scale (Jencso et al., 2009). The mechanisms that cause the changing patterns of GW-SW interactions under changing climate are poorly understood, particularly in mountainous regions (Huntington and Niswonger, 2012). Furthermore, the regional changes of GW-SW interactions and their potential reasons require more attention, especially when considering their spatio-temporal variability (Barthel and Banzhaf, 2016) and changes under climate change scenarios. It is argued that snowmelt and runoff are main drivers of GW-SW interactions (Scibek et al., 2007; Mantua et al., 2010; Maurer et al., 2010); however, additional explanation is needed to address how directly snowmelt and runoff impact GW-SW interactions, since the relation between surface water and groundwater is complex and other factors also play important roles in the formation of GW-SW (Huntington and Niswonger, 2012). Because the mechanisms related to the formation of snowmelt and runoff are different in various topography

and climate settings, it is necessary to incorporate factors such as climate, topography, and land cover, among other factors, in analyzing the significance of snowmelt runoff on GW-SW interactions. On the Canadian Prairies, where snowmelt is the main component of streamflow, a regional analysis of snowmelt and its relations with GW-SW interactions within mountainous, foothills and plains regions can give insights into the relation between these two factors in different spatial and temporal settings. This can be especially helpful in analyzing how other hydrological processes and climate factors might affect GW-SW interactions in current and future climate scenarios.

1.2 Research Objective

Given this context, the goal of this research was to elaborate on the performance and uncertainties associated with using widely-used snowmelt simulation approaches of TIM and EBM in regional hydrological modelling, followed by analysis of regional snowmelt and GW-SW interactions, and their control on each other's dynamics. This was done through simulating and projecting snowmelt and snow depth in regions with different climate and topography. After choosing the proper snowmelt module in hydrological modelling, the GW-SW interactions and their changes under future climate scenarios were analyzed, after which the effect of snowmelt on GW-SW interaction dynamics was assessed in mountainous, foothill and plain regions. The North Saskatchewan River Basin (NSRB) of central Alberta was chosen as the study area because of its hydrological and hydrogeological complexity, variety in climate, landscape, elevation and land-cover. In addition, the NSRB is one of the main providers of surface runoff to Saskatchewan River, and is the main source of drinking water to many areas in the region, including the city of Edmonton. Therefore, we evaluated TIM and EBM through implementing those modules in the SWAT model, followed by uncertainty analysis of snow depth projections.

After that, the best performing snowmelt module was chosen in the SWAT model, and the relations between snowmelt and GW-SW interactions were analyzed through an integrated GW-SW model developed using SWAT-MODFLOW. In summary, the following objectives were defined to attain the research goals of this study:

1. Analyzing the performance of EBM and TIMs, through examining spatio-temporal variability of snow depth and streamflow simulations in mountainous, foothill and plain areas;
2. Assessing the spatio-temporal changes in the cascade of uncertainty associated with snow depth projections using EBMs and TIMs as snowmelt modules under different climate change models, RCP scenarios, and downscaling methods;
3. Modelling the effect of snow density formulation on the simulations and its impact on the projected cascade of uncertainty of snow depth;
4. Regional assessment of impacts of climate change on seasonal and decadal changes of snowmelt and GW-SW interaction patterns;
5. Assessment of how spatio-temporal variation of groundwater-surface water is associated with snowmelt patterns;
6. Analyzing the interactions and correlations of snowmelt and GW-SW interactions in different hydroclimate regions such as mountainous, foothill and plain regions.

To achieve objective 1 to 3 of this research, we embedded TIM and EBM snowmelt approaches (namely SWAT-TIM and SWAT-EBM, respectively) as well as two snow density (SND) approaches in SWAT model. SWAT is a process-based, semi-distributed, eco-hydrological model which simulates various physical processes and their inter-connections on a daily basis. Such processes include snowmelt, soil moisture, surface runoff, evapotranspiration

and groundwater recharge, among others (Arnold et al. 1998, 2012). SWAT uses a simple TIM for snowmelt and snow depth simulations. Therefore, in this study SWAT-EBM and SND approaches were embedded into SWAT model by modifying its source code. At first, regional and sub-basin scale performance of different snowmelt approaches were evaluated and compared in terms of snow depth and streamflow simulations. After that, the Analysis of Variance (ANOVA) method was used for uncertainty decomposition of snow depth projections in mountainous, foothill and plain regions of the NSRB.

Based on the research related to objectives 1 to 3, the most reliable snowmelt module (in terms of simulation and uncertainties related to snow depth and streamflow) was chosen for evaluating the spatio-temporal changes in regional snowmelt (Objective 4) and for coupling to the MODFLOW groundwater model. Then, SWAT-MODFLOW model was created after calibrating SWAT and MODFLOW based on streamflow and observation well data, respectively. SWAT-MODFLOW was then used to extract the results of GW-SW interactions and their future changes under climate change models and greenhouse emission scenarios. Finally, the objectives 5 and 6 were achieved by comparison of dynamics of snowmelt and GW-SW interactions resulting from SWAT and SWAT-MODFLOW model, respectively.

1.3 Thesis Structure

Chapter 2 consist of objective 1-3 in the form of a manuscript, which is currently under review in *Journal of Hydrology*. It introduces current state of snowmelt simulations and compares the performance of TIMs and EBMs, along with two different snow density approaches, on simulation and uncertainty of snow depth and streamflow. Then, the uncertainty

associated with snow depth projections in regional hydrological modelling was evaluated and discussed in different regions of the NSRB.

Chapter 3 covers objective 4-6 in the form of a draft manuscript, which will be submitted for a journal publication. It describes the results of GW-SW interactions and their changes under future climate conditions. Also, the relations between regional snowmelt and GW-SW interactions and their possible governing factors are discussed for mountainous, foothill and plain regions of the NSRB.

Chapter 4 summarizes the findings of previous chapters and provides concluding remarks and take-home messages regarding the future of hydrological research on snowmelt and groundwater dynamics.

CHAPTER II – MANUSCRIPT 1

Uncertainty assessment of snow depth projections in watersheds of mountainous, foothills, and plain areas in northern latitudes

Majid Zaremehrjardy[1], Saman Razavi[2], Monireh Faramarzi[1,*]

[1] Watershed Science & Modelling Laboratory, Department of Earth and Atmospheric Sciences, University of Alberta, Edmonton, AB T6G 2R3, Canada.
[2] Global Institute for Water Security, School of Envionment and Sustainability, and Department of Civil, Geological, and Environmental Enigeering, University of Saskatchewan.
[*]Corresponding author: faramarz@ualberta.ca

Manuscript in review in the Journal of Hydrology

2.1 Abstract

Snowmelt is a major driver of the hydrological cycle in cold regions, as such, its accurate representation in hydrological models is key to both regional snow depth and streamflow prediction. The choice of a proper method for snowmelt representation is often improvised; however, a thorough characterization of uncertainty in such process representations, particularly in the context of climate change, has remained essential. To fill this gap, this study revisits and characterizes performance and uncertainty around the two general approaches to snowmelt representation, namely Energy-Balance Modules (EBMs) and Temperature-Index Modules (TIMs), and two common Snow Density formulations (SNDs) that map snow water equivalent (SWE) to snow depth. The major research questions we address are 'what are the dominant controls of uncertainty in snow depth and streamflow simulations across scales and in different climates', and 'how the cascade of uncertainty resulting from impact model parameters, greenhouse gases emission scenarios, climate models and their internal variability, and downscaling processes help understand effects of EBM, TIM, and snow density formulations in snow depth projections. We enable the Soil and Water Assessment Tool (SWAT) by coupling

EBM, TIM, and two SND modules for examination of different snowmelt representation methods and Analysis of Variance (ANOVA) for uncertainty decomposition and attribution. These analyses are implemented in mountainous, foothill, and plain regions in a large snow-dominated watershed in western Canada. Results show, rather counter-intuitively, that the choice of SND is a major control of uncertainty rather than the choice between TIMs and EBMs and of their uncertain parameters. The results further show that model parameter uncertainty dominantly controls uncertainty in future snow depth projections under climate change, particularly in mountainous regions. However, in plain regions, the uncertainty contribution of model parameter becomes more variable with time and less dominant compared with the other sources of uncertainty. Overall, it is shown that the hydro-climatic and topographic conditions of different regions have considerable effect on the share of different uncertainty sources when projecting regional snow depth.

Keywords: Regional hydrology, Uncertainty decomposition, Snowmelt projection, Energy Balance, Temperature Index, SWAT

2.2 Introduction

Snowmelt is one of the most important components of the hydrological cycle, as it controls the magnitude and dynamics of snow depth, streamflow, and flood frequency, especially in mountainous regions with high climate variability (Zeinivand and de Smedt, 2010; Abbas et al., 2019). The impact of climate change on snowmelt dynamics can be substantial, since snowmelt is dependent on temperature, precipitation, solar radiation and other factors whose statistical properties are expected to change in time and space under future climate conditions (Raleigh and Clark, 2014; Verdhen et al., 2014). Therefore, it is essential to understand the dynamical properties of the snow accumulation and snowmelt processes and how they might change over time under current and future conditions. An improved understanding can enable hydrologists and water managers to reduce uncertainty for future planning and management of water resources, and adaptation to climate change (Pradhanang et al., 2011).

Recently, advanced hydrological models have been used to simulate snow accumulation and snowmelt in different regions with various levels of areal extent and climate conditions (see e.g., Troin et al., 2016; Qi et al., 2017; Mas et al., 2018). Snowmelt simulation in these models, which governs snow depth dynamics as a key component of hydrological water balance, is carried out through two widely-used approaches, namely Temperature-Index Modules (TIMs) and Energy-Balance Modules (EBMs) (Debele et al., 2010). TIMs (also known as degree-day methods) are generally regarded as a simple and parsimonious approach for snowmelt estimation, as they are solely dependent on air temperature and snowpack (Hock, 2003; Debele et al., 2010). EBMs, however, are more complex and parameterized, as they try to comprehensively account for energy exchanges in air-and-snowpack and snowpack-and-soil interfaces (Dingman, 2015). While comparative assessments of TIMs and EBMs in snowmelt

simulation models have widely been studied across different regions, the choice of the best model for hydrologic modelling in particular at large scales remains a controversy (Zhang et al., 2008; Pradhanang et al., 2011).

EBMs are generally expected to outperform TIMs in simulating snowmelt dynamics, mainly because of their more realistic and physically-based nature (Todd Walter et al., 2005; Fuka et al., 2012; Qi et al., 2017; Massmann, 2019). Nevertheless, several studies have suggested that TIMs may perform equally well or even better than EBMs do in the representation of snowmelt and snow depth dynamics (see for example, Franz et al., 2008; Debele et al., 2010; Verdhen et al., 2014). In addition, a disadvantage of EBMs is that they are more data-intensive and demand numerous forcing inputs, many of which cannot be directly measured or quantified at scales larger than an instrumented site (Bavera et al., 2014; Raleigh et al., 2016; Mas et al., 2018). The issues around data demands are exacerbated in large regional studies with climate and land cover heterogeneity, especially in mountainous regions where regionalized data of energy-based variables such as snow albedo, snow surface temperature, emissivity and temperature lapse rate are difficult and costly to measure (Raleigh et al., 2016; Sun et al., 2019). Furthermore, the adequacy of any of TIMs and EBMs depends on the properties of driving climate forces in the region of interest. For instance, in maritime areas where rain-on-snow events occur more frequently, the snowmelt is dominated by turbulent heat fluxes and temperature gradients; therefore, the use of EBMs in such climates has proven more suitable (Debele et al., 2010; Qi et al., 2017). Conversely, TIMs can be considered a better option in regions where net solar radiation, which is a proxy for air temperature, is the dominant heat source (Debele et al., 2010). Consequently, the heterogeneity in climate, land cover, and topography across large river basins results in the dominancy of different snowmelt mechanisms

in different parts. Most of previous studies, however, have investigated and compared the adequacy of TIMs or EBMs in small-scale areas where extensive data is available (see for example, Franz et al., 2008; Tobin et al., 2013; Aggarwal et al., 2014; Fu et al., 2015); some other studies focused on larger but relatively homogeneous areas in terms of land cover, climate, and topography (for instance, Ficklin and Barnhart, 2014; Troin et al., 2015; Haghnegahdar et al., 2017). Hence, the performance of TIMs and EBMs in snowmelt simulation in large-scale regions with high topographic, climate, and land-use heterogeneity is yet to be properly understood.

The availability of extensive and reliable data is key to successful model parametrization and simulation of snowmelt and snow depth in regional hydrological models (Shrestha et al., 2012; Mas et al., 2018). At field scales where sufficient field data is available, high-fidelity snowmelt models can be developed (e.g., Pomeroy et al., 1998; Harder et al., 2018). At larger scales, however, where field data coverage is limited, some physical characteristics of the basin need to be represented in models by user-defined 'effective' parameters (Mas et al., 2018). Identifying such parameters that control the representation of physical processes in regional hydrological models is critical for short-term predictions and also projections of how the basin future might look like under climate change (Singh and Frevert, 2002). Parameter identification is a major area of research in the field of hydrology and beyond (Guillaume et al., 2019). It is well-known that the proper parameter values are typically *non-unique* in any given problem, a phenomenon that is commonly referred to as equifinality (Beven and Freer, 2001; Fu et al., 2015). Depending on how one wishes to address equifinality, there are two general approaches to parameter calibration to data, namely the optimization-based and uncertainty-based approaches (Razavi et al., 2010). The former attempts to identify the best set of parameter values according

to some goodness-of-fit criteria and use it for prediction and scenario runs, while the latter bases the analyses on several well-performing sets of parameter values in order to characterize prediction uncertainty arising from uncertainties in model structure, model input data, and parameters (Faramarzi et al., 2009, 2017). Many studies that projected snowmelt and/or streamflow under climate change scenarios followed the optimization-based approach (see for example, Franz et al., 2008; Zeinivand and de Smedt, 2010; Pradhanang et al., 2011; Qi et al., 2017; Liu et al., 2018). Other studies followed the uncertainty-based approach by suggesting optimal ranges for parameters to account for input data, model structure, and parameter uncertainty (Renard et al., 2010; Faramarzi et al., 2017; Wu et al., 2017).

Model parameter uncertainty is one of the many uncertainty sources in the 'cascade of uncertainty' for climate change impact assessment. Other sources include Global and Regional Climate Models (GCMs and RCMs), Representative Concentration Pathways (RCPs), and downscaling methods (Chen et al., 2011b; Bosshard et al., 2013). When dealing with the cascade of uncertainty in climate change impact assessments, it is important to decompose and apportion the uncertainty to the different uncertainty sources. The Analysis of Variance (ANOVA) has frequently been used for this purpose (see for example, Déqué et al., 2007; Yip et al., 2011; Bosshard et al., 2013), while global sensitivity analysis methods can also be used (Razavi and Gupta, 2019). The majority of studies for apportionment of uncertainty in future projections addressed only uncertainty from climate models, emission scenarios, and downscaling techniques (Kim et al., 2019). Only few studies quantified the uncertainty contribution from hydrological model parameters and input data to the uncertainty in projection of future streamflow (Wilby and Harris, 2006; Prudhomme and Davies, 2009; Poulin et al., 2011; Vetter et

al., 2017), green water and blue water flows (Ashraf Vaghefi et al., 2019), and Snow Water Equivalent (SWE) (Poulin et al., 2011).

In addition to parameter uncertainty, model structural uncertainty has remained poorly understood, particularly in cold regions hydrology where the snow processes are of significance. Only few studies have evaluated the structural uncertainty as a result of using multiple snowmelt modules on simulating streamflow and SWE (Seiller and Anctil, 2014; Troin et al., 2015). Notably, the uncertainty due to the choice of TIMs and EBMs along with their parameterizations and its impact on uncertainty in snowmelt and snow depth projections under a changing climate has not been quantified. Unlike TIMs, EBMs are more physically-based and therefore they demand more extensive spatio-temporal data to run. As such data may not be available at large scales, EBMs assign calibration parameters to unknown input variables. Therefore, it is essential to quantify the effects of TIMs (as simpler, less parametrized modules) and EBMs (as more complex, more parameterized modules) on snow depth projections under climate change scenarios in large watersheds with diverse hydrologic, climatic, and geospatial conditions.

Another major but often ignored research gap in hydrologic modelling of cold regions is the proper mapping of snow depth measurements and Snow Water Equivalent (SWE) at large scales. Snow depth measurements are the basis for the calibration and evaluation of snow modelling modules, while the representation of snow on the ground in those models is in the form of SWE (Avanzi et al., 2015). In other words, measurements of snow that are used for model evaluation are typically available as snow depths, not SWE (Sturm et al., 2010). Therefore, the accurate estimation of snow density (SND) that converts simulated SWE (i.e., in mm water) to snow depth (i.e., in mm snow depth) and vice versa becomes key to credible modelling of snow processes at large scales. An accurate estimation of SWE, SND, and the

conversion to snow depth is possible within field scales (Jost et al., 2007; Young et al., 2013; Li et al., 2017). However, field measurements in large regions are time-consuming, costly, and complicated because of heterogeneity in topography and natural conditions, and therefore, only a limited number of snow surveys can be available for a watershed (Bocchiola and Groppelli, 2010; Avanzi et al., 2015). As such, reliable estimation of SND in locations where it is not measured is essential. Notably, the variability of SND in both time and space is less than that of snow depth (Bocchiola and Groppelli, 2010) but it is still quite significant and controls snow depth simulations (Pomeroy et al., 1998; Bormann et al., 2013). The variability and distribution of SND has been widely studied using empirical relations, where the snow density is defined as a function of various variables such as air temperature, snow depth, wind speed, among other predictors (Avanzi et al., 2015). Application of empirical methods for predicting SND by using weather data also allows the hydrologists to predict the effect of climate change on SND and snow depth dynamics (Meloysund et al., 2007). Various equations, employing different types of predictors for SND estimation, have been proposed for different study areas (for example, see Avanzi et al., 2015). Because most of such equations are acquired based on a particular area of study, a careful choice of SND equation is necessary for a reliable simulation of snow depth in a new area of interest. For instance, an empirical equation developed for maritime regions might perform poorly in snow depth simulation in Canadian Prairies (Avanzi et al., 2015). Thus, it is essential to evaluate and compare the performance of various SND estimations to achieve a better understanding of the effect of density formulations on snow depth modelling and projections.

The overarching goal of this study is to provide an improved understanding of uncertainty associated with simulation and projection of snow depth and snowmelt dynamics in

regional hydrological modelling under current and future climate conditions. To this end, we enable Soil and Water Assessment Tool (SWAT) with both TIM and EBM snowmelt modules and two different SND parametrizations, by modifying its source code, to comprehensively assess the model structural and parametric uncertainty. We utilize ANOVA to apportion the total uncertainty in snow depth projections into uncertainty arising from not only model structure, parameters, and input data, but also the choice of climate models, greenhouse gas emission scenarios, and downscaling methods. The more specific objectives of this paper are threefold as it investigates: (1) the performance of EBM and TIMs, through examining spatio-temporal variability of snow depth and streamflow simulations in mountainous, foothill and plain areas by using a large snow-dominated watershed in Western Canada; (2) the spatio-temporal changes in cascade of uncertainty associated with snow depth projections using EBMs and TIMs as snowmelt modules in regional hydrological modelling under different climate change models, RCP scenarios, and downscaling methods; and (3) the effect of SND formulation on the simulations and projections of snow depth and its impact on the projected cascade of uncertainty.

2.3 Material and methods

2.3.1 Study Area

North Saskatchewan River Basin (NSRB) is a large watershed with considerable variability in climate, topography, and land cover, located in the central area of Alberta, western Canada. The area of NSRB is 59,128 km^2, forming approximately 9% of landmass in the province of Alberta (North Saskatchewan Watershed Alliance, 2005). The NSRB originates from Columbia Icefields and the foothill regions of Rocky Mountains in the west of Alberta (Figure 2.1a). The watershed is characterized by a diverse topography, with the elevation of NSRB ranging from 3478 MASL on the mountainous region down to less than 500 MASL on the plain

areas towards east of Alberta (Figure 2.1b). The land cover changes from high mountains and icefields (i.e., mountain glaciers) in the west, to evergreen forests in the foothills, and urban and agricultural areas as well as pastures are among other land cover classes in the majority of the plain region in the east of the watershed (Figure 2.1a). The historical climate data of NSRB for 1983-2007 shows a temperature range from less than -30 ℃ in winters up to +29 ℃ in summers for the watershed, and the average annual precipitation ranging from 760 mm $year^{-1}$ in mountainous areas to 400 mm $year^{-1}$ on the plains region. Snowfall and snow cover dominate the watershed for at least five months of the year (Government of Canada, 2019). This suggests a noticeable variance of climate, topography and land cover in time and space throughout the NSRB.

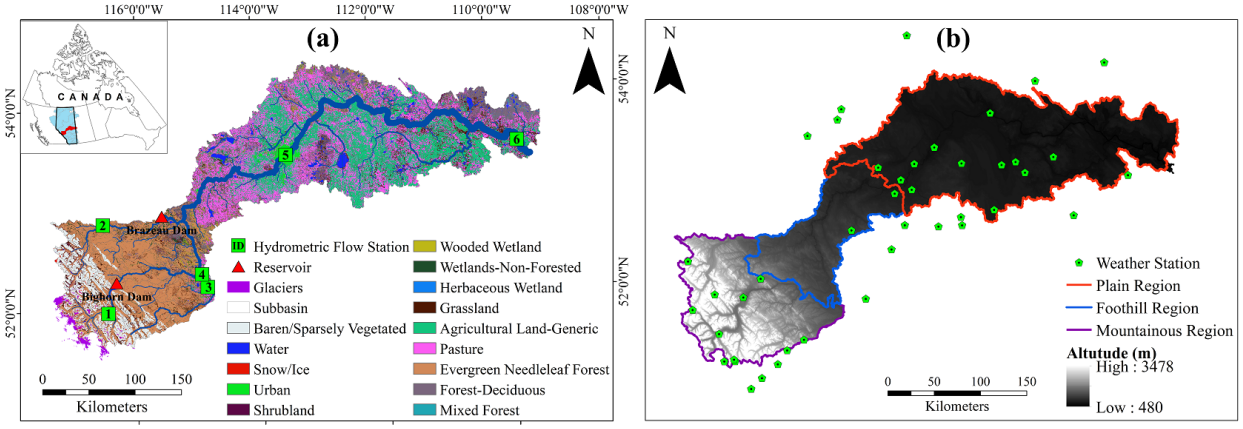

Figure 2.1. Map of NSRB representing geographic distribution of (a) the main river basin, two main dams, hydrometric stations and land use-land cover classes; and (b) topographic range, weather stations, and the three hydrologic regions used for assess.

The NSRB is a major basin draining to the Saskatchewan River in Canadian Prairies that drains into the Hudson Bay and to Atlantic Ocean. An average value of 7000 million cubic meters of water is annually discharged from North Saskatchewan River (NSR) to the Saskatchewan River at the Alberta-Saskatchewan border on the east side of NSRB (Alberta Environment and Parks, 2019). The NSR also provides the drinking water for the urban areas

within NSRB, including the city of Edmonton. Two hydro-electric dams named Bighorn and Brazeau Dams are located in the mountainous regions of NSRB, with an overall productivity of 800,000 MWh $year^{-1}$ (MacDonald et al., 2012). Moreover, numerous small and large glaciers located in the Rocky Mountains are important contributors to the streamflow in the upstream tributaries of this river (Figure 2.1a).

2.3.2 Hydrologic model setup and data

SWAT is a process-based, semi-distributed, eco-hydrological model which simulates various physical processes and their inter-connections on a daily basis (Arnold et al. 1998, 2012). Numerous hydrological variables are modelled in SWAT, including streamflow, snow accumulation, snowmelt, infiltration, evapotranspiration, vegetation growth and canopy development, groundwater recharge and base flow, among others (Neitsch et al., 2011). In SWAT, a basin is divided into several sub-basins, which are in turn subdivided into Hydrological Response Units (HRUs) as the smallest hydrological units and characterized based on soil, landuse-land cover, slope and other geospatial features. Hydrological processes are then calculated at HRU scale, and can be aggregated at sub-basin and basin levels. In this study, we delineated a total of 174 sub-basins using a 90m × 90m DEM and a pre-defined river network delineated previously based on a 10m × 10m DEM (Table A.1). Historical climate data including daily precipitation, temperature, solar radiation, humidity, and wind speed were used from Faramarzi et al. (2015), who used a suit of four climate time series from local meteorological, gridded produscts, and satellite data at a provincial coverage to reproduce historical streamflow records by implementing a calibrated SWAT hydrologic model. Other data including vegetation cover, soil characteristics, operation of dams, and glacial maps and their daily time series were obtained from Faramarzi et al. (2017). In order to examine the effects of

snowmelt simulation approaches (i.e., EBM and TIM) on streamflow dynamics in different regions of NSRB, six important hydrometric stations were considered for observing model performance and uncertainty analysis within different regions of this watershed. The locations and properties of these stations are shown in Figure 2.1 and the details are provided in Table A.2. Observed streamflow data for multiple hydrometric stations were collected from Environment Canada (Table A.1). Finally, in order to assess the performance of snow depth simulations using the two EBM and TIM approaches, the simulated depth data were compared with the monthly gridded snow depth data acquired from Canadian Meteorological Centre (CMC) Daily Snow Depth Analysis Data, Version 1 (Brown and B. Bransnett, 2010). The monthly CMC snow depth data were available from January 1999 at a spatial resolution of 24 km × 24 km, and they were used to validate SWAT-EBM and SWAT-TIM simulations for 1999-2007 period. The daily simulation of snowmelt and snow depth was performed for each sub-basin. However, for demonstration and comparison of the model performance in snow depth simulation in mountainous, foothill, and plain regions (Figure 2.1b), the monthly sub-basin data were calculated and aggregated using a weighted average of sub-basins' snow depth.

2.3.3 Snowmelt simulation approaches

We embeded two snowmelt simulation modules into SWAT2012 model by modifying its source code, thereby producing what we refer to as the SWAT-TIM and SWAT-EBM models. The SWAT-TIM model used in this study is the SWAT built-in snowmelt module, while the SWAT-EBM is based on the energy balance scheme developed by U.S. Army Corps of Engineers (USACE, 1998). This formulation was also embedded in the SWAT2009 by Qi et al., (2017) for simulation of snowmelt in a small catchement. For the purpose of this study, we used

a similar approach as Qi et al., (2017) and embedded the modified version of EBM in the SWAT2012 by modifying its source code.

In the SWAT model, regardless of the snowmelt module used, the snowfall is stored at the ground surface in the form of snow pack. The amount of the stored snow pack is reported as SWE. The mass balance for the snow pack for day t is simulated as follows (Neitsch et al., 2011):

$$SNO_t = SNO_{t-1} + SF_t - E_{sub} - SNO_{mlt} \quad (1)$$

where SNO_t is the water content of snow pack on the ground at the end of a given day (mm H_2O), SNO_{t-1} is the water content of snowpack on the ground at the end of the previous day (mm H_2O), SF_t is the total amount of snowfall within a given day (mm H_2O), E_{sub} is the amount of sublimation on a given day (mm H_2O), and SNO_{mlt} is the amount of snowmelt within a given day (mm H_2O). SWAT considers the whole precipitation for each day as snowfall if the air temperature is less than snowfall temperature (i.e., SFTMP, Table 2.1); otherwise, the whole precipitation is considered as rainfall. Also, the sublimation from the snow surface is calculated as a function of potential evapotranspiration of the given day. More information about the formulation of snowfall and snow sublimation can be found in Neitsch et al. (2011).

In the following, the formulations and corresponding parameters of SWAT-TIM and SWAT-EBM are discussed.

2.3.3.1 SWAT-TIM

In TIMs, temperature is the main driver of snowmelt. The snowmelt simulation in SWAT is based on snow cover, melt factor, and temperature variables:

$$SNO_{mlt} = b_{mlt} \cdot sno_{cov} \cdot [\frac{T_{snow} + T_{mx}}{2} - SMTMP] \quad (2)$$

where SNO_{mlt} is the amount of snowmelt on a given day (mm H_2O), b_{mlt} is the melt factor of the day (mm $H_2O \cdot day^{-1} \cdot ℃^{-1}$), sno_{cov} is the fraction of HRU area that is covered by snow, T_{snow} is the snowpack temperature on a given day (℃), T_{mx} is the maximum daily air temperature (℃), and $SMTMP$ is the threshold temperature at which the snowmelt will occurs (℃). The melt factor for snowmelt is a function of maximum and minimum melt factor of the year and the day of the year in order to account daily and seasonal variability of snowmelt:

$$b_{mlt} = \frac{SMFMX + SMFMN}{2} + \frac{SMFMX - SMFMN}{2} \cdot \sin\left(\frac{2\pi}{365} \cdot (d_n - 81)\right) \quad (3)$$

where $SMFMX$ is the maximum melt factor of the year (mm $H_2O \cdot day^{-1} \cdot ℃^{-1}$); $SMFMN$ is the minimum melt factor of the year (mm $H_2O \cdot day^{-1} \cdot ℃^{-1}$); and d_n is the day number of the year (Neitsch et al., 2011).

The temperature dynamics of snowpack is formulated as:

$$T_{snow,t} = T_{snow,t-1} \cdot (1 - TIMP) + T_a \cdot TIMP \quad (4)$$

where $T_{snow,t}$ is the snow pack temperature on a given day (℃), $T_{snow,t-1}$ is the snow pack temperature on the previous day (℃), T_a is the average air temperature in that given day (℃), and $TIMP$ is the temperature lag factor in SWAT model (Neitsch et al., 2011). It should be noted that Equations (1) and (4) are included in both SWAT-TIM and SWAT-EBM formulations.

In order to account for the spatial variability of snowmelt process within each sub-basin in our study, five elevation bands were applied to each sub-basin in SWAT model. The elevation

bands divide sub-basins into different zones based on the elevation, thereby allowing the model to discretize the hydrological processes based on sub-basins topography (Pradhanang et al., 2011). SWAT defines the temperature and precipitation of each band using the following equations:

$$P_B = P_{st} + (Z_B - Z_{st}) \times PLAPS \times 10^{-3} \quad (5)$$

$$T_B = T_{st} + (Z_B - Z_{st}) \times TLAPS \times 10^{-3} \quad (6)$$

where P_B is precipitation at elevation band (mm), P_{st} is station precipitation (mm), Z_B is midpoint elevation of band (m), Z_{st} is station elevation (m), T_B is temperature at elevation band ($°C$), T_{st} is station temperature ($°C$), $PLAPS$ is precipitation lapse rate (mm/km) and $TLAPS$ is temperature lapse rate ($°C$/km) (Rahman et al., 2013). In this study, TLAPS values for each sub-basin were assumed to be between -10 to 0 $°C$/km, and PLAPS values were defined to vary in the range 0-250 mm/km (Zhang et al., 2008; Anand et al., 2018).

In order to compute SNO_t using Equations (1) through (6), the five input parameters SMTMP, SMFMX, SMFMN, TLAPS and PLAPS need to be measured through empirical studies or calibrated. Table 2.1 shows the physically meaningful ranges assigned to these parameters for evaluating the performance of SWAT-TIM in snow simulations.

2.3.3.2 SWAT-EBM

In EBMs, the energy used for snowmelt comes from various sources including shortwave (Q_{sh}) and longwave (Q_l) net radiation, latent (Q_e) and sensible (Q_h) heat fluxes, ground heat flux (Q_g), and the energy contained in the rainfall (Q_p). Therefore, the total available energy for snowmelt (Q_m) is expressed as below (all units in $kJ.m^{-2}$):

$$Q_m = Q_{sh} + Q_l + Q_e + Q_h + Q_g + Q_p - \Delta Q_{in} \quad (7)$$

where ΔQ_{in} is the internal energy stored in snow, which includes changes in freeze and thaw processes, as well as snow temperature. This study adopted the snowmelt scheme suggested by USACE (1998) as a detailed and comprehensive EBM, which considers vegetation cover and rain-on-snow events in snowmelt modelling (Qi et al., 2017). In this snowmelt module, the amount of snowmelt for each energy component in Equation (7) is calculated as:

$$M_j = \frac{Q_j}{334.9 \cdot \rho_w \cdot B} \quad (8)$$

where M_j is the snowmelt resulted from the jth component of energy in Equation (7), i.e., Q_j $(kJ.m^{-2})$; 334.9 $(kJ.kg^{-1})$ is the latent heat of fusion of ice; ρ_w is the density of water (1000 $kg.m^{-3}$); and B is the thermal quality of snow or the fraction of ice in a unit mass of wet snow (0.95-0.97) (Gray and Landine, 1988). As a result, Equation (7) is re-written as:

$$M = M_{sh} + M_l + M_e + M_h + M_g + M_p - M_{in} \quad (9)$$

where M is the total daily snowmelt (mm), and the terms on the right side of Equation (9) are daily snowmelt values (mm) corresponded to energy sources described in Eq. 7. The USACE snowmelt module is dependent on different precipitation (i.e., rain-on-snow or rain-free) and vegetation (i.e., the value of Leaf Area Index, LAI) conditions (USACE, 1998). The equations of melt components in Equation (9) along with related parameters and data used are described in detail in USACE (1998) and Qi et al. (2017). For the sake of brevity, Table A.3 shows the equations for total daily snowmelt in mm (i.e., M in Eq. 9) based on different vegetation and precipitation conditions. Numerous parameters and input data types are required to solve the equations listed in Table A.3. Table 2.2 shows such data and assumptions used for calculating

snowmelt in SWAT-EBM. The mathematical equations outlined in Table 2.2 are also functions of user-defined parameters, which intensifies the role of model parameters in uncertainties of snowmelt simulations. For the purpose of this study and to examine the effect of the parameter estimation of EBM and TIM in the cascade of uncertainty for future snow depth projections, we summarized in Table 2.1, the physically meaningful ranges for the parameters of the SWAT-TIM and SWAT-EBM. The ranges were defined based on experiments and field measurements found in various studies in the literature. It should be noted that the ranges of k_{s1},k_{v1} and k_{v2} were defined based on the meaningful ranges of k_s and k_v values reported in USACE (1998) (see Table 2.1 and Table 2.2 and for more details). As mentioned before, the snowfall temperature and snowpack temperature lag factor were implemented in both SWAT-TIM and SWAT-EBM snowmelt modules used in this study.

Table 2.1. Parameters used in this study and their physically meaningful ranges for snowmelt modules in SWAT-TIM and SWAT-EBM approaches.

Snowmelt	Parameter	Parameter description	Range	Reference
SWAT-EBM and SWAT-TIM	SFTMP	Snowfall temperature (℃)	[-5 , 5]	Neitsch et al. (2011)
	TIMP	Snowpack temperature lag (℃)	[0 , 1]	
SWAT-TIM	TLAPS	Temperature lapse rate (℃/km)	[-10 , 0]	Zhang et al. (2008); Anand et al. (2018)
	PLAPS	Precipitation lapse rate (mm)	[0 , 250]	
	SMTMP	Snowmelt temperature (℃)	[-5 , 5]	Neitsch et al. (2011)
	SMFMX	Maximum melt factor (℃)	[0 , 10]	
	SMFMN	Minimum melt factor (℃)	[0 , 10]	
SWAT-EBM	k_{s1}	melt coefficient parameter	[0 , 2]	USACE (1998), Qi et al. (2017)
	k_{v1}	Wind control parameter	[0 , 2]	
	k_{v2}	Vegetation surface dynamics parameter	[1 , 5]	
	B	Snow thermal quality	[0.95 , 0.97]	Dingman (2015)
	ε	Snow emissivity	[0.95 , 0.99]	
	α	Snow surface albedo	[0.45 , 0.85]	
	T_{ss}	Snow surface temperature (℃)	[-10 , 0]	Negi et al. (2007); Singh et al. (2013); Jamieson and Schirmer (2016)

2.3.3.3 Snow density formulation

As mentioned in previous sections, SWAT-TIM and SWAT-EBM calculate the amount of snowmelt and snow depth in the form of snow water equivalent (SWE). In order to compare SWAT results with observed snow depth data for model performance evaluation, the conversion of SWE to snow depth is necessary, which is based on SND formulations. In this study, we tested two SND formulations. The first formulation, which has already been evaluated on maritime regions of Canada (Qi et al., 2017), is referred to as SND1 in this study and is computed by:

$$SND_t = \begin{cases} SND_{t-1} + d_s \cdot (0.6 - SND_{t-1}) & no\ snowfall \\ 0.1 \cdot SF_t / SNO_t + SND_{t-1}(SNO_t - SF_t)/(150 \cdot SNO_t) & snowfall \\ SND_{t-1} + 0.5/\exp(1/M) & snowmelt \end{cases} \quad (10)$$

where SND_t is the snow density of the current day ($g.cm^{-3}$), SND_{t-1} is the snow density of the previous day ($g.cm^{-3}$), d_s is the days since the last snowfall has happened (in days), and SF_t is the snowfall of the given day.

The second snow density formulation, which has been suggested by Pomeroy et al. (1998) for Canadian Prairies, is referred to as SND2 hereafter and computed by:

$$SND_t = \begin{cases} 0.06792 + 0.05125 \cdot \exp\left(\frac{T_a}{2.59}\right) & fresh\ snow \\ 0.45 + \frac{20.470}{d}\left(1 - e^{-\frac{d}{673}}\right) & aged\ snow \end{cases} \quad (11)$$

where T_a is the average temperature of a given day (℃), and d is the snow depth (mm). Because the snow depth of the same day is not available in SWAT before snow density is calculated, it is assumed that the d in Eq. 11 is the snow depth of the previous day. Finally, the snow depth will be calculated as:

$$D_t = \frac{SNO_t}{SND_t} \tag{12}$$

where D_t is the snow depth for day t (mm), and SND_t is calculated through Eq. 10 or Eq. 11, known as SND1 and SND2, respectively.

Table 2.2. Input parameters, formulations, and assumptions used in SWAT-EBM approach.

Symbol	Description	Formulation
α	Snow surface albedo	User defined
B	Snow thermal quality	User defined
C_c	Cloud cover	$C_c = 1 - R_s/R_{s,max}$
h_c	Cloud base height (m)	$h_c = 121.92 \cdot (T_a - T_d)$
k_s	Shortwave melt coefficient	$k_s = k_{s1} \cdot [1 + \sin(\pi \cdot (S_a - 90°)) . S]$; k_s usually varies between 0.9 and 1.1 (USACE, 1998)
k_{s1}	Calibration parameter for k_s	User defined
k_v	Wind coefficient	$k_v = k_{v1}/\exp(k_{v2} \cdot LAI)$; k_v is 1 for unforested plains and close to zero for heavily forested areas (USACE, 1998)
k_{v1}	Calibration parameter #1 for k_v	User defined
k_{v2}	Calibration parameter #2 for k_v	User defined
LAI	Leaf Area Index	Calculated by SWAT
M	Total snowmelt (mm)	Calculate through SWAT-EBM
R	Rainfall (mm)	Calculated by SWAT based on SFTMP
R_s	Solar radiation ($MJ\ m^{-2}$)	Input data to SWAT
$R_{s,max}$	Daily maximum solar radiation ($MJ\ m^{-2}$)	Calculated by SWAT
RH	Relative humidity	Input data to SWAT
S	Average surface slope	Calculated through GIS applications
SNO	Snow water equivalent (mm H_2O)	Calculated through SWAT-EBM
S_a	Average surface aspect (degree)	Calculated through GIS applications
T_a	Average daily air temperature (℃)	Input data to SWAT
T_c	Cloud base temperature (℃)	$T_c = TLAPS * h_c + T_a$
T_d	Dew point temperature (℃)	$T_d = T_a - 0.2 \cdot (100 - RH)$
$TLAPS$	Temperature lapse ratio (℃/km)	User defined
T_s	Snowpack temperature (℃)	Calculated through Equation (4)
T_{ss}	Snow surface temperature	User defined
v	Wind speed	Input data to SWAT
ε	Snow emissivity	User defined

2.3.4 Future climate projection data

To simulate future changes in the snow depth projections of NSRB, future climate projections from the Pacific Climate Impacts Consortium (PCIC) (Cannon, 2015) were used in this study. PCIC provides statistically downscaled GCM climate scenarios from 1950 to 2100 (Bürger et al., 2013) based on the Coupled Model Intercomparison Project phase 5 (CMIP5) (Taylor et al., 2012) and the actual historical daily gridded climate data for Canada (McKenney et al., 2011). On the other hand, the GCMs are forced with different Representative Concentration Pathways (RCPs), which define a specific emissions trajectory and subsequent radiative forcing in the earth-atmosphere system (van Vuuren et al., 2011). PCIC provides Canada-wide downscaled climate change projections using the Bias Correction/Constructed Analogues with Quantile mapping reordering (BCCAQ) method (http://www.pacificclimate.org/data).

To test the effect of downscaling procedures on the future projections of snow depth, we used two different downscaled products. The first one is the aforementioned downscaled data from PCIC (named DS1 in Figure 2.2). The second product is a set of further downscaled PCIC data to Alberta condition based on daily historical climate data from earlier studies by Ammar et al. (2020) and Masud et al., (2018). In their study, the delta method (Quilbé et al., 2008; Chen et al., 2011a) is used for bias correction of the projected climate time series based on historical data, which are resulted from examination of a suite of four climate data sources to reproduce historical flow records for 130 gauging stations by using a physically process-based hydrological model (named DS2, Figure 2.2). In total, two emissions scenarios (i.e., RCP 2.6 and RCP 8.5) in an ensemble of five GCMs (see Table A.4) were incorporated for future projection of snow depth under two downscaling techniques, and a set of 1000 simulations generated using SWAT-EBM

and SWAT-TIM based on the range of input parameters were sampled to run them for the 2040-2064 period (see section 2.3.5).

2.3.5 Performance assessment of SWAT-TIM and SWAT-EBM, and uncertainty analysis

The examination of the performance of the SWAT-TIM and SWAT-EBM models in this study are based on their ability to reproduce historical snow depth and streamflow data. The models were evaluated using monthly snow depth and streamflow measurements for the 1999-2007 and 1986-2007 periods, respectively. The comparison analyses were performed at both regional (i.e., the three regions of interest in this study including mountain, foothill, and plain) and local (i.e., 174 sub-basins) scales for snow depth simulations, and at the six hydrometric station for streamflow predictions. The inclusion of streamflow analysis in the performance assessment is because of its sensitivity to snowmelt, especially during the melt season over the April-June period. It should be noted that the main goal of this study is not to develop a calibrated hydrological model based on the best performance of snow depth simulation by comparing TIMs and EBMs. Rather, our focus is to understand robustness in model structure and uncertainties associated with using TIMs and EBMs as snowmelt modules. Hence, the observed snow depth and streamflow data were used for comparison of modelling simulation using SWAT-TIM and SWAT-EBM, and no validation in terms of snow depth and streamflow was carried out in this study. For the same reason, we did not include other influential parameters on streamflow than snowmelt related parameters (see Table 2.1) in our parameterization and evaluation scheme, because we opted to study only the uncertainty arising from the TIM and EBM routines not other water balance routines in the SWAT model. Therefore, for any routines other than EBM and TIM within SWAT, we relied on the model default parameters, most of

which were obtained from input data such as soil database, land-use database, DEM, climate, and other data used to setup the initial SWAT models. Moreover, the streamflow simulations when only snow-related parameters were perturbed help us characterize the performance of snowmelt approaches used in this study.

Input parameters for both SWAT-TIM and SWAT-EBM were chosen based on the number of input parameters involved in TIM and EBM routines and used for snowmelt and snow depth simulations in the SWAT2012 source code (see Tables 2.1 and 2.2). For model runs and for the purpose of uncertainty analysis, we used the widest physically meaningful range for each parameter that was found from literature (Table 2.1). Further, we used a Latin Hypercube Sampling Technique with the Sequential Uncertainty Fitting (SUFI-2) algorithm (Abbaspour, 2015) to generate 1000 samples of parameter sets from these ranges, and fed them into the models to perform 1000 simulations for each model. For computational efficiency, we parallelized our simulations in a 200-core supercomputer using an algorithm that some authors of this study developed in earlier work (Du et al., 2020).

To evaluate the goodness-of-fit of each SWAT run, the monthly observed and simulated snow depth were compared and evaluated using three widely-used criteria of efficiency, i.e., coefficient of determination (R^2), Nash-Sutcliffe (NS), and bR^2. While NS accounts for normalized variance of observed and simulated data, bR^2 is a slope weighted coefficient of determination that considers both under- or over-predictions (using the factor "b") and dynamics (through R^2) of data (Krause et al., 2005). Detailed formulation and their description of these criteria with relevant references are provided in Table A.5. For comparison of observed and simulated values of snow depth, a sub-basin scale analysis and a regional analysis were performed. In sub-basin scale analysis, for uncertainty assessment of SWAT parameters in each

sub-basin, the simulated data of sub-basins had to correspond to their closest gridded data points of observed snow depth. To do so, the observed snow depth for each sub-basin was assigned from the average of the CMC data points located within a 12-km (i.e., half of grid size) distance of each sub-basin border. After that, the simulated results and the assigned observed values of snow depth to each sub-basin were compared. For regional analysis, snow depth simulations for each sub-basin were weight-averaged over the area of the three regions of study (i.e., mountainous, foothill or plain regions), where the weight of each sub-basin was its area; then, the weight-averaged snow depth was compared with average observed snow depth acquired from gridded data for the same region (see Figure 2.1b).

In addition to the efficiency criteria corresponding to the optimal parameter set among 1000 simulations in each model, we used two other statistical factors using SUFI-2, namely p-factor and r-factor for the analysis of model uncertainty. These two factors evaluate model uncertainty arising from the parameter inputs, observed data, and model structure. The p-factor varies from 0 to 1 and it shows the percentage of measured data bracketed within the uncertainty band that is predicted by model in response to the range of parameters, e.g., 1000 samples of parameter set, provided as input. The uncertainty band in SUFI-2 is calculated as the 95 percent of the cumulative distribution of the simulated variables (Abbaspour, 2015), defined as 95 Percent Prediction Uncertainty (95PPU) hereafter. While the r-factor, which varies from 0 to ∞, represents the width of the predicted uncertainty band. The ideal values for p-factor and r-factor are 1 and 0, however due to the uncertainty related to data, model structure, and input parameters such values are not achievable in regional hydrological modelling.

In this study, comparison and performance assessment of the SWAT-TIM and SWAT-EBM models were not only based on the best performing set of parameters from a total of 1000

simulations, but also uncertainty analysis based on p-factor and r-factor. It is suggested that for streamflow simulations, values between 0.6-0.8 for p-factor and values around 1.0 for r-factor show a reasonable performance for streamflow simulation in areas at the scale of our study watershed (Abbaspour, 2015). Overall, we performed a total of 80,000 simulations with 40,000 for each of the SWAT-TIM and SWAT-EBM models (i.e., 40,000 =1000 parameter samples × 5 GCMs × 2 RCPs × 2 Downscaling techniques × 2 SNDs), albeit by parallelizing in a 200-core computer (see Figure 2.2).

2.3.6 Uncertainty decomposition and spatio-temporal apportionment

For quantifying the cascade of uncertainty associated with future projection of snow depth using SWAT-EBM and SWAT-TIM approaches, we used the Analysis of Variance (ANOVA) method, which has been successfully carried out in various studies, including hydrological studies (see for example, Déqué et al., 2007; Yip et al., 2011). The ANOVA method decomposes the projected variance and attributes its parts to different uncertainty sources and their interactions. In this study, the sources of uncertainty incorporated in ANOVA include hydrologic model parameterization (95PPU), GCMs, RCPs, and Downscaling methods (DS). According to the statistical theory of ANOVA, the total sum of squares (SST) is calculated as the sum of the variations resulting from each uncertainty source, and from their interactions. As a result, the SST for this study is defined as (Wang et al., 2018):

$$SST = SST_{GCM} + SST_{RCP} + SST_{DS} + SST_{95PPU} + SSI \quad (13)$$

where SST_{GCM} is the uncertainty share of GCMs, SST_{RCP} is the uncertainty share of RCPs, SST_{DS} is the uncertainty share of downscaling methods, SST_{95PPU} is the uncertainty share of SWAT-EBM and SWAT-TIM model parameters, and SSI is the uncertainty resulting from

interactions of uncertainty sources from all different combinations of two, three, and four variables (i.e., 95PPU, GCM, RCP, and DS). For more details see Bosshard et al. (2013).

In this study, a combination of 40 scenarios were applied to each of SWAT-TIM and SWAT-EBM in order to compare the share of uncertainty sources in the total cascade of uncertainty projection for snow depth projections (Figure 2.2). The monthly variation of the cascade of uncertainty projections were projected across the study area and the results were discussed for the three main regions, i.e., mountain, foothill, and plain, over the study watershed.

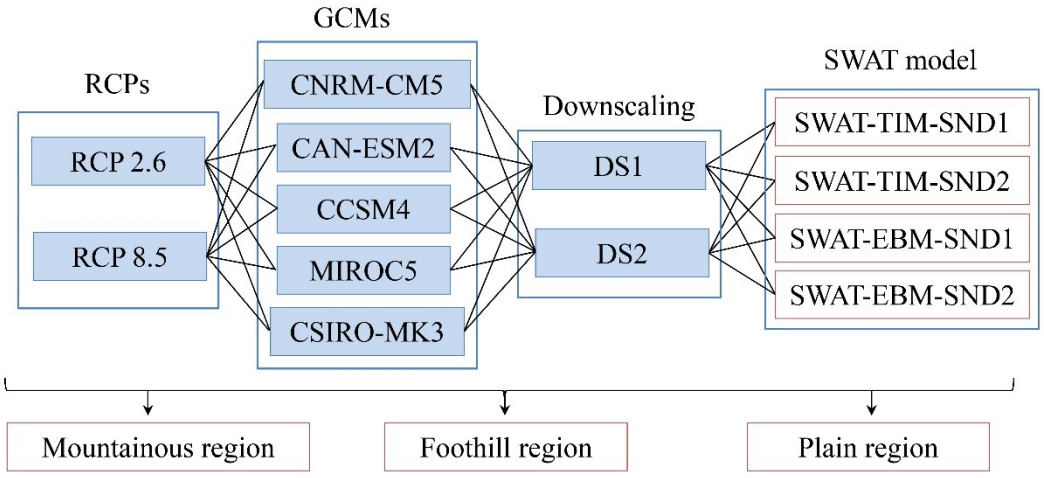

Figure 2.2. Formation of SWAT models and cascades of uncertainty framework for snow depth projections

2.4 Results and Discussion

2.4.1 Model performance of snow depth simulations at sub-basin scale

Figure 2.3 shows the sub-basin scale results of snow depth simulations related to the four combinations of SWAT models (i.e., SWAT-TIM, SWAT-EBM, SND1, and SND2). Based on the results shown in Figure 2.3a, the parameter ranges defined in both SWAT-TIM and SWAT-EBM had a moderate performance in reproducing observed snow depth data, although it is shown that SWAT-TIM was able to have a slightly higher value of average p-factor, therefore

slightly better performance as compared to EBM, especially in plain areas. It is shown in Figure 2.3a that the change of snow density formulation had a considerable effect on p-factor values, particularly in foothill and plain regions. It is however clear that none of snowmelt modules under either of the two snow density approaches had adequately reproduced historical snow depth in mountainous regions. The average p-factors shown in Table 2.3 and Figure 2.3 represent the lower level of performance for mountainous regions for any snow depth simulation approaches than the other two regions. This highlights the complexity of snow-related processes in mountainous regions,

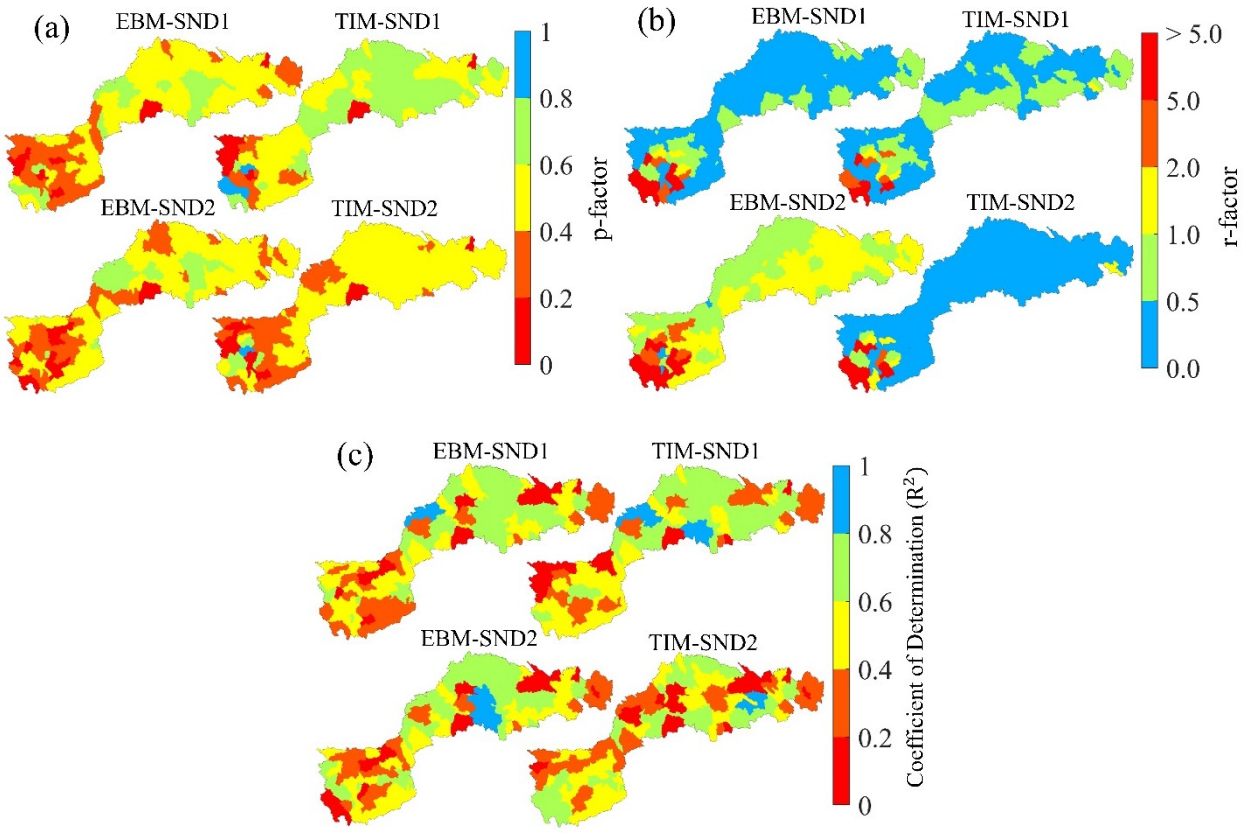

Figure 2.3. Results of (a) p-factor, (b) r-factor and (c) best R^2 calculated based on 1000 simulations of monthly snow depth using combinations of SWAT-EBM and SWAT-TIM with SND1 and SND2 for 1999-2007 period.

Table 2.3. Maximum, minimum, and average values of p-factors, r-factors and R^2 for sub-basins within different regions of NSRB.

		SND1						SND2					
		TIM			EBM			TIM			EBM		
		max	min	avg.	max	min	avg.	max	min	avg.	max	min	avg.
Mountain	p	0.85	0.06	0.45	0.71	0.00	0.37	0.82	0.04	0.35	0.73	0.00	0.34
	r	12.8	0.16	2.07	42.7	0.15	6.09	71.1	0.09	9.12	138.5	0.40	20.28
	R^2	0.76	0.08	0.39	0.75	0.09	0.40	0.77	0.18	0.49	0.75	0.09	0.40
Foothill	p	0.73	0.32	0.59	0.65	0.27	0.46	0.56	0.27	0.44	0.64	0.19	0.46
	r	0.63	0.21	0.43	0.78	0.17	0.38	0.47	0.05	0.20	2.15	0.45	1.06
	R^2	0.78	0.09	0.45	0.70	0.12	0.45	0.77	0.14	0.46	0.70	0.12	0.45
Plain	p	0.75	0.14	0.60	0.73	0.08	0.47	0.58	0.17	0.46	0.71	0.14	0.45
	r	1.03	0.16	0.50	0.68	0.25	0.39	1.04	0.00	0.15	1.93	0.64	1.08
	R^2	0.80	0.00	0.55	0.85	0.03	0.51	0.81	0.01	0.45	0.85	0.03	0.51

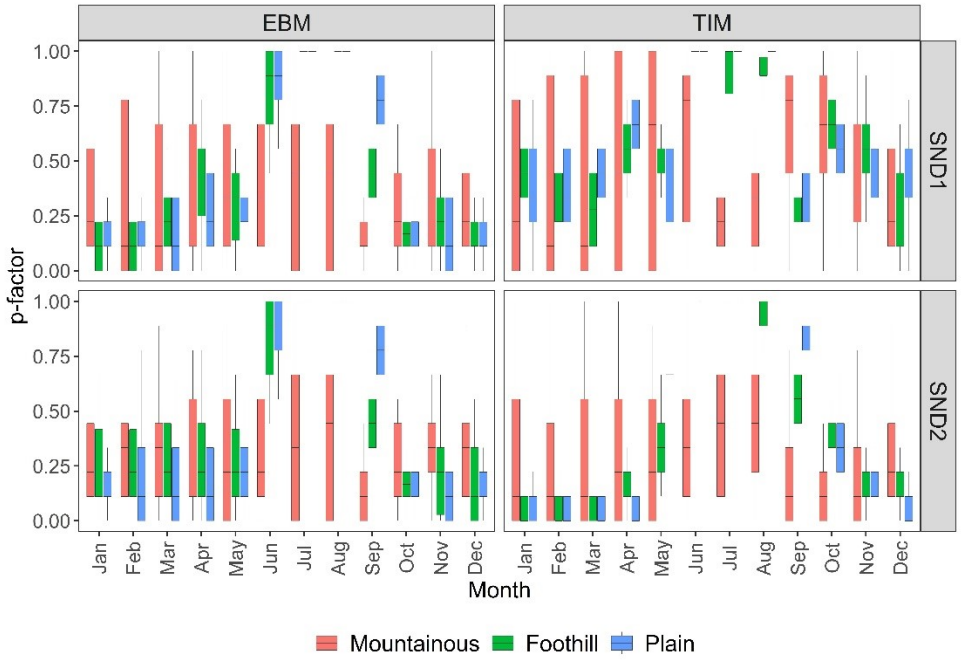

Figure 2.4. Monthly variation of the p-factor values within three regions of NSRB using four snow depth simulation approaches. The box plots show the range of p-factors obtained across sub-basins.

which is exacerbated by the lack of reliable and consistent climate data in such areas. The noticeable temporal gaps in precipitation time series, as well as their inadequate spatial coverage in mountainous regions are potentially a major reason for the poor performance of snowmelt

modules to simulate snow depths in mountainous regions (Mizukami et al., 2014; Ul Islam and Déry, 2017). On the other hand, the higher spatial variability of temperature, solar radiation, wind speed and relative humidity in mountainous regions in comparison with foothill and mountain region and the coarse spatial resolutions of such climate data compared to the topographic variability of mountainous regions (see Table A.2) may be another reason for the low performance of SWAT-TIM and SWAT-EBM in simulating historical snow depth data in most of sub-basins within mountainous region (Comola et al., 2015; Helbig et al., 2015; DeBeer and Pomeroy, 2017). Figure 2.4 shows the variation of monthly p-factors of snow depth analysis based on different subbasins within mountainous, foothill and plain regions. It is shown that in most of the months, the p-factors of subbasins across mountainous regions had the largest variability compared to those of plain and foothill regions. Nevertheless, the average values of p-factor within mountainous regions were lower than those of foothill and plain regions (see Figure 2.4 and Table 2.3). While none of the four model combinations shown in Figure 2.4 can be presented as superior to others in terms of reproducing historical snow depth, the changes in p-factor ranges under different approaches were noticeable (e.g., changes from TIM-SND1 to TIM-SND2). It is also noteworthy that in Figure 2.4, the variability of p-factor in foothill and plain regions during summer months was negligible, since foothill and plain areas of NSRB usually had minimum or no snow cover during summer. Overall, the high variability of p-factors using both TIM and EBM and under both SND1 and SND2 in mountainous region suggest unreliable snow depth simulation as a result of complex topography and lack of adequate and reliable climate datasets, even when a more comprehensive model structure (e.g., EBM combinations) is utilized (Helbig et al., 2015).

Figure 2.3b shows the r-factors corresponded to historical snow depth simulations of NSRB sub-basins. The high value of r-factor for several sub-basins in mountainous regions suggests that the effect of snow parameters in simulating snow depth can be significant in mountainous regions with high topographic and climate variability. This can be particularly related to areas with complex and highly variable hydrology, as the average and maximum values of r-factor in the non-mountainous region is noticeably smaller than those within the mountainous region. It can be interpreted from Table 2.3 that the average values of r-factors in mountainous regions were considerably greater than other areas, where the average p-factor values were less than those in other areas. This implies that a larger uncertainty is predicted in mountainous regions, where only small share of the historic data were reproduced using any of the two models under any of the SND combinations. Since EBMs are more physically-based approaches by definition than TIMs are, the poor performance of EBM models under any of the SND combinations are likely due to the poor quality of input data, i.e., spatio-temporal climate factors and input parameters used to run them. This suggests a clear need for enhancement of data collection and monitoring strategies within mountainous regions (Clow et al., 2012; Helbig et al., 2015; DeBeer and Pomeroy, 2017) than enhancement of the modelling approaches themselves. The uncertainty range (i.e., r-factor) of mountainous regions of EBMs in both SND1 and SND2 was higher than those in TIMs, suggesting that the effect of model parameterization on modelling uncertainty of snow depth simulations is intensified in complex areas (i.e., mountainous regions in this study) (Ul Islam and Déry, 2017). On the other hand, the r-factors of snow depth simulation in all regions under EBM-SND2 were increased compared to the r-factors related to EBM-SND1, with the highest level of difference within mountainous regions (see Table 2.3).

The additional modelling uncertainty resulting from using SND2 instead of SND1 could be attributed to the sensitivity of SND2 to air temperature. According to Eq. (11), under fresh snow (i.e., snowfall) conditions, snow density is solely a function of current air temperature. On the other hand, under aged snow conditions, snow density is a function of snow depth of the previous day, a variable that is calculated based on the snow density of the previous day. As a result, the snow density under SND2 is a strong function of air temperature of a given day or its previous day(s). Since the major difference between SND2 and SND1 is in incorporating the air temperature in SND2, it can be argued that incorporating air temperature factor in snow density estimation resulted in more uncertainty in snow depth simulations using SND2 because similar to other climate data, the temperature data were not abundantly available for snow depth simulation at this scale.

Finally, our analysis of the R^2 values corresponding to the best simulation results (out of 1000 model runs) is shown in Figure 2.3c. An overview of the results from four different model-SND combination shows that, in general, the snow depth in sub-basins of plain areas were simulated properly, yet demanding improvements. Although some sub-basins in the plain region had the R^2 of less than 0.4, most of the sub-basins showed a R^2 value of 0.6 or above, which can be an indicator of a proper snowpack simulation in plain areas. The comparison of observed and simulated snow depth data in the foothill and mountainous regions, however, showed poorer results compared to those of plain regions. Although sporadic sub-basins with a proper R^2 can be found in foothill and mountainous regions, most of the sub-basins showed the R^2 value of less than 0.6. This can be due to the likely error inherent in the gridded snow depth data used for our comparison, as well as their coarse resolution (i.e., 24 km × 24 km) for sub-basin-based comparison (Helbig et al., 2015). In other words, the comparison of simulated and observed data

for sub-basins was based on assigning the historical data from coarse resolution grid points to each sub-basins. Hence, the spatial heterogeneity of historical snow depth are under-represented at the sub-basin scale. For the same reason, we are not presenting NS and bR^2 results of snow depth simulation, since they provide more detailed comparison of the simulated versus observed data, which require a higher resolution measurements for a direct and comprehensive assessment. Furthermore, the lack of time-series data for precipitation in regions with high variability in topography and climate such as west side of NSRB resulted in a poorer model performance (Mizukami et al., 2014; Ul Islam and Déry, 2017). Consequently, presentation of comparison results at a regional-scale in our study would give more reliable insights than those of sub-basin scale.

2.4.2 Effect of snow density formulation on model performance at regional scale

The results in this section reveal the effect of snow density formulation on performance and uncertainty associated with simulations and projections of snow depth. The results of the best model runs out of 1000 simulations for various regions, snowmelt approaches (EBM, TIM), and snow depth approaches (SND1 and SND2) are shown in Figure 2.5 and Table A.6. As shown in Figure 2.5a, when using SND1, neither the SWAT-TIM (with an average NS, bR^2, and R^2 of 0.45, 0.19, and 0.65) nor the SWAT-EBM (NS, bR^2, and R^2 of 0.51, 0.23, 0.66) could reliably simulate the dynamics and magnitudes of regional snow depth within the mountainous regions of NSRB. However, by implementing SND2, which is an empirical formulation specifically meant for Canadian Prairies (Pomeroy et al., 1998), a considerable improvement in simulation of regional snow depth in both SWAT-TIM (with an average NS, bR^2, and R^2 of 0.79, 0.58, 0.80) and SWAT-EBM (NS, bR^2, and R^2 of 0.25, 0.69, 0.78) can be seen. Comparison of Figure 2.5a with Figure 2.5b and 5c reveals that the proper formulation of snow density function

plays an important role in quantifying snow depth, particularly in mountainous regions (Sturm et al., 2010; Bormann et al., 2013). In fact, higher variability of snow depth within mountainous regions along with high variability of temperature might be the reason why the snow depth in such regions is more sensitive to definition of snow density formulations. On the other hand, the performance of SWAT-TIM and SWAT-EBM under SND1 and SND2 in snow depth simulation within foothill and plain were nearly the same. Nevertheless, it is detected that SWAT-EBM-SND2, which is known to be more physically based and robust in snow depth simulation, mostly overestimated the snow depth in all the regions within NSRB. This can be in line with the overestimation of streamflow at the outlet of NSRB (see Figure 2.6). In other words, the overestimation of snow depth in winter might result in overestimation of streamflow in warmer periods of the year, where the snowpack is mostly melted and converted into streamflow.

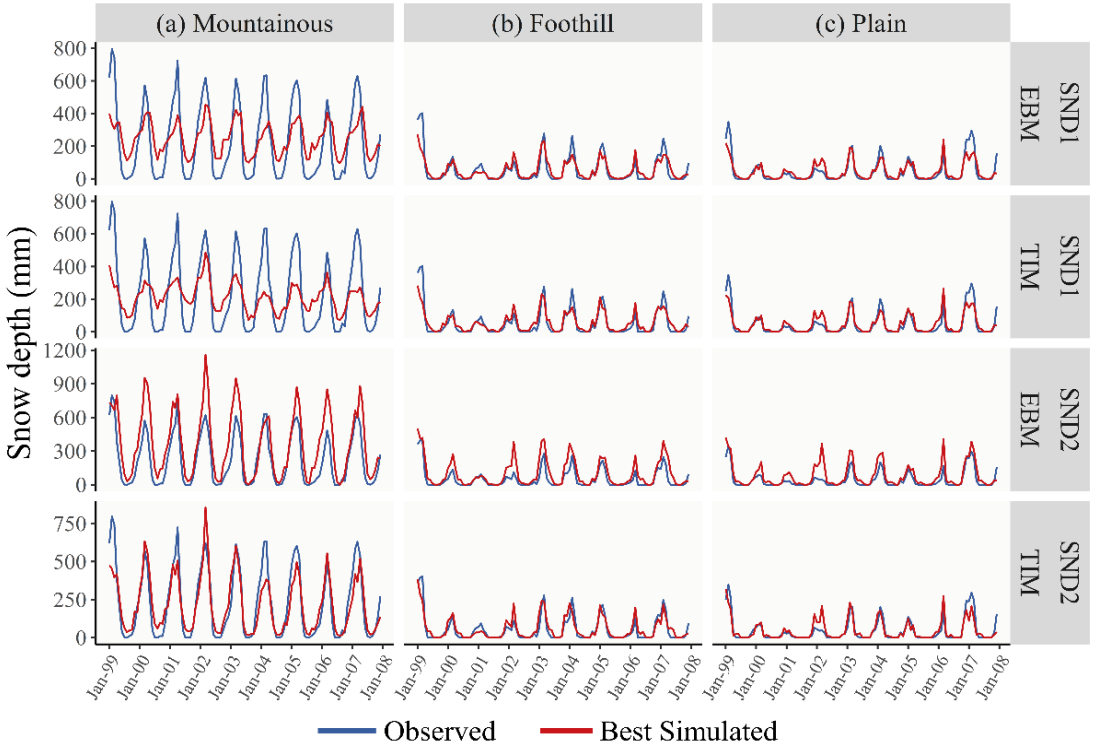

Figure 2.5. Comparison of the best simulated snow depth (red) with observed (blue) data in (a) mountainous, (b) foothill and (c) plain regions for the 1999-2007 period.

2.4.3 Assessment of SWAT-TIM and SWAT-EBM in reproducing streamflow

Since streamflow is a function of snowmelt in terms of SWE (rather than snow depth), SWE is independent from SND approaches used. Hence, streamflow reproduction results in this section are reported in terms of SWAT-TIM and SWAT-EBM approaches, because using SND1 or SND2 has no effect on streamflow values. The streamflow simulation using 1000 parameter set samples in SWAT-EBM and SWAT-TIM show that in the upstream stations (see Figure 2.1 and Table A.1), representing Mountainous region, with p-factors of 0.57 and 0.33 for stations #1 and #2 respectively, the SWAT-EBM performed slightly better than SWAT-TIM with p-factor of 0.40 and 0.16 for stations #1 and #2, respectively (Table 2.4). In terms of NS and bR^2 SWAT-EBM with NS of 0.66 and bR^2 of 0.42 performed slightly better than SWAT-TIM with NS of 0.59 and bR^2 of 0.34 in station #1; however, the performance of SWAT-TIM was much better in station #2, with NS of 0.23 and bR^2 of 0.27 for SWAT-TIM as compared to NS of -1.43 and bR^2 of 0.05 from SWAT-EBM simulations (see Table 2.4). On the other hand, SWAT-TIM had performed marginally better in simulating streamflow data within downstream hydrometric stations. Comparisons of the r-factor, NS and bR^2 shows relatively close values for SWAT-TIM and SWAT-EBM within both mountainous and plain regions, suggesting that the performance of TIM and EBM within a large watershed with diverse hydro-climate and topographic conditions was relatively similar in simulating the streamflow dynamics. These results are in line with previous studies on comparison of TIMs and EBMs for streamflow simulations (Franz et al., 2008; Zhang et al., 2008; Zeinivand and Smedt, 2009; Debele et al., 2010; Meng et al., 2017). One important point, however, is the low values of NS of SWAT-EBM in most of the hydrometric stations. It is found in the literature that the EBMs might overestimate the streamflow due to overestimation of mid-winter snow depth (Franz et al., 2008). As it can be

found by comparison of EBM and TIM in Figure 2.6, the best performing simulation results of EBM, out of 1000 simulations, was yet overestimating the peak flows, resulting in low values of NS, which highlighted the constant overestimation of the flow (Krause et al., 2005, see Table 2.4). It is noteworthy that the streamflow simulations are based on best-fitting snow parameters only, and other parameters related to soil, groundwater, runoff that are sensitive to streamflow can be adjusted in order to change simulated streamflow results in Figure 2.6, which is beyond the scope of this study. Nevertheless, the overestimation of peak flow resulting from using SWAT-EBM is noticeable (i.e., within hundreds of cubic meter per second), which might not be rectified by logical adjustment of other SWAT parameters. Hence, the potential overestimation of streamflow through using EBMs should be taken into account in hydrological studies such as analyzing extreme conditions (i.e., floods and droughts) throughout regional studies.

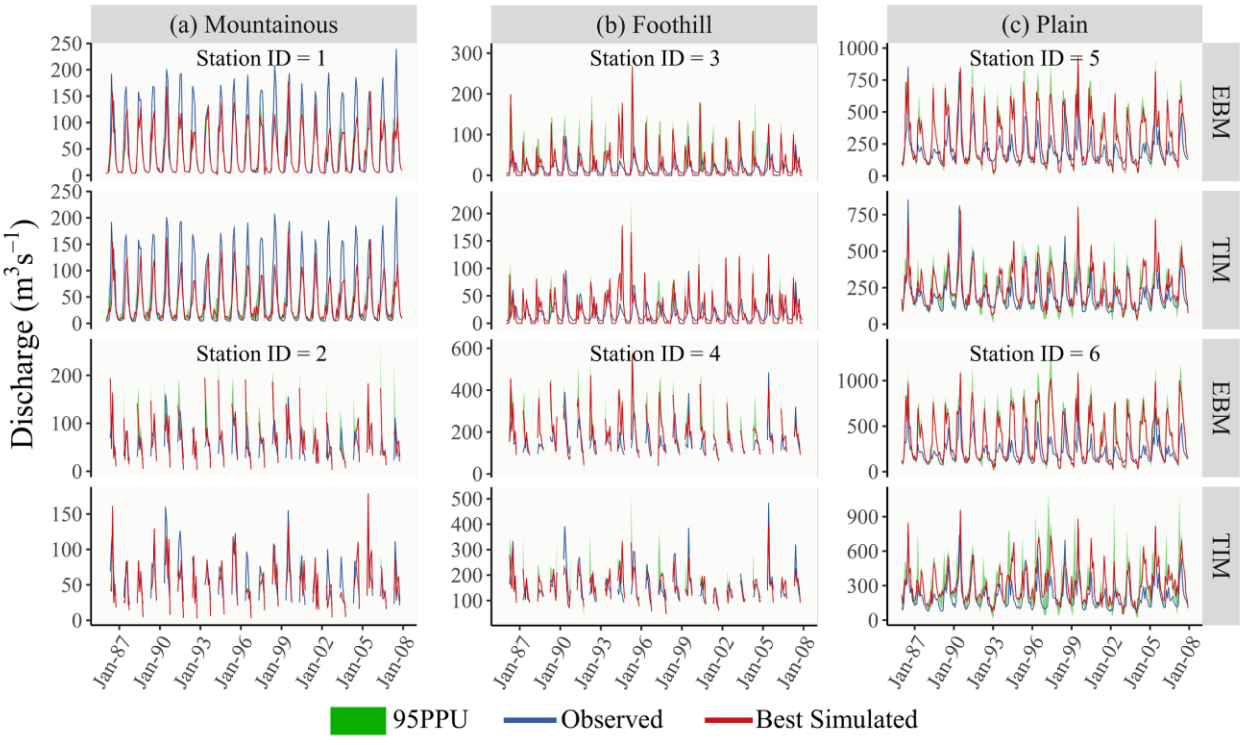

Figure 2.6. Comparison of monthly observed (blue), best simulated (red), and 95PPU (orange band) streamflow for 1986-2007 period using SWAT-EBM (left column) and SWAT-TIM (right column). 95PPU: 95 percent prediction uncertainty.

Table 2.4. Performance of average monthly streamflow simulation for SWAT-TIM and SWAT-EBM for 1986-2007.

Region	Station ID (Table A.2)	Snowmelt module	p-factor	r-factor	R^2	NS	bR^2
Mountainous	1	EBM	0.57	0.16	0.72	0.66	0.42
		TIM	0.40	0.13	0.69	0.59	0.34
	2	EBM	0.33	0.82	0.10	-1.43	0.05
		TIM	0.16	0.17	0.41	0.23	0.27
Foothill	3	EBM	0.14	0.93	0.14	-3.74	0.13
		TIM	0.08	0.28	0.18	-1.70	0.13
	4	EBM	0.34	0.76	0.21	-1.22	0.14
		TIM	0.40	0.39	0.39	0.34	0.21
Plain	5	EBM	0.23	0.49	0.57	-0.65	0.47
		TIM	0.36	0.46	0.66	0.44	0.56
	6	EBM	0.29	0.72	0.61	-2.04	0.40
		TIM	0.36	0.78	0.57	-0.10	0.52

2.4.4 Evaluation of uncertainty sources in the cascade of uncertainty projection

The average monthly results of uncertainty decomposition for snow depth projection in mountainous, foothill, and plain regions are shown in Figure 2.7. Also, the annual average values of contributions of different uncertainty sources for the same regions is outlined in Table A.7. It can be seen from the figures that the share of parameter uncertainty within all regions of NSRB is considerable, although holding different values in different regions and times. A general comparison of cascades of uncertainty of mountainous, foothill, and plain regions based on Figure 2.7 and Table A.7 shows that 95PPU arising from SWAT-EBM and SWAT-TIM holds the largest share of uncertainty in mountainous regions, compared to foothill and plain regions. This uncertainty range was resulted from 1000 set of parameter combination sampled from a physically meaningful range defined from literature (see Table 2.1). This suggest the importance of model parameterization and the input data in complex regions for snow depth simulations and projections (Mizukami et al., 2014; Ul Islam and Déry, 2017). As we move from mountainous to foothill and plain regions, the average annual share of parameter uncertainty becomes less than that of mountainous regions as the share of annual PPU, under NSD2, changes from 75.4% and

57.0% for EBM and TIM, respectively in mountainous to 57.8% and 42.1% in foothill, and to 59%, and 27.5% in plain region, respectively (see Table A.7). In the Mountainous region and under SND1 and SND2 formulations, both SWAT-TIM and SWAT-EBM showed a relatively similar trend in sharing the formation of cascade of uncertainty. The average value of 95PPU contribution to cascade of uncertainty for EBM-SND1, TIM-SND1 and TIM-SND2 ranges between 55% to 60%, presenting a relatively similar behavior of parameter uncertainty within these approaches. The average parameter uncertainty from EBM-SND2, however, is 75%, which suggests the noticeable effect of snow density approach in the formation of cascade of uncertainty in EBM model. EBM-SND2 also holds the largest share of parameter uncertainty for foothill and plain regions. It is also shown in Figure 2.7a that the share of parameter uncertainty decreased in warmer seasons (i.e., May to August). This indicates that as the weather gets warmer in mountainous regions, the effect of various GCMs, RCPs, downscaling methods and their interactions on snow depth projections increased, since they directly affect the precipitation, air temperature and solar radiation, which are major drivers of snowmelt and snow depth, therefore forcing a larger variation in projection of snowfall and therefore snow depth than hydrologic model parameters. On the other hand, snowfall events are less frequent in warm seasons (MacDonald et al., 2012), which makes the effect of snowmelt parameters within EBM and TIM less than those for colder seasons. As a result, the effect of GCMs, RCPs, downscaling methods and their interactions was increased in warm seasons. In colder seasons, however, GCMs, RCPs, downscaling methods and their interactions had less contribution to the cascade of uncertainty in mountainous regions, possibly because temperature variability is less effective of snow formation in cold seasons. In cold seasons, the air temperature within mountainous regions are well below freezing point; therefore, the variability of temperature among various GCMs,

RCPs and downscaling methods does not effect the conversion of precipitation to snowfall or rainfall. Because of that, EBM and TIM parameter uncertainty controls most of the uncertainty associated with snow depth simulations in these months than the GCMs, RCPs, and DS. As the study region moves from mountainous areas to the plain region, the share of different uncertainty sources changes for different months. The comparison of Figures 2.7a, 2.7b and 2.7c shows that by shifting from mountainous to plain regions, the contribution of parameter uncertainty to cascade of uncertainty decreased, while other sources of uncertainty contributed more to the overall uncertainty of snow depth projections. In particular, the contribution of GCM to the uncertainty cascade increased from mountainous region to foothill and plain regions. This is an interesting finding as it provides insight into the conflicting assessments in the literature with some studies concluded GCMs as the largest contributor to the uncertainty projection (Prudhomme and Davies, 2009; Vetter et al., 2017) and others introduced emission scenarios (Vetter et al., 2015), and fewer studies underscored the effects of hydrologic models (Ashraf Vaghefi et al., 2019) in the cascade of uncertainty projections. Our study provides a comprehensive assessment of all contributing factors across spatial and temporal scales and under diverse hydro-climatic and topographic conditions, and it describes how changes from mountainous to plain regions result in different pattern in the share of uncertainty contribution. Same as warm months within mountainous regions, the increased share of GCM uncertainty in foothill and plain regions in comparison with mountainous regions might be partially related to the effect of air temperature on considering precipitation as snowfall or rainfall in SWAT model (see Section 2.3.3).

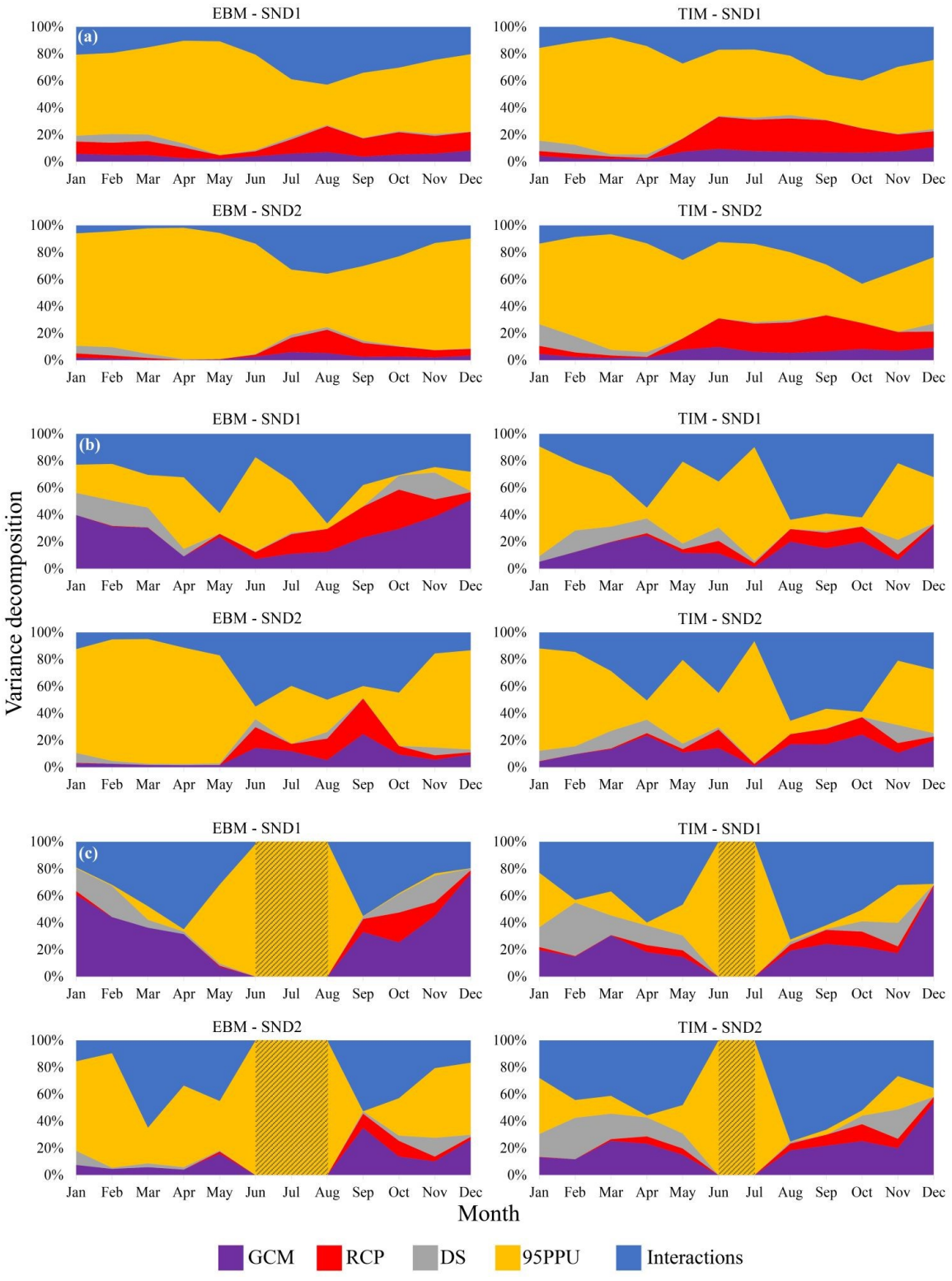

Figure 2.7. Variance decomposition of the uncertainty in snow depth projection within (a) mountainous, (b) foothill, and (c) plain regions throughout NSRB using SWAT-TIM and SWAT-EBM under SND1 and SND2 scenarios. Note: diagonal lines indicate times when snow depth

Furthermore, since the parameter uncertainty had decreased from mountainous to foothill and plain regions (Figure 2.7), this mathematically resulted in the share of other uncertainty sources to increase, which is possibly one other reason for the increase of GCM contribution to uncertainty cascades in foothill and plain regions. The contribution of interactions of different uncertainty sources is the second most important contributor to the cascade of uncertainty of mountainous regions and among the largest contributors in foothill and plain regions, suggesting the non-linear effect of uncertainty sources on snow depth projections (Chawla and Mujumdar, 2018).

Another important point to mention is related to the contribution of model parameter uncertainty to the cascade of uncertainty within plain regions in warm months (i.e., May to August), which is close to 100%, while this contribution is much lower in other months of the year (Figure 2.7c). The large contribution of model parameters to the cascade of uncertainty in warmer months is due to the high temperature of plain regions in warm months. The temperature of this region is significantly higher than the snowfall temperature (especially in June, July and August), which makes the snowfall to rarely happen, therefore resulting in a zero contribution of GCM, RCP, and DS. On the other hand, the amount of snow depth in warm months is almost zero, as almost all the snow depth has been melted throughout the spring (e.g., April and May). As a result, a meager change in snow depth simulation right before or during the warm months will numerically result in a large variance calculation for the 95PPU, using ANOVA method, as compared to the small value of snow depth. As presented with diagonal lines in Figure 2.7c, due to the zero share of GCM, RCP, and DS during warm months in plain region, the 95PPU gained the maximum share of the uncertainty despite its negligible variation due to the parameter uncertainty.

2.5 Conclusion and future directions

Snowmelt and snow depth processes are among the most significant hydrological processes in most of high elevation watersheds in the northern latitudes and mountainous watersheds with cold hydrology. However, the contribution of uncertainty due to the use of Temperature Index Modules (TIMs) and Energy Balance Modules (EBMs) in projection of snowmelt and snow depth in regional studies is poorly understood. We implemented the ANOVA uncertainty decomposition approaches, where a process-based TIM and EBM snowmelt routines, as well as two different snow density modules were coupled within the Soil and Water Assessment Tool (SWAT) source code and future projections were performed based on an ensemble climate datasets of five GCMs, under the two future scenarios of RCP 2.6 and RCP 8.5 and using two downscaling approaches. This allowed spatio-temporal assessment of the uncertainty projections of snow melt and snow depth across heterogeneous landscapes, from mountainous and foothill to plain areas using a large river basin in Alberta, western Canada as the study region. The main conclusions of this study are:

1. The performance of EBM and TIM approaches in simulating snowmelt and snow depth is different across scales and time; therefore, conclusions from a small-scale study with a homogeneous landscape and hydro-climate condition cannot be generalized to a larger regional scale and for a longer period of time.

2. While the performances of EBM and TIM were relatively similar in mountainous regions and both produced a relatively large uncertainty, the spatio-temporal analysis of the p-factor, r-factor, NSE, bR^2, and R^2 indicated that SWAT-TIM performed better in foothill and plain regions as compared to the SWAT-EBM combinations and the SWAT-EBM approach

overestimated streamflow in most regions and snow depth in all the regions within the study watershed.

3. While snowmelt simulation modules are key in hydrologic modelling of snow dominated regions, the performance of the models in snow depth simulations is more dependent on the formulation of snow density simulation, rather than using TIM or EBM. This highlights the importance of the selection of a proper snow density (SND) approach in accordance with the study area and climatic conditions.

4. All EBM, TIM, SND1, and SND2 model combinations predicted larger uncertainty in simulation of snow depth and streamflow in the mountainous regions as compared to foothill and plain areas. Since EBMs are a more physically-based approach by definition than TIMs, the poor performance of SWAT-EBM model under any of the SND combinations are likely due to the poor quality of input data, i.e., spatio-temporal climate factors and input parameters used to run them. This observation suggests a clear need for enhancement of data collection and monitoring strategies within mountainous regions.

5. The analysis of the cascade of uncertainty for future snow depth simulation indicated that the share of uncertainty from different sources varies over time and across regions. While the share of uncertainty was dominated by EBM and TIM parameterization in the highland areas and in cold months, it was conquered by the GCMs, RCPs, and DS in lower elevation foothill and plain areas. The share of uncertainty was also affected by the choice of snow density approach, and the SWAT-EBM-SN2 modelling approach resulted in a larger share of uncertainty in future snow depth projection, due to a more physically-based nature of the model combination, as compared to all other model combinations.

6. The larger share of parameter uncertainty in cold months is related to the air temperature that are well below freezing point making the variability of temperature among various GCMs, RCPs and downscaling methods ineffective in the conversion of precipitation to snowfall or rainfall in the mountainous regions, while the larger parameter uncertainty in warm months in the plain regions is related to a significantly higher than the snowfall temperature, which makes the snowfall to rarely happen, therefore resulting in a zero contribution of GCM, RCP, and DS and numerically allocating a large uncertainty share to the parameters.

This research facilitates better understanding of the performance and uncertainties associated with the projection of snow melt and snow depth using EBM and TIM approaches in large regional studies, where hydro-climate and geospatial features vary across regions and times. It also demonstrates that a multi-scale and temporal analysis is needed for understanding the cascade of uncertainties in future snowmelt and snow depth simulations. Our study underscores the importance of the input climate data in simulation of hydrological processes in the high elevation areas that is likely more significant than the choice of model structure and process representation. Furthermore, in regional station-based observed data do not represent the average snow depth within a large region of study (i.e., with scales of hundreds of square kilometers), a fact that highlights the need of spatial gridded data for comparison of snow depth simulations. On the other hand, the gridded data of historical snow depth or SWE within Canadian Prairies are scarce, and it is difficult to acquire proper gridded data for snow depth at a fine spatial resolution. Therefore, any improvement in historical climate data of precipitation and temperature, as well as historical snow depth data can result in an improved quality of snowmelt and snow depth analysis within large regions.

2.6 Acknowledgement

We would like to thank Dr. Junyu Qi for guiding us about EBM formulations and operation within SWAT model. Funding for this study has been received from Campus Alberta Innovation Program Chair (Grant# RES0034497), and Natural Sciences and Engineering Research Council of Canada Discovery Grant (Grant# RES0043463).

2.7 References

Abbas, T., Hussain, F., Nabi, G., Boota, M.W., Wu, R.-S., 2019. Uncertainty evaluation of SWAT model for snowmelt runoff in a Himalayan watershed. Terr. Atmos. Ocean. Sci. 30, df. https://doi.org/10.3319/tao.2018.10.08.01

Abbaspour, K.C., 2015. SWAT-CUP: SWAT Calibration and Uncertainty Programs- A User Manual, Department of Systems Analysis, Intergrated Assessment and Modelling (SIAM),EAWAG. Swiss Federal Institute of Aqualtic Science and Technology, Duebendorf, Switzerland. https://doi.org/10.1007/s00402-009-1032-4

Aggarwal, S.P., Thakur, P.K., Nikam, B.R., Garg, V., 2014. Integrated approach for snowmelt run-off estimation using temperature index model, remote sensing and GIS. Curr. Sci. 106, 397–407.

Alberta Environment and Parks, 2019. Alberta river basins [WWW Document]. URL https://web.archive.org/web/20160409210242/http://www.environment.alberta.ca/apps/basins/default.aspx (accessed 7.30.19).

Ammar, M.E., Gharib, A., Islam, Z., Davies, E.G.R., Seneka, M., Faramarzi, M., 2020. Future floods using hydroclimatic simulations and peaks over threshold: An alternative to nonstationary analysis inferred from trend tests. Adv. Water Resour. 136, 103463. https://doi.org/10.1016/j.advwatres.2019.103463

Anand, J., Gosain, A.K., Khosa, R., Srinivasan, R., 2018. Regional scale hydrologic modeling for prediction of water balance, analysis of trends in streamflow and variations in streamflow: The case study of the Ganga River basin. J. Hydrol. Reg. Stud. 16, 32–53. https://doi.org/10.1016/j.ejrh.2018.02.007

Arnold, J., Moriasi, D., Gassman, P., Abbaspour, K., White, M., Srinivasan, R., Santhi, C., Harmel, R., van Griensven, A., Van Liew, M., Kannan, N., Jha, M., 2012. SWAT: Model Use, Calibration, and Validation. Trans. ASABE 55, 1317–1335. https://doi.org/10.13031/2013.42244

Arnold, J., Srinivasan, R., Muttiah, R., Williams, J., 1998. Large Area Hydrologic Modeling and Assessment; Part I: Model Development. J. Am. Water Resour. Assoc. 17, 73. https://doi.org/10.1016/S0899-9007(00)00483-4

Ashraf Vaghefi, S., Iravani, M., Sauchyn, D., Andreichuk, Y., Goss, G., Faramarzi, M., 2019. Regionalization and parameterization of a hydrologic model significantly affect the cascade of uncertainty in climate-impact projections. Clim. Dyn. 0, 0. https://doi.org/10.1007/s00382-019-04664-w

Avanzi, F., De Michele, C., Ghezzi, A., 2015. On the performances of empirical regressions for the estimation of bulk snow density. Geogr. Fis. Dinam. Quat. 38, 105–112. https://doi.org/10.4461/GFDQ.2015.38.10

Bavera, D., Bavay, M., Jonas, T., Lehning, M., De Michele, C., 2014. A comparison between two statistical and a physically-based model in snow water equivalent mapping. Adv. Water

Resour. 63, 167–178. https://doi.org/10.1016/j.advwatres.2013.11.011

Beven, K., Freer, J., 2001. Equifinality, data assimilation, and uncertainty estimation in mechanistic modelling of complex environmental systems using the GLUE methodology. J. Hydrol. 249, 11–29. https://doi.org/https://doi.org/10.1016/S0022-1694(01)00421-8

Bocchiola, D., Groppelli, B., 2010. Spatial estimation of snow water equivalent at different dates within the Adamello Park of Italy. Cold Reg. Sci. Technol. 63, 97–109. https://doi.org/10.1016/j.coldregions.2010.06.001

Bormann, K.J., Westra, S., Evans, J.P., McCabe, M.F., 2013. Spatial and temporal variability in seasonal snow density. J. Hydrol. 484, 63–73. https://doi.org/10.1016/j.jhydrol.2013.01.032

Bosshard, T., Carambia, M., Georgen, K., Kotlarski, S., Krahe, P., Zappa, M., Schar, C., 2013. Quantifying uncertainty sources in an emsemble of hydrological climate-impact projections. Water Resour. Res. 49, 1523–1536. https://doi.org/10.1007/s00704-017-2359-3

Brown, R.D., B.Bransnett, 2010. Canadian Meteorological Centre (CMC) Daily Snow Depth Analysis Data, Version 1. [WWW Document]. Boulder, Color. USA. NASA Natl. Snow Ice Data Cent. Distrib. Act. Arch. Cent. https://doi.org/10.5067/W9FOYWH0EQZ3

Bürger, G., Sobie, S.R., Cannon, A.J., Werner, A.T., Murdock, T.Q., 2013. Downscaling extremes: An intercomparison of multiple methods for future climate. J. Clim. 26, 3429–3449. https://doi.org/10.1175/JCLI-D-12-00249.1

Cannon, A.J., 2015. Selecting GCM scenarios that span the range of changes in a multimodel ensemble: Application to CMIP5 climate extremes indices. J. Clim. 28, 1260–1267. https://doi.org/10.1175/JCLI-D-14-00636.1

Chawla, I., Mujumdar, P.P., 2018. Partitioning uncertainty in streamflow projections under nonstationary model conditions. Adv. Water Resour. 112, 266–282. https://doi.org/10.1016/j.advwatres.2017.10.013

Chen, J., Brissette, F.P., Leconte, R., 2011a. Uncertainty of downscaling method in quantifying the impact of climate change on hydrology. J. Hydrol. 401, 190–202. https://doi.org/10.1016/j.jhydrol.2011.02.020

Chen, J., Brissette, F.P., Poulin, A., Leconte, R., 2011b. Overall uncertainty study of the hydrological impacts of climate change for a Canadian watershed. Water Resour. Res. 47, 1–16. https://doi.org/10.1029/2011WR010602

Clow, D.W., Nanus, L., Verdin, K.L., Schmidt, J., 2012. Evaluation of SNODAS snow depth and snow water equivalent estimates for the Colorado Rocky Mountains, USA. Hydrol. Process. 26, 2583–2591. https://doi.org/10.1002/hyp.9385

Comola, F., Schaefli, B., Ronco, P. Da, Botter, G., Bavay, M., Rinaldo, A., Lehning, M., 2015. Scale-dependent effects of solar radiation patterns on the snow-dominated hydrologic response. Geophys. Res. Lett. 42, 3895–3902. https://doi.org/10.1002/2015GL064075

DeBeer, C.M., Pomeroy, J.W., 2017. Influence of snowpack and melt energy heterogeneity on

snow cover depletion and snowmelt runoff simulation in a cold mountain environment. J. Hydrol. 553, 199–213. https://doi.org/10.1016/j.jhydrol.2017.07.051

Debele, B., Srinivasan, R., Gosain, A.K., 2010. Comparison of process-based and temperature-index snowmelt modeling in SWAT. Water Resour. Manag. 24, 1065–1088. https://doi.org/10.1007/s11269-009-9486-2

Déqué, M., Rowell, D.P., Lüthi, D., Giorgi, F., Christensen, J.H., Rockel, B., Jacob, D., Kjellström, E., De Castro, M., Van Den Hurk, B., 2007. An intercomparison of regional climate simulations for Europe: Assessing uncertainties in model projections. Clim. Change 81, 53–70. https://doi.org/10.1007/s10584-006-9228-x

Dingman, L., 2015. Physical Hydrology. Waveland Press.

Du, X., Loiselle, D., Alessi, D.S., Faramarzi, M., 2020. Hydro-climate and biogeochemical processes control watershed organic carbon inflows: Development of an in-stream organic carbon module coupled with a process-based hydrologic model. Sci. Total Environ. 718, 137281. https://doi.org/10.1016/j.scitotenv.2020.137281

Faramarzi, M., Abbaspour, K.C., Adamowicz, W.L.V., Lu, W., Fennell, J., Zehnder, A.J.B., Goss, G.G., 2017. Uncertainty based assessment of dynamic freshwater scarcity in semi-arid watersheds of Alberta, Canada. J. Hydrol. Reg. Stud. 9, 48–68. https://doi.org/10.1016/j.ejrh.2016.11.003

Faramarzi, M., Abbaspour, K.C., Schulin, R., Yang, H., 2009. Modelling blue and green water resources availability in Iran. Hydrol. Process. 26, 1–16. https://doi.org/10.1002/hyp

Faramarzi, M., Srinivasan, R., Iravani, M., Bladon, K.D., Abbaspour, K.C., Zehnder, A.J.B., Goss, G.G., 2015. Setting up a hydrological model of Alberta: Data discrimination analyses prior to calibration. Environ. Model. Softw. 74, 48–65. https://doi.org/10.1016/j.envsoft.2015.09.006

Ficklin, D.L., Barnhart, B.L., 2014. SWAT hydrologic model parameter uncertainty and its implications for hydroclimatic projections in snowmelt-dependent watersheds. J. Hydrol. 519, 2081–2090. https://doi.org/10.1016/j.jhydrol.2014.09.082

Franz, K.J., Hogue, T.S., Sorooshian, S., 2008. Operational snow modeling: Addressing the challenges of an energy balance model for National Weather Service forecasts. J. Hydrol. 360, 48–66. https://doi.org/10.1016/j.jhydrol.2008.07.013

Fu, C., James, A.L., Yao, H., 2015. Investigations of uncertainty in SWAT hydrologic simulations: A case study of a Canadian Shield catchment. Hydrol. Process. 29, 4000–4017. https://doi.org/10.1002/hyp.10477

Fuka, D.R., Easton, Z.M., Brooks, E.S., Boll, J., Steenhuis, T.S., Walter, M.T., 2012. A Simple Process-Based Snowmelt Routine to Model Spatially Distributed Snow Depth and Snowmelt in the SWAT Model. J. Am. Water Resour. Assoc. 48, 1151–1161. https://doi.org/10.1111/j.1752-1688.2012.00680.x

Government of Canada, 2019. Historical Climate Data [WWW Document]. URL

http://climate.weather.gc.ca/historical_data/search_historic_data_e.html (accessed 8.6.19).

Gray, D.M., Landine, P.G., 1988. An energy-budget snowmelt model for the Canadian Prairies. Can. J. Earth Sci. 25, 1292–1303. https://doi.org/10.1139/e88-124

Guillaume, J.H.A., Jakeman, J.D., Marsili-Libelli, S., Asher, M., Brunner, P., Croke, B., Hill, M.C., Jakeman, A.J., Keesman, K.J., Razavi, S., Stigter, J.D., 2019. Introductory overview of identifiability analysis: A guide to evaluating whether you have the right type of data for your modeling purpose. Environ. Model. Softw. 119, 418–432. https://doi.org/10.1016/j.envsoft.2019.07.007

Haghnegahdar, A., Razavi, S., Yassin, F., Wheater, H., 2017. Multicriteria sensitivity analysis as a diagnostic tool for understanding model behaviour and characterizing model uncertainty. Hydrol. Process. 31, 4462–4476. https://doi.org/10.1002/hyp.11358

Harder, P., Helgason, W.D., Pomeroy, J.W., 2018. Modeling the Snowpack Energy Balance during Melt under Exposed Crop Stubble. J. Hydrometeorol. 19, 1191–1214. https://doi.org/10.1175/jhm-d-18-0039.1

Helbig, N., Van Herwijnen, A., Magnusson, J., Jonas, T., 2015. Fractional snow-covered area parameterization over complex topography. Hydrol. Earth Syst. Sci. 19, 1339–1351. https://doi.org/10.5194/hess-19-1339-2015

Hock, R., 2003. Temperature index melt modelling in mountain areas. J. Hydrol. 282, 104–115. https://doi.org/10.1016/S0022-1694(03)00257-9

Jamieson, B., Schirmer, M., 2016. Measuring snow surface temperature: why, why not, and how?

Jost, G., Weiler, M., Gluns, D.R., Alila, Y., 2007. The influence of forest and topography on snow accumulation and melt at the watershed-scale. J. Hydrol. 347, 101–115. https://doi.org/10.1016/j.jhydrol.2007.09.006

Kim, Y., Ohn, I., Lee, J.K., Kim, Y.O., 2019. Generalizing uncertainty decomposition theory in climate change impact assessments. J. Hydrol. X 3, 100024. https://doi.org/10.1016/j.hydroa.2019.100024

Krause, P., Boyle, D.P., Bäse, F., 2005. Comparison of different efficiency criteria for hydrological model assessment. Adv. Geosci. 5, 89–97. https://doi.org/10.5194/adgeo-5-89-2005

Li, H., Wang, Z., He, G., Man, W., 2017. Estimating snow depth and snow water equivalence using repeat-pass interferometric SAR in the northern piedmont region of the Tianshan Mountains. J. Sensors 2017. https://doi.org/10.1155/2017/8739598

Liu, W., Wang, L., Sun, F., Li, Z., Wang, H., Liu, J., Yang, T., Zhou, J., Qi, J., 2018. Snow Hydrology in the Upper Yellow River Basin Under Climate Change: A Land Surface Modeling Perspective. J. Geophys. Res. Atmos. 123, 12,676-12,691. https://doi.org/10.1029/2018JD028984

MacDonald, R.J., Byrne, J.M., Boon, S., Kienzle, S.W., 2012. Modelling the Potential Impacts of Climate Change on Snowpack in the North Saskatchewan River Watershed, Alberta. Water

Resour. Manag. 26, 3053–3076. https://doi.org/10.1007/s11269-012-0016-2

Mas, A., Baraer, M., Arsenault, R., Poulin, A., Préfontaine, J., 2018. Targeting high robustness in snowpack modeling for Nordic hydrological applications in limited data conditions. J. Hydrol. 564, 1008–1021. https://doi.org/10.1016/j.jhydrol.2018.07.071

Massmann, C., 2019. Modelling snowmelt in ungauged catchments. Water (Switzerland) 11. https://doi.org/10.3390/w11020301

Masud, M.B., Ferdous, J., Faramarzi, M., 2018. Projected changes in hydrological variables in the agricultural region of Alberta, Canada. Water (Switzerland) 10. https://doi.org/10.3390/w10121810

McKenney, D.W., Hutchinson, M.F., Papadopol, P., Lawrence, K., Pedlar, J., Campbell, K., Milewska, E., Hopkinson, R.F., Price, D., Owen, T., 2011. Customized Spatial Climate Models for North America. Bull. Am. Meteorol. Soc. 92, 1611–1622. https://doi.org/10.1175/2011BAMS3132.1

Meloysund, V., Leira, B., Hoiseth, K. V., Liso, K.R., 2007. Review: Predicting snow density using meteorological data. Meteorol. Appl. 14, 413–423. https://doi.org/10.1002/met

Meng, T., Carewa, R., Florkowski, W.J., Klepacka, A.M., 2017. Analyzing temperature and precipitation influences on yield distributions of canola and spring wheat in Saskatchewan. J. Appl. Meteorol. Climatol. 56, 897–913. https://doi.org/10.1175/JAMC-D-16-0258.1

Mizukami, N., Clark, M.P., Slater, A.G., Brekke, L.D., Elsner, M.M., Arnold, J.R., Gangopadhyay, S., 2014. Hydrologic implications of different large-scale meteorological model forcing datasets in mountainous regions. J. Hydrometeorol. 15, 474–488. https://doi.org/10.1175/JHM-D-13-036.1

Negi, H.S., Thakur, N.K., Mishra, V.D., 2007. Estimation and validation of snow surface temperature using modis data for snow-avalanche studies in NW-Himalaya. J. Indian Soc. Remote Sens. 35, 287. https://doi.org/10.1007/BF02990785

Neitsch, S., Arnold, J., Kiniry, J., Williams, J., 2011. Soil & Water Assessment Tool Theoretical Documentation Version 2009. Texas Water Resour. Inst. 1–647. https://doi.org/10.1016/j.scitotenv.2015.11.063

North Saskatchewan Watershed Alliance, 2005. The State of the North Sask River Watershed Report.

Pomeroy, J.W., Gray, D.M., Shook, K.R., Toth, B., Essery, R.L.H., Pietroniro, A., Hedstrom, N., 1998. An evaluation of snow accumulation and ablation processes for land surface modelling. Hydrol. Process. 12, 2339–2367. https://doi.org/10.1002/(SICI)1099-1085(199812)12:15<2339::AID-HYP800>3.0.CO;2-L

Poulin, A., Brissette, F., Leconte, R., Arsenault, R., Malo, J.S., 2011. Uncertainty of hydrological modelling in climate change impact studies in a Canadian, snow-dominated river basin. J. Hydrol. 409, 626–636. https://doi.org/10.1016/j.jhydrol.2011.08.057

Pradhanang, S.M., Anandhi, A., Mukundan, R., Zion, M.S., Pierson, D.C., Schneiderman, E.M., Matonse, A., Frei, A., 2011. Application of SWAT model to assess snowpack development and streamflow in the Cannonsville watershed, New York, USA. Hydrol. Process. 25, 3268–3277. https://doi.org/10.1002/hyp.8171

Prudhomme, C., Davies, H., 2009. Assessing uncertainties in climate change impact analyses on the river flow regimes in the UK. Part 2: Future climate. Clim. Change 93, 197–222. https://doi.org/10.1007/s10584-008-9461-6

Qi, J., Li, S., Jamieson, R., Hebb, D., Xing, Z., Meng, F.R., 2017. Modifying SWAT with an energy balance module to simulate snowmelt for maritime regions. Environ. Model. Softw. 93, 146–160. https://doi.org/10.1016/j.envsoft.2017.03.007

Quilbé, R., Rousseau, A.N., Moquet, J.S., Trinh, N.B., Dibike, Y., Gachon, P., Chaumont, D., 2008. Assessing the effect of climate change on river flow using general circulation models and hydrological modelling - Application to the chaudière River, Québec, Canada. Can. Water Resour. J. 33, 73–94.

Rahman, K., Maringanti, C., Beniston, M., Widmer, F., Abbaspour, K., Lehmann, A., 2013. Streamflow Modeling in a Highly Managed Mountainous Glacier Watershed Using SWAT: The Upper Rhone River Watershed Case in Switzerland. Water Resour. Manag. 27, 323–339. https://doi.org/10.1007/s11269-012-0188-9

Raleigh, M.S., Clark, M.P., 2014. Are temperature-index models appropriate for assessing climate change impacts on snowmelt? Proc. 82nd West. Snow Conf. 45–51.

Raleigh, M.S., Livneh, B., Lapo, K., Lundquist, J.D., 2016. How does availability of meteorological forcing data impact physically based snowpack simulations? J. Hydrometeorol. 17, 99–120. https://doi.org/10.1175/JHM-D-14-0235.1

Razavi, S., Gupta, H. V., 2019. A multi-method Generalized Global Sensitivity Matrix approach to accounting for the dynamical nature of earth and environmental systems models. Environ. Model. Softw. 114, 1–11. https://doi.org/10.1016/j.envsoft.2018.12.002

Razavi, S., Tolson, B.A., Matott, L.S., Thomson, N.R., MacLean, A., Seglenieks, F.R., 2010. Reducing the computational cost of automatic calibration through model preemption. Water Resour. Res. 46, 1–17. https://doi.org/10.1029/2009WR008957

Renard, B., Kavetski, D., Kuczera, G., Thyer, M., Franks, S.W., 2010. Understanding predictive uncertainty in hydrologic modeling: The challenge of identifying input and structural errors. Water Resour. Res. 46, 1–22. https://doi.org/10.1029/2009WR008328

Seiller, G., Anctil, F., 2014. Climate change impacts on the hydrologic regime of a Canadian river: Comparing uncertainties arising from climate natural variability and lumped hydrological model structures. Hydrol. Earth Syst. Sci. 18, 2033–2047. https://doi.org/10.5194/hess-18-2033-2014

Shrestha, R.R., Dibike, Y.B., Prowse, T.D., 2012. Modelling of climate-induced hydrologic changes in the Lake Winnipeg watershed. J. Great Lakes Res. 38, 83–94.

https://doi.org/10.1016/j.jglr.2011.02.004

Singh, K.K., Mishra, V.D., Singh, D.K., Ganju, A., 2013. Estimation of snow surface temperature for NW Himalayan regions using passive microwave satellite data. Indian J. Radio Sp. Phys. 42, 27–33.

Singh, V.P., Frevert, D.K., 2002. Mathematical Models of Large Watershed Hydrology. Water Resources Publications.

Sturm, M., Taras, B., Liston, G.E., Derksen, C., Jonas, T., Lea, J., 2010. Estimating snow water equivalent using snow depth data and climate classes. J. Hydrometeorol. 11, 1380–1394. https://doi.org/10.1175/2010JHM1202.1

Sun, N., Yan, H., Wigmosta, M.S., Leung, L.R., Skaggs, R., Hou, Z., 2019. Regional Snow Parameters Estimation for Large-Domain Hydrological Applications in the Western United States. J. Geophys. Res. Atmos. 124, 5296–5313. https://doi.org/10.1029/2018JD030140

Taylor, K.E., Stouffer, R.J., Meehl, G.A., 2012. An overview of CMIP5 and the experiment design. Bull. Am. Meteorol. Soc. 93, 485–498. https://doi.org/10.1175/BAMS-D-11-00094.1

Tobin, C., Schaefli, B., Nicótina, L., Simoni, S., Barrenetxea, G., Smith, R., Parlange, M., Rinaldo, A., 2013. Improving the degree-day method for sub-daily melt simulations with physically-based diurnal variations. Adv. Water Resour. 55, 149–164. https://doi.org/10.1016/j.advwatres.2012.08.008

Todd Walter, M., Brooks, E.S., McCool, D.K., King, L.G., Molnau, M., Boll, J., 2005. Process-based snowmelt modeling: Does it require more input data than temperature-index modeling? J. Hydrol. 300, 65–75. https://doi.org/10.1016/j.jhydrol.2004.05.002

Troin, M., Arsenault, R., Brissette, F., 2015. Performance and Uncertainty Evaluation of Snow Models on Snowmelt Flow Simulations over a Nordic Catchment (Mistassibi, Canada). Hydrology 2, 289–317. https://doi.org/10.3390/hydrology2040289

Troin, M., Poulin, A., Baraer, M., Brissette, F., 2016. Comparing snow models under current and future climates: Uncertainties and implications for hydrological impact studies. J. Hydrol. 540, 588–602. https://doi.org/10.1016/j.jhydrol.2016.06.055

Ul Islam, S., Déry, S.J., 2017. Evaluating uncertainties in modelling the snow hydrology of the Fraser River Basin, British Columbia, Canada. Hydrol. Earth Syst. Sci. 21, 1827–1847. https://doi.org/10.5194/hess-21-1827-2017

USACE, 1998. Runoff From Snowmelt. Eng. Des. 142.

van Vuuren, D.P., Edmonds, J., Kainuma, M., Riahi, K., Thomson, A., Hibbard, K., Hurtt, G.C., Kram, T., Krey, V., Lamarque, J.F., Masui, T., Meinshausen, M., Nakicenovic, N., Smith, S.J., Rose, S.K., 2011. The representative concentration pathways: An overview. Clim. Change 109, 5–31. https://doi.org/10.1007/s10584-011-0148-z

Verdhen, A., Chahar, B.R., Sharma, O.P., 2014. Springtime snowmelt and streamflow predictions in the Himalayan Mountains. J. Hydrol. Eng. 19, 1452–1461.

https://doi.org/10.1061/(ASCE)HE.1943-5584.0000816

Vetter, T., Huang, S., Aich, V., Yang, T., Wang, X., Krysanova, V., Hattermann, F., 2015. Multi-model climate impact assessment and intercomparison for three large-scale river basins on three continents. Earth Syst. Dyn. 6, 17–43. https://doi.org/10.5194/esd-6-17-2015

Vetter, T., Reinhardt, J., Flörke, M., van Griensven, A., Hattermann, F., Huang, S., Koch, H., Pechlivanidis, I.G., Plötner, S., Seidou, O., Su, B., Vervoort, R.W., Krysanova, V., 2017. Evaluation of sources of uncertainty in projected hydrological changes under climate change in 12 large-scale river basins. Clim. Change 141, 419–433. https://doi.org/10.1007/s10584-016-1794-y

Wang, B., Liu, D.L., Waters, C., Yu, Q., 2018. Quantifying sources of uncertainty in projected wheat yield changes under climate change in eastern Australia. Clim. Change 151, 259–273. https://doi.org/10.1007/s10584-018-2306-z

Wilby, R.L., Harris, I., 2006. A framework for assessing uncertainties in climate change impacts: Low-flow scenarios for the River Thames, UK. Water Resour. Res. 42, 1–10. https://doi.org/10.1029/2005WR004065

Wu, Q., Liu, S., Cai, Y., Li, X., Jiang, Y., 2017. Improvement of hydrological model calibration by selecting multiple parameter ranges. Hydrol. Earth Syst. Sci. 21, 393–407. https://doi.org/10.5194/hess-21-393-2017

Yip, S., Ferro, C.A.T., Stephenson, D.B., Hawkins, E., 2011. A Simple, Coherent Framework for Partitioning Uncertainty in Climate Predictions. J. Clim. 4634–4643. https://doi.org/10.1175/2011JCLI4085.1

Young, K.L., Assini, J., Abnizova, A., Miller, E.A., 2013. Snowcover and melt characteristics of upland/lowland terrain: Polar bear pass, bathurst island, nunavut, Canada. Hydrol. Res. 44, 2–20. https://doi.org/10.2166/nh.2012.083

Zeinivand, H., de Smedt, F., 2010. Prediction of snowmelt floods with a distributed hydrological model using a physical snow mass and energy balance approach. Nat. Hazards 54, 451–468. https://doi.org/10.1007/s11069-009-9478-9

Zeinivand, H., Smedt, F., 2009. Hydrological modeling of snow accumulation and melting on river basin scale. Water Resour. Manag. 23, 2271–2287. https://doi.org/10.1007/s11269-008-9381-2

Zhang, X., Srinivasan, R., Debele, B., Hao, F., 2008. Runoff simulation of the headwaters of the yellow river using the SWAT model with three snowmelt algorithms. J. Am. Water Resour. Assoc. 44, 48–61. https://doi.org/10.1111/j.1752-1688.2007.00137.x

CHAPTER III – MANUSCRIPT 2

Assessment of snowmelt and groundwater-surface water dynamics in mountainous, foothills, and plain regions in northern latitudes

Majid Zaremehrjardy[1], Justin Victor[1], Daniel Alessi[1], Brian Smerdon[2], Seonggyu Park[3], Monireh Faramarzi[1,*]

[1] Department of Earth and Atmospheric Sciences, University of Alberta, Edmonton, AB T6G 2R3, Canada.
[2] Alberta Geological Survey, Alberta Energy Regulator, Edmonton, AB, T6B 2X3, Canada.
[3] Department of Civil and Environmental Engineering, Colorado State University, 1372 Campus Delivery, A207G Engineering Bldg., Fort Collins, CO 80523-1372, USA.

[*]Corresponding author: faramarz@ualberta.ca

Manuscript to be submitted to journal

3.1 Abstract

Snowmelt and groundwater-surface water (GW-SW) dynamics are of the most dominant controllers of hydrological processes and water availability in northern latitudes, particularly in warm seasons. The dynamics and changes of snowmelt and GW-SW interactions and their relations is poorly understood in regional analysis. To fill this gap, this study implements process-based hydrological modelling of SWAT-MODFLOW to map snowmelt and GW-SW dynamics in regional scales. The major research questions are "what is the effect of climate change on snowmelt and GW-SW dynamics?" and "how are GW-SW interactions altered by snowmelt dynamics?" We coupled the surface water hydrological model of Soil and Water Assessment Tool (SWAT) with groundwater model of MODFLOW in order to analyze snowmelt and groundwater dynamics across scales that included: (1) historical periods, (2) their projections using an ensemble of five global climate models (GCMs) based on two emission scenarios (i.e., RCP2.6 and RCP8.5), and (3) their spatio-temporal relations. These analyses are

implemented in mountainous, foothill and plain regions in a large snow-dominated watershed in western Canada. Results show that under climate change scenarios, earlier snowmelt is predicted to occur in mountainous and foothill regions, while less snow accumulation and melt is anticipated in plain regions. Future projections of GW-SW interactions show an increase of groundwater discharge to streams in winter and spring seasons, particularly as a result of earlier snowmelt in winter and spring. On the other hand more surface water loss to groundwater in summer and fall is predicted, which can be caused by low level of groundwater under future conditions. In the end, the correlation analysis between regional snowmelt and GW-SW interactions for historical (1983-2007) simulations show high correlation (R^2 =0.494) in mountainous regions, compared to very low correlation ($R^2 < 0.01$) in foothill and plain regions. The low correlation in downstream regions can be attributed to (1) the effect of evapotranspiration (ET) on altering groundwater and sub-surface water resources in foothill and plain regions; (2) the dominance of rainfall in groundwater recharge, especially in growing seasons; (3) GW flow connectivity and flow gradient that may create upstream-downstream cumulative effects under the ground and influence GW dynamics in the plain regions than in mountains. It is hypothesized that aquifers in the mountainous region of the study watershed are less influenced from their adjacent aquifers but only from surface water recharge, resulting in a higher correlation with snowmelt dynamics than plain regions. Overall, it is shown that the hydro-climatic variability and topographic conditions of different regions play an important part in the governing factors of snowmelt and GW-SW dynamics.

3.2 Introduction

Water is of the utmost importance, both as a basic need for consumption and as the commodity input for agriculture and industry (Kundzewicz and Döll, 2009; Harma et al., 2012). The spatial and temporal availability of water throughout the world is heavily dependent on the hydrological cycles at a global scale (Harding et al., 2011). In cold regions, particularly the Canadian Prairies, snowmelt is the main source of streamflow during spring and early summer, and its recharge is the main source of base flow during low flow seasons (Dumanski et al., 2015). All of these processes control the availability of water resource in dynamic (e.g., surface run-off) and static (e.g., groundwater storage) environments (Flerchinger et al., 1992). Furthermore, the susceptibility of water to climate change is expressed in the relations between human effects and natural climate variability, which is not sustainable at current rates of industrial activity and environmental conservation (Vogel et al., 2019). It is therefore critical to consider climate change as a variable in hydrological research due to the impact it has on snowmelt, groundwater, and their combined effect on streamflow and other sources of water availability (F. Cochand et al., 2019).

To address future concerns of climate change and its impacts on the spatio-temporal variations of water resources, various hydrologic modelling approaches must be employed to establish the most accurate and encompassing tactics for proper watershed planning and management (Hagemann et al., 2013; Guevara Ochoa et al., 2020). Usage of such models becomes particularly important for systems where groundwater and surface water are used conjunctively to satisfy multiple social sectors (Aliyari et al., 2019). Variations in the water content of watershed basins are controlled by multiple processes, but the movement of groundwater and surface water (including their interactions) in relation to snowmelt dynamics

play a significant role in dictating future trends of water availability and distribution (Maurya et al., 2018), especially in northern latitudes (Aygün et al., 2020). Although some literature has focused on snowmelt and groundwater-surface water interactions, with majority of them at field scale in different basins, some aspects of these processes require more attention, including (1) an analysis of snowmelt dynamics and groundwater-surface water (GW-SW) interactions under changing climate at a regional scale, a scale of which often neglected in GW-SW modelling but crucial for policy and planning; (2) the spatio-temporal relations of the dynamics of these two processes; and (3) assessment of the effects of natural factors such as climate, topography, and land-use, as well as geospatial features related to prehistoric and contemporary times on the dynamics of these processes.

The widespread impacts of climate change have become heavily publicized and attributed to numerous weather phenomena around the world. These phenomena include heat waves, floods, droughts, glacier ablation, more severe and frequent storms, and inundation of coastal societies (Qi et al., 2019; Vogel et al., 2019). In cold regions and northern latitudes, the role of snowmelt in controlling the storage and flow of water within hydrological systems and by extension, access to water for human use and consumption, is extremely valuable (Hayashi and Farrow, 2014; Lundberg et al., 2016). Streamflow in the summertime is particularly vulnerable to changes in snowmelt pattern, which was found to have an even greater effect on these flows when compared to precipitation and groundwater recharge (Huntington and Niswonger, 2012). Snowmelt also has the ability to initiate interactions between streamflow and groundwater, as any deficits in the soil water profile or groundwater system prohibits these exchanges from taking place, unless they are restored by sources such as spring snowmelt or winter precipitation (Chauvin et al., 2011). Several field-scale studies elaborated on snowmelt dynamics and its

variations under climate change (Clilverd et al., 2011; Hayashi and Farrow, 2014). However, the regional analysis of snowmelt cannot be done at field-scales resolution because it is costly, complex, and time-consuming (Bocchiola and Groppelli, 2010; Avanzi et al., 2015). On the other hand, inference from field analysis to a large regional-scale assessment is subjective, since response of hydrogeological processes across spatio-temporal scales are highly variable. Therefore, hydrological modelling is used as an alternative for evaluating snowmelt dynamics in current and future climates. Hydrological modelling is particularly of interest because future climate models and greenhouse emission scenarios can be used as forcing to such models in order to assess the effect of climate change on hydrological processes and their interactions (Haddeland et al., 2014). Several hydrological models such as Snowmelt-Runoff Model (SRM, Kult et al., 2012; Saydi et al., 2019), Cold Region Hydrological Model (CRHM, Zhou et al., 2014) and Soil and Water Assessment Tool (SWAT, Debele et al., 2010; Qi et al., 2017) were used for snowmelt analysis in the literature. However, the main focus of these models were mostly to study detailed hydrological processes at small areas of study (Chauvin et al., 2011; Gao et al., 2019), or key processes in large watershed but homogeneous in terms of climate, land-use, and topographic variability (Finger et al., 2012; Kure et al., 2013; Lucas-Picher et al., 2015). In more complex regions in terms of topography, land-use, and climate, such as the eastern slopes of the Canadian Rocky Mountains, snowpack is a critical source of water for multiple prairie provinces and warmer air temperatures produced by climate change can create a shift from snow to rain, reducing water storage in snowpack and compromising its reliability and predictability as a resource that must be used and managed diligently (Schindler and Donahue, 2006; MacDonald et al., 2012). Municipal development and drinking waters could be vulnerable to variations in snowmelt patterns, where they heavily rely on groundwater and reduced

snowmelt can urge groundwater shortage. Agriculture can be particularly susceptible to variations in snowmelt patterns where irrigation is heavily relied upon. The association of climate change with reduced snowmelt runoff and a shift in its peak of occurrence to earlier in the season has the potential to induce later water shortages (Bai et al., 2019). Therefore, it is important to evaluate the regional response of snowmelt to climate change, particularly in various topographical and climate settings.

On the other hand, there are abundant, intimate relations between surface water and groundwater in hydrological systems, requiring an assessment of both components as a collective in order to establish effective and encompassing strategies for optimal water utilization and management (Field et al., 2014; Qi et al., 2019; Lewandowski et al., 2020). The simplest and most direct relations between groundwater and surface water involves recharge and discharge, which typically consists of exchanging large volumes of water (Kornelsen and Coulibaly, 2014). This can occur on local or much greater scales, with variables such as season, climate, and vegetation creating sets of expected or average values for water exchange. This is exemplified in mountainous environments, where the properties of soils and subsurface media control the discharge of groundwater to streams that are in transit from a high elevation catchment to a low elevation valley bottom, or in other words, where there is a change in topography (Allen et al., 2010; Jutebring Sterte et al., 2018). These interactions become substantially more significant in the winter, where contributions to streamflow from glacier melt, rainfall, and snowmelt are minimal at best, and unregulated streams are ultimately maintained by groundwater discharge, which is controlled by stationary aspects such as the spatial variation of geology, topography, and climate (Paznekas and Hayashi, 2016). The importance of subsurface geology is applicable to other environments such as wetlands, where variations in the thickness of units below the

surface can produce changes in groundwater flow, leading to contrasting seasonal trends in water table fluctuation and surface hydrology (Devito et al., 1996). It is also critical to acknowledge that the likelihood of changes in the relations between groundwater and surface water is significantly higher when moving from a local to regional scale analysis, as there are more abundant aquifers and surface bodies and thus interactions, which vary temporally and spatially (Barthel and Banzhaf, 2016). When considering these relations, it is important to not only view them as dynamic within a span of weeks or months, but as sensitive interactions that can be variable on seasonal and decadal time scales, such as in response to snowmelt and precipitation patterns (Hayashi and Farrow, 2014; Bailey et al., 2016). In spite of all the past and present research utilizing various programs for hydrological modelling, the regionalized analysis of GW-SW interactions demand improvements (Zhou and Li, 2011; Candela et al., 2014). The literature produced from the study of the impacts these variables have on partitioning of resources in hydrologic systems is significant and diverse (Akiyama Sakai et al., 2007; Lewandowski et al., 2020), but is underrepresented for regional scale landscapes, where physical properties can vary dramatically from a spatio-temporal perspective (Barthel and Banzhaf, 2016). Therefore, understanding the regional dynamics of GW-SW interactions is vital, particularly because such dynamics can be interpreted in terms of distinct climatic and topographic properties of different regions, in addition to their hydrological processes and their interactions.

In climates cold enough to produce snowfall and sustain snowpack seasonally or permanently, snowmelt input to groundwater and surface water has the potential to be a significant contributor to hydrological processes (Schilling et al., 2019). The distribution and availability of groundwater and surface water in these environments are limited by some of the same constraints as those placed on snowmelt, such as its timing and spatial distribution, the

structure of the basin, and the properties of the aquifers (Deng et al., 1994; Foster and Allen, 2015; Zhang et al., 2018). The areal extent of snow cover directly impacts groundwater levels and the timing of subsurface water flow (Flerchinger et al., 1992). On the other hand, the climate change effects on snow accumulation and snowmelt can raise concerns around water availability in different regions, because warmer air temperatures can promote the conversion of snowfall to rainfall (MacDonald et al., 2012), which will ultimately have widespread impacts on surface and subsurface water dynamics. The complex relations between snowmelt and GW-SW interactions depend on numerous properties that are present in the water and the surrounding environment. This implies the necessity to accommodate conditions such as elevation, climate, topography, and vegetation cover in the analysis of the relations between these processes, as they will undoubtedly impact the ability and extent of processes to facilitate the relations between water sources in various settings (Smith et al., 2014; Carroll et al., 2018). The high susceptibility of water resource partitioning is exhibited effectively in mountainous environments, where the transition from high elevations to foothills and plain areas provides valuable opportunities for studying how variations in the characteristics of each of these settings controls water dynamics. At lower elevations, where vegetation density is high, the lower snowfall accumulation translates to less snowmelt and occurs prior to peak consumption demand, producing small amounts of groundwater recharge. Nevertheless, snowmelt rapidly drops off as the growing season begins and the water availability ultimately depends on the land features produced by topography (Carroll et al., 2019). Overall, the relation and feedback between snowmelt and GW-SW interactions and the variables facilitating them are extensively documented (Assani et al., 2012). However, to the best of our knowledge, the direct effect of snowmelt on GW-SW interactions and their inter-relations in different regional settings is not evaluated. The analysis of

correlations between snowmelt and GW-SW interactions can provide good insights into the factors governing these processes and how these relations might vary under variable topography, land-cover, and climate conditions.

The goal of this study is to provide a framework for regional analysis of snowmelt and GW-SW interactions, as well as their changes under future climate conditions. We also focused on improving the understanding of correlations between snowmelt and GW-SW interactions and how they are inter-connected in different regions of study. Finally, the effect of climate conditions, topography, and land-use on such changes and interactions are examined. To this end, we coupled the surface hydrological model of the Soil and Water Assessment Tool (SWAT) with groundwater model of MODFLOW to evaluate the dynamics of snowmelt and GW-SW interactions at a regional-scale. These analysis are performed in mountainous, foothill and plain regions of a large and complex watershed in central Alberta. The more specific objectives of this paper include: (1) the regional assessment of the impacts of climate change on the seasonal and decadal changes of snowmelt patterns; (2) analysis of response of seasonal and decadal changes in GW-SW interactions to future climate; (3) assessment of how spatio-temporal variation of groundwater-surface water is associated with snowmelt patterns; and (4) comparison of snowmelt and GW-SW interactions in different hydroclimate regions such as mountainous, foothill and plain regions in regional hydrological models.

3.3 Material and methods

3.3.1 Study Area

North Saskatchewan River Basin (NSRB) has been chosen for the study area as an example of a large region with high variability of climate and land use/land cover (Figure 3.1).

NSRB is a relatively large basin with an approximate drainage area of 60,000 km^2, which comprises more than 9% of landmass area in the province of Alberta (North Saskatchewan Watershed Alliance, 2005). The elevation of NSRB ranges from 3478 MASL on the west side to just 500 MASL on the Alberta/Saskatchewan border, with its extent ranging from 52-55 °N and 110-120 °W. The average annual precipitation within NSRB for 1983-2007 ranges from 400 mm $year^{-1}$ on the east side to 760 mm $year^{-1}$ on the mountainous region of NSRB on the west. Also, the historical temperature data for NSRB suggests that the temperature can range from -30 ℃ in winters up to +29 ℃ in summer, with high spatial and temporal variability of the temperature (Government of Canada, 2019).

The North Saskatchewan River (NSR) originates from headwaters in highlands of the Rocky Mountains, where Columbia Icefields in Banff National Park are the major contributing glaciers to this river. The river flows more than a thousand kilometers before reaching the Alberta/Saskatchewan border. The NSR later joins the South Saskatchewan River, which will ultimately drain into Hudson Bay (North Saskatchewan Watershed Alliance, 2005). The NSR is a major tributary to the Saskatchewan River, as the annual discharge of NSR at Alberta-Saskatchewan border is more than 7 cubic kilometers (Alberta Environment 2019). This river is regulated by two headwater dams, namely Bighorn dam on the main stem of NSR, and Brazeau dam on Brazeau River, to provide water supply for the City of Edmonton. These factors along with the existence of glaciers, forests, mountain snowpacks, and wetlands (North Saskatchewan Watershed Alliance, 2005) have resulted in a relatively complex area in terms of hydrological process, GW-SW interactions, and climate variability.

An analysis of historical pattern of river flow at HYDAT Station 05df001 at the City of Edmonton (see Figure 3.1) shows an overall decrease of streamflow on the main river channel

from 1911 to 2013 (North Saskatchewan Watershed Alliance, 2005). Also, trend analysis of observed data from four selected climate stations within NSRB, namely Nordegg (1915 to 2007), Rocky Mountain House (1978 to 2007), Vermilion (1913 to 2007) and the City of Edmonton (1880 to 2007) show an increasing pattern for temperature. Climate change studies on the NSRB suggest an increase of temperature between 0.3 ℃ to 2.2 ℃ for different areas of the basin by 2035. Therefore, there is a need for watershed planners to understand the climate projections and their uncertainty within NSRB in order to adapt their plans for surface water and groundwater management and the most effective mitigation strategies (Golder Associates, 2008).

3.3.2 Hydrological Model and Input Data

3.3.2.1 SWAT model

The Soil and Water Assessment Tool (SWAT) is a process-based, semi-distributed hydrological modelling with the ability of simulating the quality and quantity of surface water in daily time steps (Arnold et al. 1998, 2012). SWAT is capable of being applied for studying climate change impact assessment and effects of land management practices on dynamics of surface water quality and quantity over large and complex watersheds. Numerous hydrological processes can be simulated by SWAT, including but not limited to streamflow, snowmelt, subsurface flow, evapotranspiration, and soil moisture dynamics (Neitsch et al., 2011).

SWAT model formation demands input climate data of precipitation, temperature, humidity, wind speed and solar radiation. The delineation of sub-basins and Hydrological Response Units (HRUs) can be done through application of GIS maps for Digital Elevation Models (DEMs), land-use and land cover, soil, and their physical properties. HRUs are delineated within subbasins, and they are the smallest spatial units for process simulations in the model that are characterized with homogeneous soil, landuse, and slope parameters. Table A.1

shows the name, extent and sources of different datasets for building the SWAT model in this study. In this study, the 90m × 90m DEM was used to set up the SWAT model for the NSRB. A total of 174 sub-basins were delineated using a pre-defined river network which was previously delineated using 10m × 10m DEM (Table A.1). Historical climate data including precipitation, temperature, wind speed, solar radiation and relative humidity is derived from Faramarzi et al. (2015), who used various climate datasets from meterological stations and gridded product to reproduce historical streamflow throughout the province of Alberta.

We used Sequential Uncertainty Fitting (SUFI-2) algorithm (Abbaspour, 2015) to calibrate and validate the NSRB SWAT model for the periods of 1993-2007 and 1983-1995, respectively, with a warm-up period of three years for each time window. The choice of parameters and their ranges for model calibration and validation were obtained from Faramarzi et al. (2017). In model calibration, each iteration contained 1000 samples of parameter sets from their physically meanful ranges to be fed into SWAT model, resulting in 1000 SWAT simulations. For each simulation the monthly observed and simulated streamflow were compared in six important hydrometric stations within NSRB. Also, several iterations (each containing 1000 simulations) were needed for acquiring appropriate ranges of SWAT parameters. For time effective calculation, this process were parallelized over 200 cores using a parallelization algorithm developed by Du et al. (2020). The locations and properties of those hydrometric stations are shown in Figure 3.1a and Table A.2, respectively. In order to evaluate the goodness-of-fit of SWAT model, we considered three widely-used criteria of efficiency, i.e., coefficient of determination (R^2), bR^2, and Nash-Sutcliffe (NS). Detailed formulation and description of these criteria can be found in Table A.5.

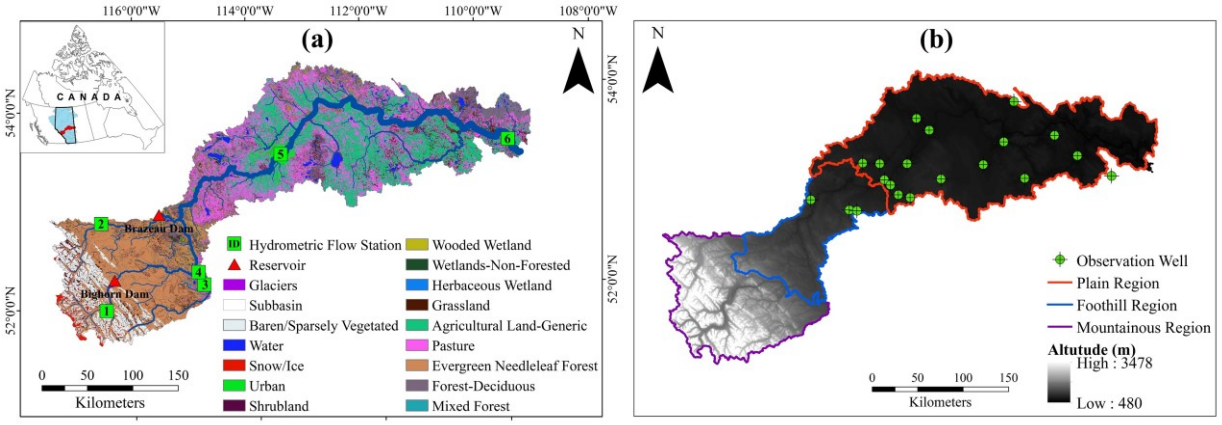

Figure 3.1. Map for NSRB representing (a) land-use classification, main river network, two main dams, and six hydrometric stations for SWAT calibration, (b) topographic range, three hydrologic regions for analysis of modelling results, and locations of observation wells for MODFLOW calibration.

In addition to the performance criteria related to optimal SWAT parameter sets among 1000 simulations in each iteration, we used two statistical factors from SUFI-2 algorithm, namely p-factor and r-factor, to evaluate the uncertainty associated with model parameters, structure and observed data. The p-factor ranges from 0 to 1 and determines the percentage of the measured data bracketed within the uncertainty band generated by SWAT. The uncertainty band in SUFI-2 is calculated as the 95 percent of the cumulative distribution of the simulated variables, defined as 95 Percent Prediction Uncertainty (95PPU) hereafter. On the other hand, r-factor (ranging from 0 to ∞) represent the width of the predicted uncertainty band. When calibrating a model using SUFI-2 approach, the ideal outcome can be a p-factor of 1, indicating that 100% of the measured data are reproduced using simulations; and r-factor of zero, indicating a minimum uncertainty prediction or a perfect simulation. However, due to uncertainty related to input and measured data, model structure, and parameters within hydrological modelling, a p-factor value of more than 0.5 and r-factor of close to 1 might be a sign of proper model calibration, depending on the research objectives, modeller's view point and their expertise in interpretation of results, as well as status of input data availability (Faramarzi et al., 2009).

3.3.2.2 MODFLOW model

The MODFLOW model for NSRB was developed using Visual MODFLOW Flex 6.0. The Newton formulation of MODFLOW-2005 (namely, MODFLOW-NWT) has been used to effectively take into account the nonlinearities involved with groundwater flow equations of MODFLOW cells during drying and rewetting phases (Bailey et al., 2016). The MODFLOW model developed for NSRB covers 181,500 sq.km of area. The area of the MODFLOW project is larger than SWAT project area in order for the MODFLOW grids to cover the whole SWAT area of study (i.e. NSRB area, Figure 3.1). A total of 55 × 33 grid cells were defined in the MODFLOW model to cover study area, with the dimensions of each grid to be 10 km × 10 km. Although a coarse resolution was chosen for MODFLOW setup, the structure of MODFLOW and SWAT-MODFLOW for the NSRB remained relatively complex because of a high variability in formations and elevations of MODFLOW layers in different regions of NSRB. Each of the MODFLOW layers is corresponded to a geological unit. In this study, five geological formations are included in MODFLOW setup for NSRB. The data for the extent and elevation of geological formations, as well as the hydraulic properties of each formation, has been acquired from Alberta Geological Survey (Smerdon et al. 2017; Alberta Geological Survey 2019). The possible ranges of horizontal hydraulic conductivity (K_H) values for each geological formation has been provided based on the maximum and minimum K_H values measured from various boreholes throughout the west-central part of Alberta province (Smerdon et al. 2017). Table 3.1 shows the names and property value ranges of each geological formation considered for this study. After assigning five geological formations to MODFLOW model, a constant value of 500 meters below ground surface was assigned to the bottom of MODFLOW model in order to keep the lower boundary of the model far away from surface water features. This allowed for

possible groundwater flows in areas where deeper geological formations might connect to the surface (Chunn et al., 2019). The elevation data for top and bottom of geological formations were not available for a part of mountainous region of the study area (i.e. western side of NSRB, close to Rocky Mountains). As a result, it was assumed that the elevation of geological formation at the west side of the NSRB are constant, with a value equal to the most western side of the study area with available elevation data. Finally, we used the information from DEM data of NSRB to fill the missing elevation data for top of the upmost layer (the layer that is closest to ground surface) in MODFLOW.

Besides the information related to geological formations for setting up the MODFLOW, initial heads, as well as boundary conditions such as rivers and recharge data need to be defined to the model for a more precise representation of hydraulic head fluctuations within NSRB. In addition, the basis of integrating MODFLOW with SWAT is required (see Section 3.3.2.3). In the MODFLOW model of NSRB, initial conditions are at first defined to be equal to ground surface for each MODFLOW cell. However, after running MODFLOW for one time, initial heads are updated based on MODFLOW.HDS output file in order to provide a better initial condition for SWAT-MODFLOW integration. On the other hand, River (RIV) and Recharge (RCH) boundary conditions have been imported from NSRB SWAT model into MODFLOW in order to facilitate the integration process of SWAT-MODFLOW model. The details of complete processes of importing RIV and RCH data from SWAT to MODFLOW can be found in Chunn et al. (2019).

Table 3.1. Geological formations used for setting up NSRB MODFLOW model.

Layer No.	Layer name	Elevation range of layer top (meter)	Horizontal hydraulic conductivity (K_h) range (m/s) (Smerdon et al., 2017)	K_h/K_v range (Chen et al., 2017; Tanachaichoksirikun et al., 2020)
1	Mountainous region/Displaced bedrock	500.21 – 3413.05	$1.48 \times 10^{-10} - 1.94 \times 10^{-7}$	1-100
2	Bedrock – Paskapoo	466.97 – 1390.48	$1.09 \times 10^{-10} - 5.49 \times 10^{-5}$	1-100
3	Bedrock – Scollard	366.78 – 963.13	$9.53 \times 10^{-10} - 3.55 \times 10^{-6}$	1-100
4	Bedrock – Battle	53.06 – 920.88	$7.73 \times 10^{-10} - 1.34 \times 10^{-7}$	1-100
5	Bedrock - Horseshoe	42.83 – 913.79	$4.34 \times 10^{-10} - 3.57 \times 10^{-6}$	1-100

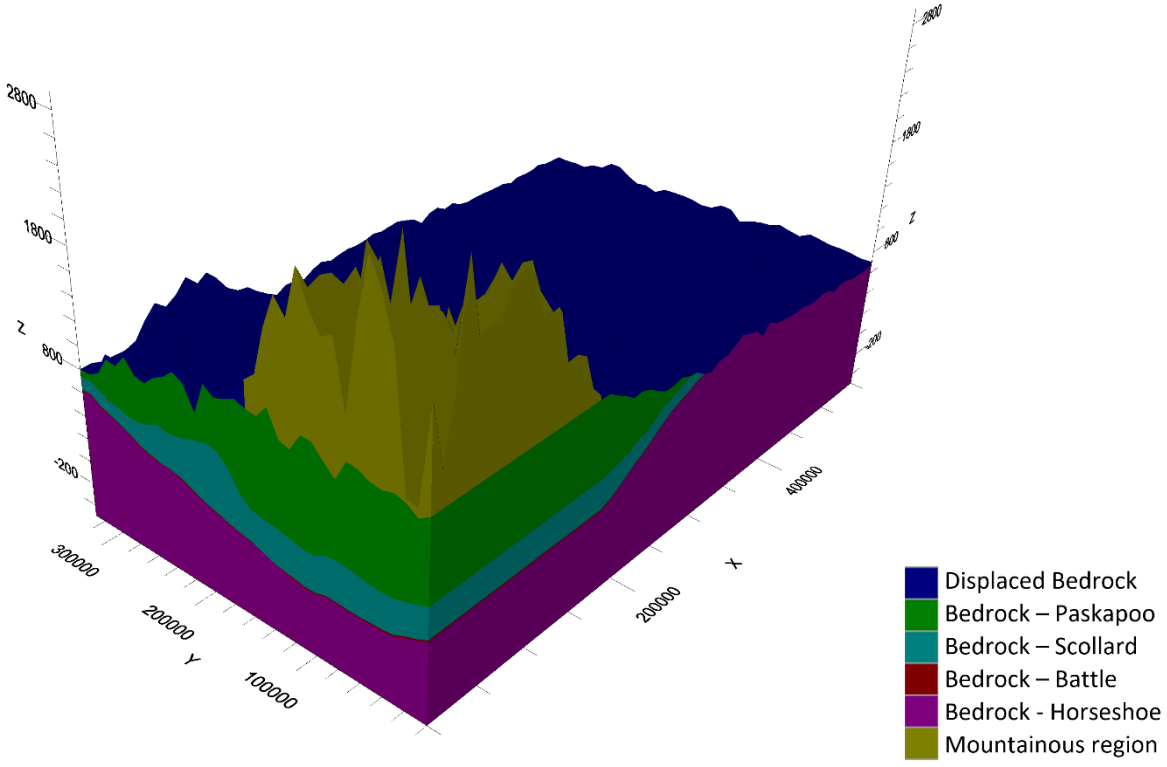

Figure 3.2. Geographic formations related to NSRB MODFLOW model. The mountainous region has been modeled with the same properties as the first geological formation i.e. displaced bedrock. X and Y axes shows easting and northing (in meters) of NSRB MODFLOW model, which is mapped on Cartesian coordinate system in MODFLOW. Z axis shows the elevation (MASL) in meters.

MODFLOW simulates hydraulic head in all the cells within a model, which is the sum of actual groundwater elevation and pressure head. Since observation wells collect the historical data for hydraulic head, they can be beneficial in calibration and validation of groundwater flow models. Therefore, historical data for 20 observation wells within NSRB geological system was collected for 1983-2007. In order to calibrate MODFLOW model, the horizontal (K_h) hydraulic conductivity and its ratio to vertical hydraulic conductivity (i.e., K_h/K_v) values was adjusted in each layer and the model was forced to reproduce hydraulic head throughout NSRB. Although specific storage and yield are also adjustable in MODFLOW for calibration, the hydraulic conductivity values in MODFLOW are the key variables for simulating hydraulic heads (Chunn et al., 2019). Also, to the best of our knowledge, no observed data related to storage of geological units were available for NSRB; hence, we used MODFLOW default values of 10^{-5} m^{-1} for specific storage and 0.2 for specific yield for all geological units. Furthermore, the initial ranges of K_h values were derived from borehole studies (Smerdon et al., 2017), which could facilitate model calibration in terms of assigning hydraulic properties to different layers. On the other hand, the initial range of K_h/K_v was derived from the suggested ranges in the literature (Chen et al., 2017; Tanachaichoksirikun et al., 2020, see Table 3.1). We used SUFI-2 approach to sample 1000 sets of MODFLOW parameters (i.e., five K_h and five K_h/K_v parameters related to five layers) to compare simulated and measured hydraulic heads acquired from 20 observation wells for 1983-2007 period. The locations of observation wells can be found in Figure 3.1. Three criteria of R^2, Mean Absolute Error (MAE) and Normalized Root Mean Squared Error (NRMSE) were used to compare month-by-month (i.e., first day of each month) simulations of MODFLOW to their corresponding observed data. The ideal values of R^2, MAE, and RMSE are 1, 0, and 0, respectively.

3.3.2.3 SWAT-MODFLOW

In this study, we used an integration of SWAT (as surface hydrology model) with MODFLOW (as groundwater model) in order to analyze the dynamics of GW-SW interactions throughout the NSRB. The linkage between SWAT and MODFLOW can be done though GIS applications, where the elevation and locations of each MODFLOW grid is corresponded to the same properties related to SWAT HRUs (Park & Bailey, 2017). Due to the differences between the resolution and boundaries of spatial units of SWAT and MODFLOW (i.e., HRU in SWAT and grid cells in MODFLOW), some geolocations need to be done before integrating SWAT and MODFLOW. For this purpose, the HRUs within SWAT model are disaggregated and geo-located to establish the connection between SWAT and MODFLOW cells. The Disaggregated HRUs (DHRUs) pass location and amount of groundwater recharge from ground surface within subbasins to their corresponding MODFLOW cells across the watershed, and return calculated hydraulic head values from MODFLOW to SWAT at the stream locations, so that the GW-SW interaction can be made throughout this process on a daily basis. Furthermore, location of stream network of SWAT is needed to be projected on MODFLOW cells in order to geographically specify the location of GW-SW interactions and river formations (Guzman et al., 2015; Bailey et al., 2016). Hence, some data conversions and modifications are needed in GIS environment to connect SWAT DHRUs to MODFLOW grid cells. The details of creating linking files and setting up SWAT-MODFLOW model are available in Park & Bailey (2017).

3.3.3 Future climate projection data

In order to project climate change impact on the hydrological system of NSRB, climate projections of five climate models acquired from the Pacific Climate Impacts Consortium (PCIC) (Cannon, 2015) were used in this study. PCIC provides downscaled GCM climate scenarios from

1950 to 2100 (Bürger et al., 2013) based on the Coupled Model Intercomparison Project phase 5 (CMIP5) (Taylor et al., 2012) and historical daily gridded climate data for Canada (McKenney et al., 2011). The data provided by PCIC is Canada-wide downscaled climate change projections, which are provided using the Bias Correction/Constructed Analogues with Quantile mapping reordering (BCCAQ) method (http://www.pacificclimate.org/data). In this study, we further downscaled PCIC data to Alberta condition based on historical climate data (Ammar et al., 2020 and Masud et al., 2018). We used the delta method (Quilbé et al., 2008; Chen et al., 2011) for bias correction of projected climate time series based on historical data, which were resulted from analyzing a suite of four climate data sources used for reproducing historical flow for 130 hydrometric stations across Alberta through a process-based hydrological model.

On the other hand, GCMs were forced with different Representative Concentration Pathways (RCPs), which define different emission scenarios and subsequent radiative forcing in the earth-atmospheric system (van Vuuren et al., 2011). Therefore, two emission scenarios, namely RCP 2.6 and RCP 8.5 in an ensemble of five GCMs were used for evaluating the climate change effects on snowmelt and GW-SW dynamics for 2040-2064 period. The details of GCMs used in this study can be found in Table A.4.

3.4 Results and Discussion

3.4.1 Calibration, Validation and Uncertainty Analysis

3.4.1.1 SWAT

The calibration of the SWAT model was performed for 1993-2007 (i.e., three years of warm-up and 12 years of calibration), whereas the validation was completed for 1983-1995 (i.e., three years of warm-up followed by 10 years of validation). As it is shown in Table 3.2, the

statistics of each hydrometric station under calibration and validation is very similar. It can also be seen that in mountainous regions, where stations #1 and #2 are located, the values of p-factor and r-factor are both low, albeit the statistics of the best simulation is comparable to other regions. However, increase of r-factor in mountainous regions would result in increase of r-factor in foothill and plain regions. This suggests the importance of proper availability of historical data in hydrological simulations in mountainous areas and its effect on downstream. The lack of climate reliable data (both spatially and temporally) in mountainous regions could have contributed to low ranges of p-factor.

According to streamflow calibration and validation results shown in Figure 3.3 and Table 3.2, more than 60% of the observed data are bracketed within modelling simulations between 1986-2007, with desirable statistics for SWAT best simulation in most of the regions. It should be noted that the performance of model calibration at stations #2 and #4 is marginally lower than other areas, which could be attributed to seasonal availability of observed data in such stations (see Table A.2). The observed data for stations #2 and #4 was not available for November to March, meaning that the low-flow simulations were not evaluated in these stations. However, proper statistics (i.e., R^2, NS and bR^2) can be seen from the statistics of other two stations in upstream regions (i.e., stations #1 and #3), with the same level of p-factor and r-factor with stations #2 and #4 respectively. This suggests that the performance of stations #2 and #4 could be improved if observed data was available for all seasons, which could enable a comprehensive calibration of streamflow at those stations.

Table 3.2. Calibration (1996-2007) and validation (1986-1995) results for streamflow reproduction in NSRB SWAT model.

Region	Station ID (Table S2)	Period	p-factor	r-factor	R^2	NS	bR^2
Mountainous	1	Calibration	0.44	0.47	0.70	0.68	0.57
		Validation	0.45	0.47	0.74	0.70	0.66
	2	Calibration	0.47	0.57	0.52	0.43	0.36
		Validation	0.53	0.67	0.62	0.45	0.46
Foothill	3	Calibration	0.74	0.92	0.80	0.80	0.71
		Validation	0.59	1.02	0.83	0.76	0.82
	4	Calibration	0.68	0.99	0.65	0.47	0.51
		Validation	0.64	0.91	0.66	0.58	0.52
Plain	5	Calibration	0.58	0.93	0.68	0.58	0.59
		Validation	0.63	0.75	0.74	0.74	0.54
	6	Calibration	0.62	0.86	0.67	0.65	0.52
		Validation	0.59	0.78	0.72	0.71	0.47

3.4.1.2 MODFLOW

As it was mentioned in Section 3.3.2.2 and shown in Figure 3.1b, the observed hydraulic heads from 20 observation wells were taken into consideration for calibrating hydraulic heads in MODFLOW. Observed heads at the 1st day of each month were used for evaluating model performance in order to account for the hydraulic head fluctuations in a more sensible way. In total, approximately 3600 data points were extracted from 20 observation wells between 1983 and 2007 for comparison with model simulations. Out of 1000 parameter sets defined from initial ranges in Table 3.1, the best performance statistics and their corresponding parameters were acquired, and the hydraulic head values are shown in Figure 3.4. The performance of best chosen MODFLOW parameters were shown as $R^2 = 0.95$, $\mathrm{MAE} = 22.9$ m and $\mathrm{NRMSE} = 0.108$, and the corresponding parameters of the best simulation are shown in Table 3.3.

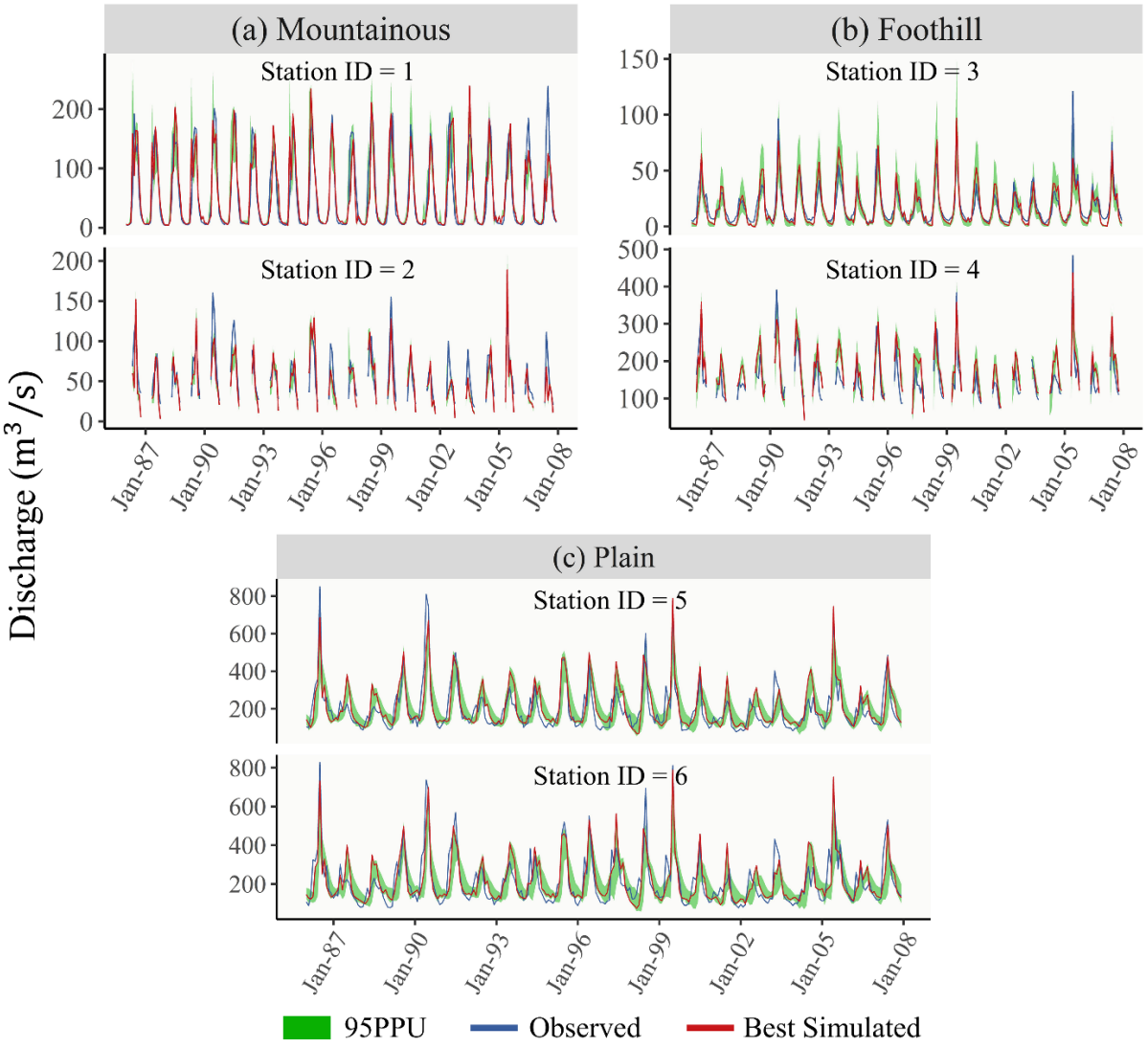

Figure 3.3. Calibration (1996-2007) and validation (1986-1995) results for simulation of historical streamflow in different regions of NSRB.

Table 3.3. Calibrated values of K_h and K_h/K_v related to best simulation in MODFLOW.

Layer No.	Layer name	Horizontal hydraulic conductivity (K_h)	K_h/K_v	Statistics
1	Mountainous region/Displaced bedrock	5.87×10^{-9}	6.5	$R^2 = 0.951$
2	Bedrock – Paskapoo	1.99×10^{-5}	36.6	$MAE = 22.9$
3	Bedrock – Scollard	2.88×10^{-6}	29.1	$NRMSE = 0.108$
4	Bedrock – Battle	9.04×10^{-8}	23.1	
5	Bedrock - Horseshoe	5.8×10^{-9}	76.6	

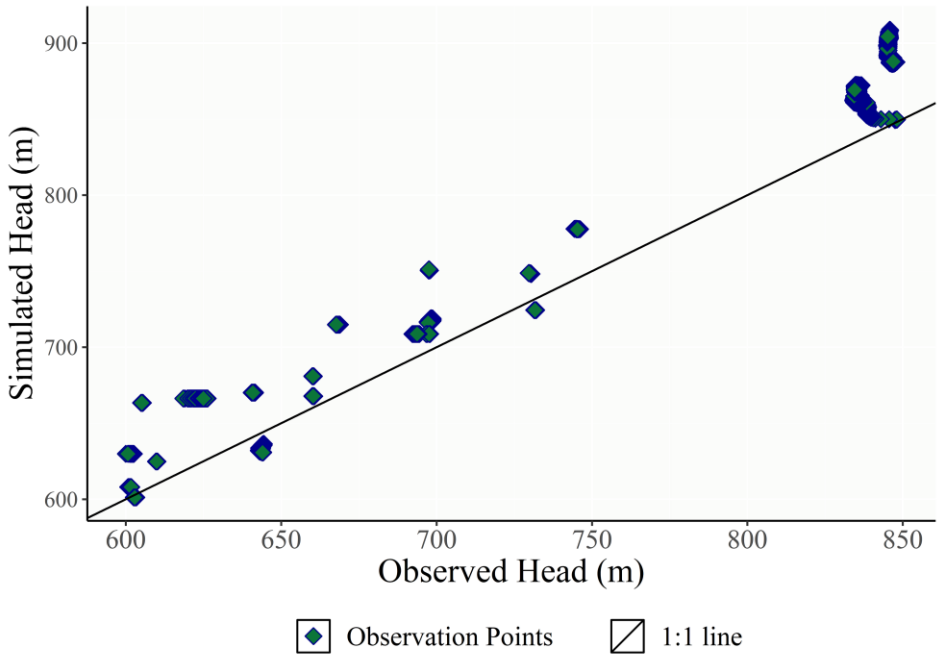

Figure 3.4. Comparison of observed and simulated hydraulic head values using SUFI-2 algorithm in MODFLOW.

3.4.2 Analysis of spatio-temporal changes in snowmelt dynamics under changing climate

The comparison results of historical (1983-2007) and future projections (2040-2064) of regional snowmelt along with their driving factors are presented in this section. Since five GCMs are used under RCP2.6 and RCP8.5 emission scenarios (see Table A.4), the future projections of model responses are presented in the form of possible ranges, encompassing the minimum and maximum projected value for each time step. The results are presented based on 7-day moving averages in order to smooth the daily outputs of SWAT and SWAT-MODFLOW. As shown in Figure 3.5a, the peak of snowmelt in mountainous regions occurs around May and June for historical period, while the peak snowmelt of foothill and plain areas happens earlier, particularly in March and April. This could be because of the lower temperatures in mountainous regions before the start of spring (i.e., before March, Figure 3.6c). As it is depicted in Figure 3.6, the

average temperature of all regions in almost every season is projected to increase. This increase, along with changing snowfall patterns has resulted in different snowmelt projections in different seasons of NSRB mountainous region. However, an increased snowmelt is projected in April and May for the mountainous regions, which can be mostly related to the increase of temperature in those months. Although temperature increase occurs in almost every month of the mountainous region, its increase in colder seasons is more significant because where air temperature increases from freezing point to melting points (i.e., with temperatures close to 0 ℃), more snowmelt events will initiate. As shown in Figure 3.6c, air temperature in April and May is projected to increase and at some points pass the melting point, resulting in more snowmelt events to occur in cold season. It is also found in the literature that climate change in mountainous regions might result in earlier snowmelts than present (Clilverd et al., 2011; Aygün et al., 2020). The earlier snowmelt, along with decreased projected snowfall in mountainous regions (Figure 3.6b) has also resulted in slower snowmelt in summer times. These results are in line with numerous findings in the literature (see for example, Moore et al., 2007; Kobierska et al., 2011; Elias et al., 2015; Sadro et al., 2018).

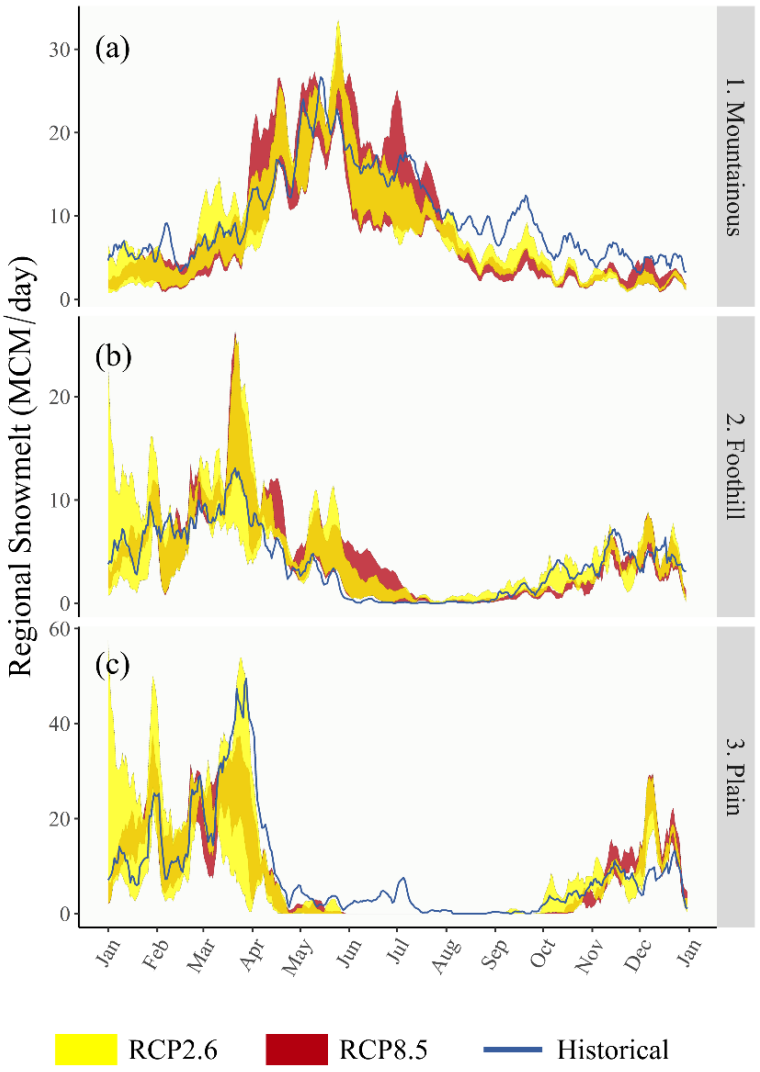

Figure 3.5. Comparison of historical (1983-2007) average of snowmelt with future projections (2040-2064) in NSRB regions (presented in 7-day moving averages)

On the other hand, it can be seen from Figure 3.5c that the spring snowmelt in plain region is projected to decrease, although no significant change in snowmelt peak timing can be witnessed. Also, the snowmelt of plain region is predicted to increase in winter (i.e., December to February). Although there is no significant change in snowfall pattern predicted for the plain region, the projected increase in temperature of this area is noticeable, which can result in increased snowmelt in cold seasons. Another important point related to the plain region is the projected decrease of snowmelt predicted from March to September (i.e., spring and summer),

where the projected snowmelt is mostly zero from June to September. This is due to the decrease in snowfall and snow accumulation, leaving less or no snow pack on the ground to be melted in warm seasons. Finally trends of snowmelt and climate indicators related to foothill region lays between those of mountainous and plain regions, since this region holds the characteristics of both mountainous and plain regions in terms of climate, topography and elevation variations.

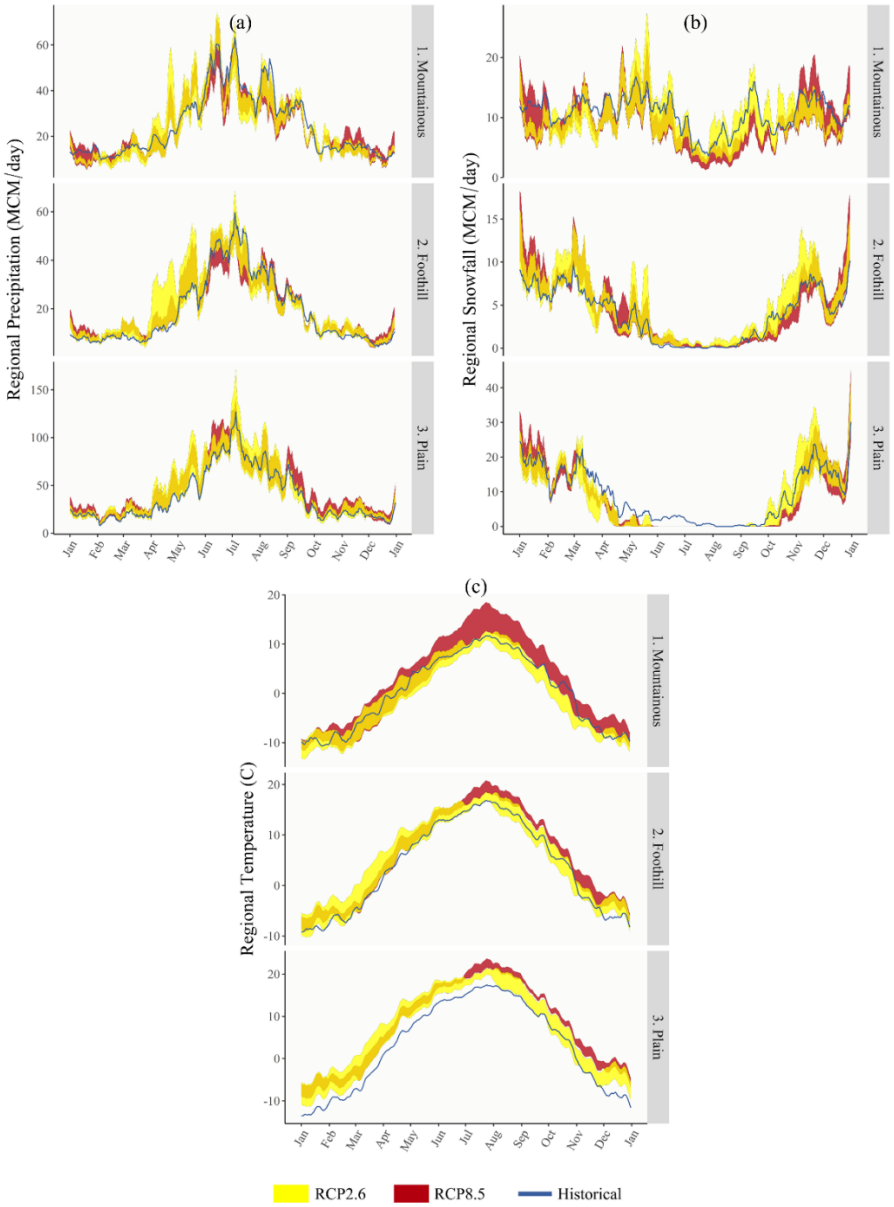

Figure 3.6. Historical simulation (1983-2007) and future projection (2040-2065) of (a) precipitation, (b) snowfall and (c) temperature in mountainous, foothill and plain regions of NSRB. The data are presented as 7-day moving averages of modelling results.

Analysis of precipitation, snowfall, and temperature patterns of NSRB regions (see Figure 3.6) suggest an overall increase of precipitation projected for the future of all regions, except for warm seasons of the mountainous region. These trends, however, are not repeated for snowfall patterns, where it is predicted that the snowfall will notably decrease in almost all seasons of mountainous regions and warm seasons of the plain region. Based on such results, more rainfall events can be anticipated under future conditions, while snowfall is mostly projected to decrease or remain unchanged under climate change scenarios.

3.4.3 Analysis of spatio-temporal changes in GW-SW interactions under changing climate

The results of GW-SW interactions and their changes under climate change scenarios are presented in this section. Four seasons namely winter (December, January and February), spring (March, April, May), summer (June, July, August), and fall (September, October, November) are considered for the analysis of spatial GW-SW interactions. In Figure 3.7, the average of historical GW-SW for 1983-2007 are shown in each MODFLOW cell. Positive values of GW-SW interactions show the groundwater discharge to surface water in the streams, while negative values denote water loss from streams to groundwater. It can be seen in Figure 3.7 that in general, groundwater discharge to surface water has occurred in greater values than groundwater recharge, especially in most parts of mountainous and foothill regions. Nevertheless, in some parts of the mountainous regions there is a groundwater recharge, and the values of GW-SW interactions are mostly small compared to foothill region. In foothill region, most of groundwater contribution to surface water within NSRB occurs. This is intensified in spring and summer months, where the increased level of groundwater has resulted in more contribution of groundwater to surface water. On the other hand, most of the groundwater recharge has occurred

in plain region. This can be related to the evapotranspiration (ET) resulting from vegetation cover and dry soil, which has played an important part in decreasing soil moisture and therefore increasing groundwater recharge from streamflow (Carroll et al., 2019). Also, the surface water gain from groundwater in plain region is minimum, suggesting that the volumes of GW-SW interactions (in both terms of groundwater recharge and discharge) are low in all seasons of plain region. Apart from ET, the lower exchanges between GW and SW can also be related to groundwater table in plain region, which might still be not high enough to interact with surface water (Foster and Allen, 2015). The results of historical GW-SW interactions are in line with Chunn et al. (2019) and Foster and Allen (2015), where most of the interactions had occurred in the form of groundwater discharge to the streams.

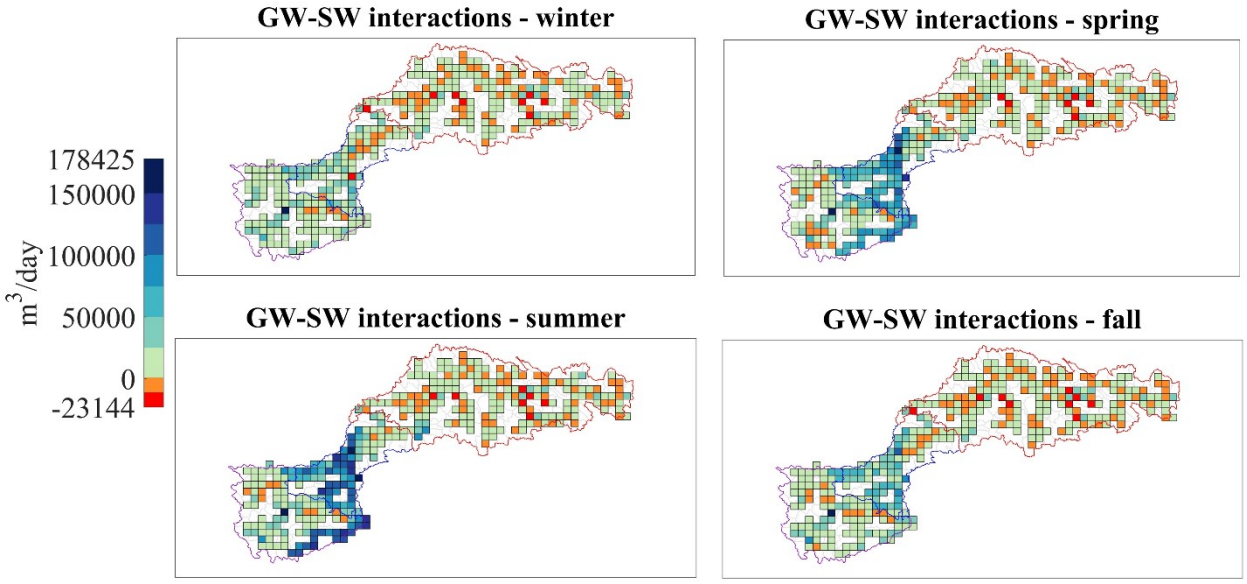

Figure 3.7. Average historical GW-SW interaction for MODFLOW cells. Positive values of GW-SW interactions show the groundwater discharge to surface water in the streams, while negative values denote water loss from streams to groundwater.

Figure 3.8 shows the averaged changes in GW-SW interactions based on average results from five GCMs and two RCPs used in this study. In this figure, negative values denote

increased surface water loss to groundwater, and positive values shows increased groundwater discharge to surface water. It can be said from Figure 3.8 that some regions might experience more groundwater recharge in the future; on the other hand, regional analysis show an increase in groundwater discharge to surface water in various months for different regions (see Figure 3.9). In mountainous regions, especially in warmer seasons, it is predicted that groundwater contribution to the rivers water will increase in the future. This also stands for plain regions in most of warm seasons. However, GW-SW interactions and their changes are not significant in plain regions between September to February (see Figure 3.9) which highlights the effect of snowmelt and streamflow on GW-SW interactions (Huntington and Niswonger, 2012; Foster and Allen, 2015). In fact, higher projected groundwater discharge to surface water in the future of mountainous and plain regions can be attributed to snowmelt recession and its effect on streamflow formations. Comparisons of changes in GW-SW interactions (Figure 3.9a) and in snowmelt (Figure 3.5a) in mountainous regions indicates the same patterns of increase in both processes in spring. This pattern, however, cannot be seen for the plain region, which suggests that the changes in GW-SW interactions in such areas are not solely controlled by snowmelt (Hayashi and Farrow, 2014).

According to Figure 3.8 and Figure 3.9b, the changes in GW-SW interactions of foothill region show two different patterns: (1) a noticeable increase of groundwater discharge to surface water in winter and spring, (2) increase of surface water loss to groundwater in July to September (mainly in summer). This can be related to earlier snowmelt in mountain regions, which will increase groundwater levels in mountainous regions as well. Such an increase will therefore result in contribution of groundwater to surface water in mountainous and, particularly, foothill regions. On the other hand, the opposite trend can be seen in future projections of foothill

region in summer. In fact, earlier and slower snowmelt in mountainous regions (see Figure 3.5a) has resulted in decreased snowmelt flow in summer, ultimately lowering the hydraulic gradient of groundwater. This results in soil moisture deficit in foothill regions in comparison to historical simulations, which has resulted in surface water loss to groundwater. Analysis of changes of GW-SW interactions shows that the areas within foothill region that are affected by climate change the most are very close to mountain regions, rather than plain region. This shows the close connection of mountainous region and upstream of foothill region, where the groundwater level of mountainous region has a direct influence on foothill region.

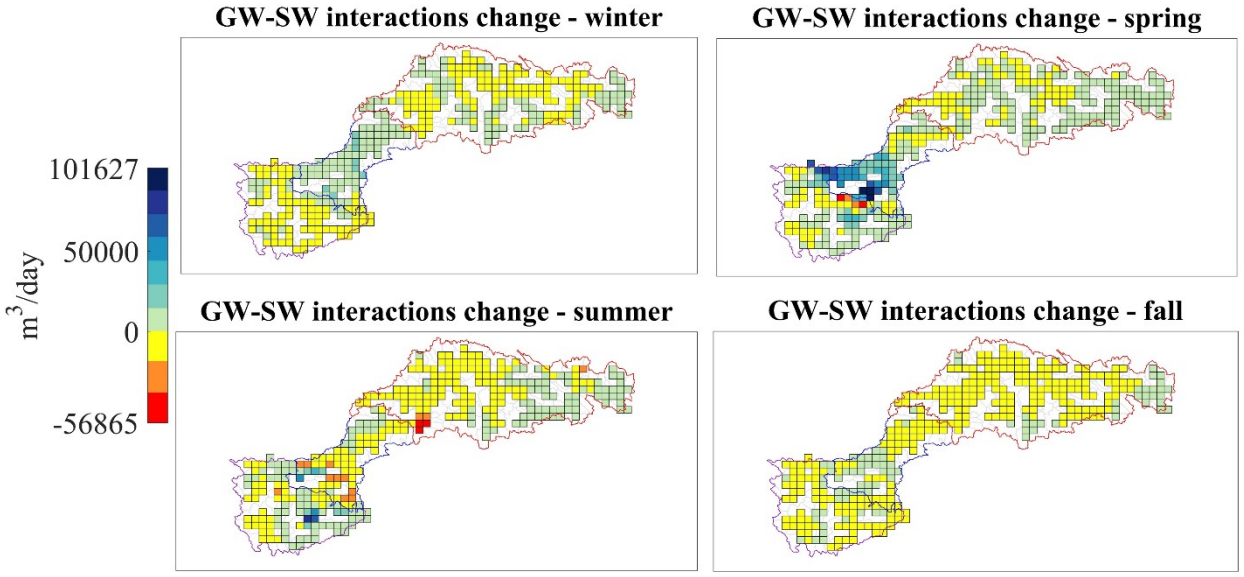

Figure 3.8. Averaged changes in GW-SW interactions under future climate conditions. Positive and negative values indicate increase of groundwater discharge to surface water and groundwater recharge, respectively. The changes calculated as Future (m^3/day) – Historical (m^3/day).

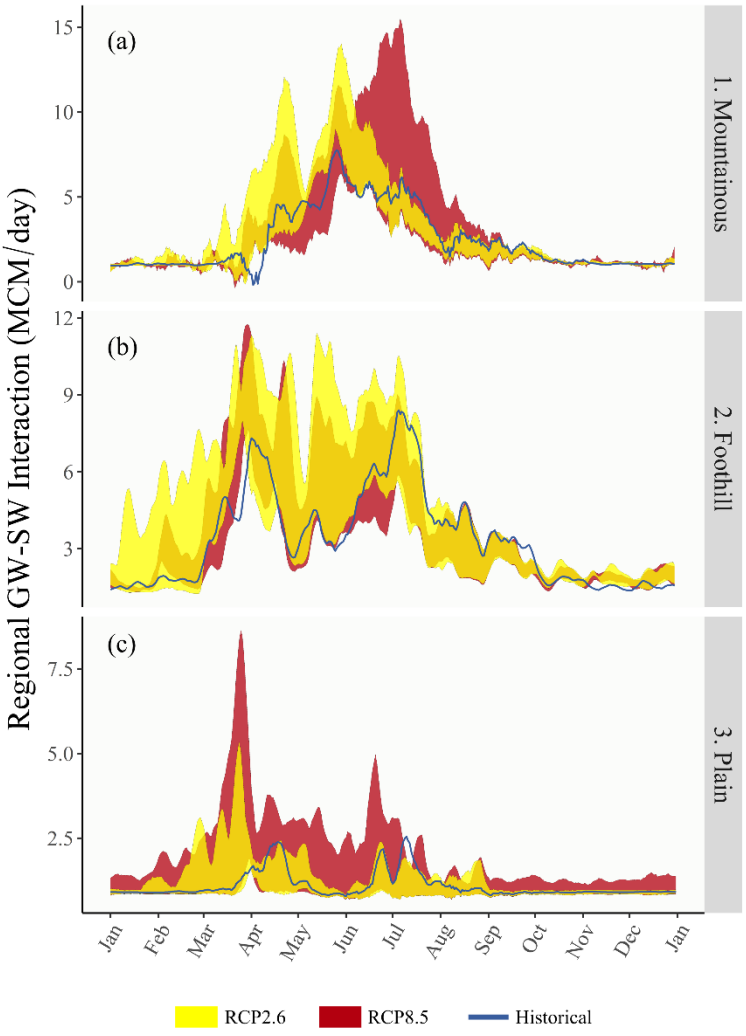

Figure 3.9. Comparison of historical average of GW-SW interactions with future projections in NSRB regions (presented in 7-day average values)

3.4.4 Analysis of relations between GW-SW Interactions and Snowmelt

The results of this section show the influence of snowmelt on dynamics of GW-SW interactions in different regions of NSRB. Comparison of monthly snowmelt and GW-SW interactions in Figure 3.10 suggest that the correlation between these two processes is only meaningful in mountainous regions, where the R^2 of these two factors is 0.494. This correlation is significant, considering the fact that many factors play role in the formation of snowmelt and GW-SW interactions. This clearly shows that snowmelt plays a key role in GW-SW formation in

mountainous regions, because these two processes have showed a similar trend (see Figure 3.5a and Figure 3.9a). On the other hand, the correlation between snowmelt and GW-SW interactions in foothill and plain regions is marginal, with the R^2 of both regions being less than 0.01. A more detailed view of the relations between these two factors can be found in Figure 3.11. As shown in Figure 3.11a, dynamics of snowmelt and GW-SW interactions show similar trends throughout the simulation period (i.e., 1983-2007) in mountainous region, which suggests the direct influence of snowmelt on groundwater dynamics and interactions with surface water. These results are in line with findings of Carroll et al. (2019), where a high correlation was found between snowmelt and groundwater recharge in a mountain system. According to Figure 3.11b, the response of GW-SW interactions to snowmelt has been delayed, and the dynamics (trends) of GW-SW interactions do not directly follow that of snowmelt. The lagged GW-SW interactions might be the result of upstream contribution of GW and SW to foothill region, while the snowmelt is only occurring within foothill areas. It can be seen in Figure 3.11b that GW-SW interactions (i.e., the y-axis on the right) had considerable values in comparison to snowmelt (i.e., the y-axis on the left). This highlights the important effect of GW discharge to SW from mountainous regions in forming significant amounts of GW-SW interactions in the foothill regions. As we approach the plain region, GW-SW interactions become very small in comparison to snowmelt. Although small GW-SW interactions in plain region might be effective on its weak correlation with snowmelt (see Figure 3.11c), same correlation has also been witnessed in foothill region, where the GW-SW interactions are very high. Hence, other factors can potentially play parts in lack of relations between GW-SW interactions and snowmelt in foothill and plain regions. It is discussed in the literature that GW-SW interactions are highly

dependent on topography (Carroll et al., 2019). Potential reasons for low correlations of snowmelt and GW-SW interactions in foothill and plain regions are:

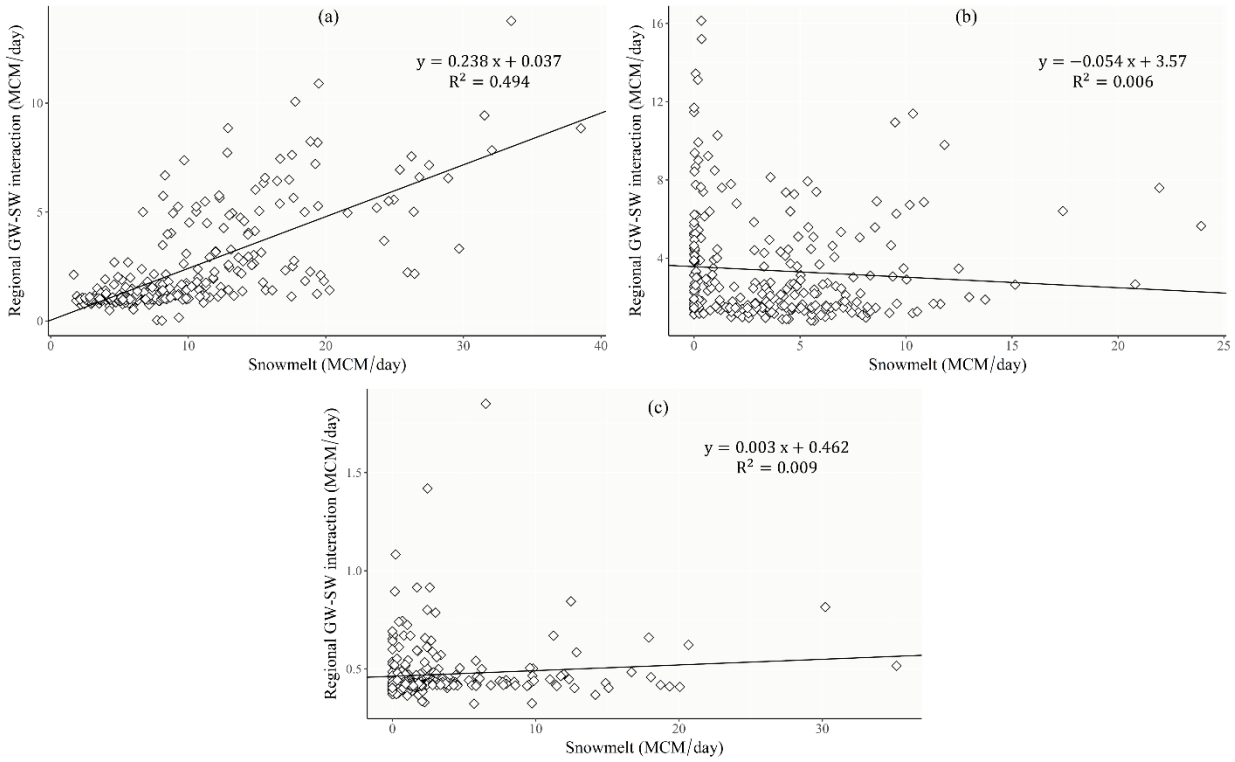

Figure 3.10. Monthly snowmelt and GW-SW interactions in (a) mountainous, (b) foothill, and (c) plain region of NSRB.

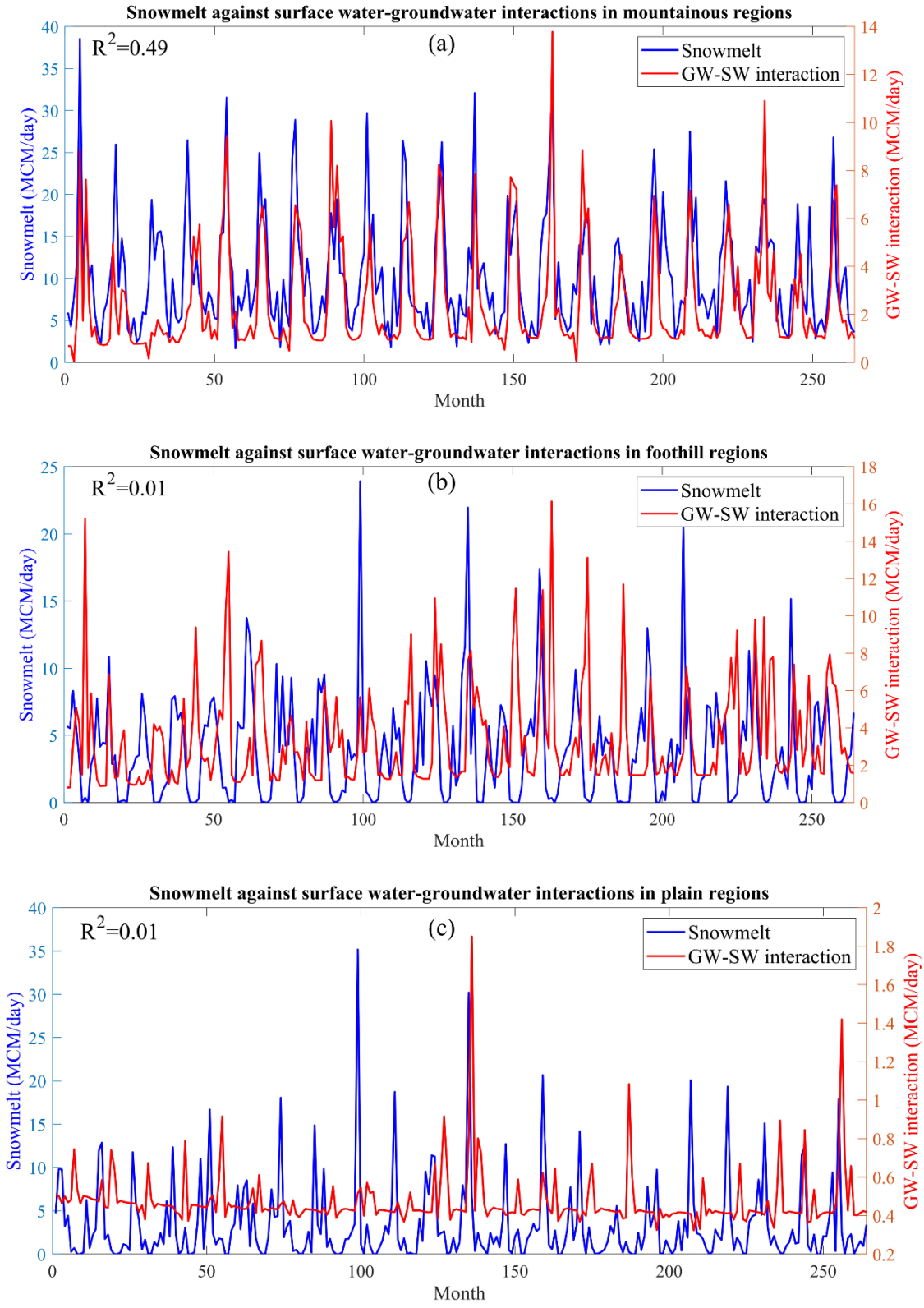

Figure 3.11. Monthly time-series simulation results of snowmelt and SW-GW interactions for (a) mountainous, (b) foothill and (c) plain regions of NSRB (1983-2007), the results for first three years (i.e., 1983-1985) as the warm-up period are excluded from the graph.

(1) Land cover type, soil type, and vegetation cover can play a very important role in groundwater recharge in the terrestrial part of a given sub-basin and in the SW-GW interactions in the streams (Hayashi and Farrow, 2014; Hayashi et al., 2016). These effects are mostly are represented through actual ET from land and vegetation cover. A large ET from the soil and vegetation cover can reduce terrestrial soil moisture and decrease potential recharge to ground water, which eventually dwindles GW levels, and therefore changes the dynamics of GW-SW interactions (Condon et al., 2020). Since most parts of the mountainous region of NSRB is sparsely vegetated (see Figure 3.1), and evaporative demand from soil is low due to higher elevation and colder climate (Shi et al., 2014), the value of ET is small. Also SWAT simulations for 1983-2007 show that the average annual ET for mountainous, foothill, and plain regions are 236 mm/year, 418 mm/year and 396 mm/year, respectively. The low ET from mountains can leave a large volume of soil moisture for potential recharge to GW, which had a considerable effect on high correlation between snowmelt and GW-SW interactions (Carroll et al., 2019). On the contrary, the foothill and plain regions are mainly covered by evergreen forests, pastures, and agricultural lands (see Figure 3.1). The amount of ET resulting from such vegetation covers and soil groups, particularly in growing seasons when evaporative demand of atmosphere is high due to warmer temperature, has inhibited groundwater discharge to uptake the water to plant roots, instead of surface water (Hayashi et al., 2016; Carroll et al., 2019; M. Cochand et al., 2019). Such effects can be seen in Figure 3.11b and Figure 3.11c, where GW-SW interaction is moderated at the times of peak snowmelt. As a result, it can be argued that the effect of ET on the correlation of snowmelt and GW-SW interactions is considerable.

(2) Groundwater recharge and GW-SW interactions in mountainous regions is mostly dependent on snowmelt, and permeability of geological formations (Carroll et al., 2019), since

snowfall is the dominant precipitation in this region. On the other hand, rainfall precipitation occurs more and plays a more important role in foothill and plain regions (see Figure 3.6 for details). Therefore in these regions, the effect of summer rainfall should be considered in addition to snowmelt runoff in order to have a comprehensive assessment of GW-SW interaction drivers. Hayashi and Farrow (2014) suggested that by taking into account the effect of snowmelt and growing-season rainfall, the correlation between the precipitation and groundwater level rises was improved. This suggests the importance of summer rainfall and snowmelt together for analysis of the response of GW-SW system to precipitation and snowmelt events.

(3) The historical simulation of MODFLOW in this study show that the groundwater level is higher in mountainous regions, and the flow of groundwater is from mountainous regions towards foothill and plain regions (results are not shown). This is also found in line with findings of Bekele et al. (2003) and Adams et al. (2004), where the groundwater flow of Alberta basin was found to be topography-driven, as opposed to recharge-controlled flows (Gleeson et al., 2011). As a result, the foothill and plain regions of NSRB are impacted by the groundwater flow from mountainous region. On the other hand, while all the regions are impacted by aquifers from north and south sides of NSRB, the mountainous region is less impacted by upstream (i.e., west to east) groundwater flow. As a result, the impact of upstream groundwater flow from mountainous region to downstream regions (i.e., foothill and plain regions) might potentially result in changing the GW-SW interactions and their correlation with snowmelt. It should be noted that regional snowmelt is localized to each region of interest, while GW-SW interaction of each region is impacted by the groundwater flow and surface water dynamics of their upstream and surrounding regions as well.

3.5 Conclusion and Future Directions

Snowmelt and GW-SW interactions are among the most important and dynamic hydrological processes in high elevation watersheds in cold regions, particularly in warmer seasons. In this study, we coupled surface hydrological model of Soil and Water Assessment Tool (SWAT) with MODFLOW model to assess the historical trend of snowmelt and GW-SW interactions, as well as their projections under future climate scenarios by using an ensemble climate datasets of five GCMs under two future RCP scenarios. Furthermore, we evaluated and discussed the correlations between snowmelt and GW-SW interactions in different regions of study. This allowed spatio-temporal assessment of snowmelt and GW-SW interaction dynamics across heterogeneous landscapes, extending from mountainous to foothill and plain regions, using NSRB as a large river basin in central Alberta as the study area. The main conclusions of this study can be summarized below:

1. Based on regional analysis, the historical reproductions of snowmelt and GW-SW interactions is different within mountainous, foothill and plain regions. These processes also showed distinct responses to climate change in different regions.
2. Under climate change scenarios, it is predicted that precipitation will increase in spring (March to May) and early summer in all regions of NSRB. However, air temperature is projected to mostly increase in all regions and all seasons throughout NSRB. As a result of the dominancy of air temperature increase over precipitation increase, snowfall is projected to decrease in every season of mountainous regions. Except for the winter and early-spring snowfall, no considerable change in snowfall is predicted for foothill region. Finally, the spring and summer snowfall on the plain region is predicted to decrease, while no apparent changes can be witnessed in other seasons of this region.

3. Analysis of regional snowmelt projections under future climate scenarios showed that mountainous region of NSRB will predictably experience an earlier snowmelt, where the snowmelt is predicted to increase in April and May, while decreasing in June and July. Also, considerable snowmelt decrease is predicted in fall and winter (September to February) in mountainous regions, possibly because of less snow accumulation projected for this area. In the foothill region, snowmelt is projected to increase in warm seasons (i.e., spring and summer), with no considerable changes in snowmelt peak time. In contrary to mountainous and foothill regions, plain region is projected to experience increased snowmelt in winter, and less snowmelt in spring and summer. The increased winter snowmelt of the plain region can be attributed to increased air temperature in winter, whereas the decreased snowmelt of spring and summer is due to less snow cover available in the future for melting to occur.
4. Historical analysis of GW-SW interactions show that groundwater discharge to surface water dominates such interactions in most areas of NSRB and in all seasons. Both mountainous and foothill regions mostly showed a groundwater discharge to streams in historical analysis. The groundwater contribution to surface water is particularly larger in spring and summer, suggesting the important effect of snowmelt percolation on increasing groundwater levels in mountainous regions, and recharging surface water through GW-SW interactions in mountainous and foothill regions. Finally, most of the historical groundwater recharge occurs in plain regions, which can be related to lower groundwater level as a result of ET, land-cover and soil types.
5. Results of climate change scenarios and future projections of GW-SW interactions show a general increase of groundwater discharge to surface water in mountainous and plain regions. The increased contribution of groundwater to surface water under climate change in

mountainous regions predictably occurs in warm seasons, which can be related to the earlier snowmelt projected in this region. In plain regions, increased amount of precipitation, especially in warm seasons, could be an important factor in increasing groundwater discharge to surface water. Furthermore, the foothill region is projected to have an increased groundwater discharge in winter and spring, followed by a noticeable increase in groundwater recharge in summer. It is argued that this trend can be a direct result of earlier snowmelt and its percolation in both mountainous and foothill region, followed by groundwater level drop in summer as a result of less snowmelt and increased air temperature within the foothill region.

6. Analysis of correlations between regional snowmelt and GW-SW interactions in mountainous, foothill and plain regions showed high correlations ($R^2 = 0.494$) in mountainous regions, but negligible correlations in foothill and plain regions ($R^2 < 0.01$ for both regions). Three major factors can potentially affect the relations between snowmelt and GW-SW interactions. First, the average ET in mountainous regions is much smaller than those in foothill and plain regions (average historical ET is 236 mm/year in mountainous region, compared to 418 mm/year and 396 mm/year in foothill and plain regions, respectively). The higher ET in foothill and plain region might have played an important role in the small correlation between snowmelt and GW-SW interactions, since higher ET alters the water balance, and surface and sub-surface water availability. Second, while snow is the dominant type of precipitation in mountainous regions, rainfall is more common in downstream areas such as foothill and plain regions. Third, since the groundwater flow in Alberta is mostly topography-driven, groundwater flow of high-elevated areas such as mountainous regions affects those of downstream regions such as plain and foothill regions.

Thus, future studies can focus on the possible improvements in analysis of relations of snowmelt vs. GW-SW interactions by incorporating land-use and seasonal precipitation into comparisons.

This research facilitates a better understanding of dynamics of snowmelt and GW-SW interactions, their possible changes under future climate scenarios in regional scale. It also demonstrates how regional snowmelt might affect GW-SW interactions, and how and why such effects are different in various climate, topographic and land-use conditions. Our study shows that although a complex relation among climate, topography, vegetation and other related factors results in formation of GW-SW interactions, snowmelt runoff is potentially the main driver of this process in mountainous regions. Future studies can also focus on other effective factors on GW-SW dynamics in regions with various topography and land-use settings, in order to achieve a better understanding of major drivers of groundwater recharge and its connection to surface water. Also, recent studies have shown the vital role of depression-based recharge, especially in Canadian Prairies, on GW-SW interactions (Hayashi and Farrow, 2014; Brannen et al., 2015; Hayashi et al., 2016). As a result, it is important to consider the effect of wetlands, potholes, and other water bodies on groundwater recharge in the modelling process using high-quality input data and appropriate setup of fill-and-spill processes within hydrological models. Another limitation of this study is the assumption that land-use/land-cover, soil properties, and hydraulic conductivity of geological formations do not change over time. It is argued that the K values of underlying formations are changed based on groundwater level dynamics (Brannen et al., 2015). Moreover, the effect of frozen soil and low permeability lenses on infiltration, groundwater recharge and GW-SW interactions can be substantial in cold region hydrology and hydrogeology (Aygün et al., 2020; Zhang et al., 2020). Finally, the effect of historical water bodies, and

geospatial features related to prehistoric and contemporary times can greatly control and impact GW-SW dynamics and their correlation with different hydrological processes (Gomez-Velez et al., 2014; Lewandowski et al., 2020). We acknowledge that such effects are not explicitly taken into account in hydrological modelling within this study, but improvements can be made in future research on a better representation of the aforementioned factors in regional modelling. This will result in a better understanding of the governing processes in the formation of groundwater recharge and its connection to surface water.

3.6 Acknowledgement

Funding for this study has been received from Campus Alberta Innovation Program Chair (Grant# RES0034497), and Natural Sciences and Engineering Research Council of Canada Discovery Grant (Grant# RES0043463).

3.7 References

Abbaspour, K.C., 2015. SWAT-CUP: SWAT Calibration and Uncertainty Programs- A User Manual, Department of Systems Analysis, Intergrated Assessment and Modelling (SIAM),EAWAG. Swiss Federal Institute of Aqualtic Science and Technology, Duebendorf, Switzerland. https://doi.org/10.1007/s00402-009-1032-4

Adams, J.J., Rostron, B.J., Mendoza, C.A., 2004. Coupled fluid flow, heat and mass transport, and erosion in the Alberta basin: Implications for the origin of the Athabasca oil sands. Canadian Journal of Earth Sciences 41, 1077–1095. https://doi.org/10.1139/E04-052

Akiyama Sakai, A., Yamazaki, Y., Wang, G., Fujita, K., Nakawo, M., Kubota, J., and Konagaya, Y., T., 2007. Surfacewater-groundwater interaction in the Heihe River basin, Northwestern China. Bull Glaciol Res.

Alberta Environment and Parks, 2019. Alberta river basins [WWW Document]. URL https://web.archive.org/web/20160409210242/http://www.environment.alberta.ca/apps/basins/default.aspx (accessed 7.30.19).

Alberta Geological Survey, 2019. 3D provincial geological framework model of Alberta, version 2.

Aliyari, F., Bailey, R.T., Tasdighi, A., Dozier, A., Arabi, M., Zeiler, K., 2019. Coupled SWAT-MODFLOW model for large-scale mixed agro-urban river basins. Environmental Modelling and Software 115, 200–210. https://doi.org/10.1016/j.envsoft.2019.02.014

Allen, D.M., Whitfield, P.H., Werner, A., 2010. Groundwater level responses in temperate mountainous terrain: Regime classification, and linkages to climate and streamflow. Hydrological Processes 24, 3392–3412. https://doi.org/10.1002/hyp.7757

Ammar, M.E., Gharib, A., Islam, Z., Davies, E.G.R., Seneka, M., Faramarzi, M., 2020. Future floods using hydroclimatic simulations and peaks over threshold: An alternative to nonstationary analysis inferred from trend tests. Advances in Water Resources 136, 103463. https://doi.org/10.1016/j.advwatres.2019.103463

Arnold, J., Moriasi, D., Gassman, P., Abbaspour, K., White, M., Srinivasan, R., Santhi, C., Harmel, R., van Griensven, A., Van Liew, M., Kannan, N., Jha, M., 2012. SWAT: Model Use, Calibration, and Validation. Transactions of the ASABE 55, 1317–1335. https://doi.org/10.13031/2013.42244

Arnold, J., Srinivasan, R., Muttiah, R., Williams, J., 1998. Large Area Hydrologic Modeling and Assessment; Part I: Model Development. Journal of the American Water Resources Association 17, 73. https://doi.org/10.1016/S0899-9007(00)00483-4

Assani, A.A., Landry, R., Laurencelle, M., 2012. Comparison of interannual variability modes and trends of seasonal precipitation and streamflow in southern quebec (canada). River Research and Applications. https://doi.org/10.1002/rra.1544

Avanzi, F., De Michele, C., Ghezzi, A., 2015. On the performances of empirical regressions for the estimation of bulk snow density. Geogr. Fis. Dinam. Quat. 38, 105–112. https://doi.org/10.4461/GFDQ.2015.38.10

Aygün, O., Kinnard, C., Campeau, S., 2020. Impacts of climate change on the hydrology of northern midlatitude cold regions, Progress in Physical Geography. https://doi.org/10.1177/0309133319878123

Bai, Y., Fernald, A., Tidwell, V., Gunda, T., 2019. Reduced and Earlier Snowmelt Runoff Impacts Traditional Irrigation Systems. Journal of Contemporary Water Research & Education. https://doi.org/10.1111/j.1936-704x.2019.03318.x

Bailey, R.T., Wible, T.C., Arabi, M., Records, R.M., Ditty, J., 2016. Assessing regional-scale spatio-temporal patterns of groundwater–surface water interactions using a coupled SWAT-MODFLOW model. Hydrological Processes 30, 4420–4433. https://doi.org/10.1002/hyp.10933

Barthel, R., Banzhaf, S., 2016. Groundwater and Surface Water Interaction at the Regional-scale – A Review with Focus on Regional Integrated Models. Water Resources Management. https://doi.org/10.1007/s11269-015-1163-z

Bekele, E.B., Rostron, B.J., Person, M.A., 2003. Fluid pressure implications of erosional unloading, basin hydrodynamics and glaciation in the Alberta Basin, Western Canada. Journal of Geochemical Exploration 78–79, 143–147. https://doi.org/10.1016/S0375-6742(03)00148-1

Bocchiola, D., Groppelli, B., 2010. Spatial estimation of snow water equivalent at different dates within the Adamello Park of Italy. Cold Regions Science and Technology 63, 97–109. https://doi.org/10.1016/j.coldregions.2010.06.001

Brannen, R., Spence, C., Ireson, A., 2015. Influence of shallow groundwater-surface water interactions on the hydrological connectivity and water budget of a wetland complex. Hydrological Processes 29, 3862–3877. https://doi.org/10.1002/hyp.10563

Bürger, G., Sobie, S.R., Cannon, A.J., Werner, A.T., Murdock, T.Q., 2013. Downscaling extremes: An intercomparison of multiple methods for future climate. Journal of Climate 26, 3429–3449. https://doi.org/10.1175/JCLI-D-12-00249.1

Candela, L., Elorza, F.J., Tamoh, K., Jiménez-Martínez, J., Aureli, A., 2014. Groundwater modelling with limited data sets: The Chari-Logone area (Lake Chad Basin, Chad). Hydrological Processes. https://doi.org/10.1002/hyp.9901

Cannon, A.J., 2015. Selecting GCM scenarios that span the range of changes in a multimodel ensemble: Application to CMIP5 climate extremes indices. Journal of Climate 28, 1260–1267. https://doi.org/10.1175/JCLI-D-14-00636.1

Carroll, R.W.H., Bearup, L.A., Brown, W., Dong, W., Bill, M., Willlams, K.H., 2018. Factors controlling seasonal groundwater and solute flux from snow-dominated basins.

Hydrological Processes 32, 2187–2202. https://doi.org/10.1002/hyp.13151

Carroll, R.W.H., Deems, J.S., Niswonger, R., Schumer, R., Williams, K.H., 2019. The Importance of Interflow to Groundwater Recharge in a Snowmelt-Dominated Headwater Basin. Geophysical Research Letters 46, 5899–5908. https://doi.org/10.1029/2019GL082447

Chauvin, G.M., Flerchinger, G.N., Link, T.E., Marks, D., Winstral, A.H., Seyfried, M.S., 2011. Long-term water balance and conceptual model of a semi-arid mountainous catchment. Journal of Hydrology 400, 133–143. https://doi.org/10.1016/j.jhydrol.2011.01.031

Chen, J., Brissette, F.P., Leconte, R., 2011. Uncertainty of downscaling method in quantifying the impact of climate change on hydrology. Journal of Hydrology 401, 190–202. https://doi.org/10.1016/j.jhydrol.2011.02.020

Chen, M., Izady, A., Abdalla, O.A., 2017. An efficient surrogate-based simulation-optimization method for calibrating a regional MODFLOW model. Journal of Hydrology 544, 591–603. https://doi.org/10.1016/j.jhydrol.2016.12.011

Chunn, D., Faramarzi, M., Smerdon, B., Alessi, D.S., 2019. Application of an integrated SWAT-MODFLOW model to evaluate potential impacts of climate change and water withdrawals on groundwater-surface water interactions in west-central Alberta. Water (Switzerland) 11. https://doi.org/10.3390/w11010110

Clilverd, H.M., White, D.M., Tidwell, A.C., Rawlins, M.A., 2011. The sensitivity of northern groundwater recharge to climate change: A case study in Northwest Alaska. Journal of the American Water Resources Association 47, 1228–1240. https://doi.org/10.1111/j.1752-1688.2011.00569.x

Cochand, F., Therrien, R., Lemieux, J.M., 2019. Integrated Hydrological Modeling of Climate Change Impacts in a Snow-Influenced Catchment. Groundwater. https://doi.org/10.1111/gwat.12848

Cochand, M., Christe, P., Ornstein, P., Hunkeler, D., 2019. Groundwater Storage in High Alpine Catchments and Its Contribution to Streamflow. Water Resources Research 55, 2613–2630. https://doi.org/10.1029/2018WR022989

Condon, L.E., Atchley, A.L., Maxwell, R.M., 2020. Evapotranspiration depletes groundwater under warming over the contiguous United States. Nature communications 11, 873. https://doi.org/10.1038/s41467-020-14688-0

Debele, B., Srinivasan, R., Gosain, A.K., 2010. Comparison of process-based and temperature-index snowmelt modeling in SWAT. Water Resources Management 24, 1065–1088. https://doi.org/10.1007/s11269-009-9486-2

Deng, Y., Flerchinger, G.N., Cooley, K.R., 1994. Impacts of spatially and temporally varying snowmelt on subsurface flow in a mountainous watershed: 2. Subsurface processes. Hydrological Sciences Journal. https://doi.org/10.1080/02626669409492772

Devito, K.J., Hill, A.R., Roulet, N., 1996. Groundwater-surface water interactions in headwater forested wetlands of the Canadian Shield. Journal of Hydrology. https://doi.org/10.1016/0022-1694(95)02912-5

Dumanski, S., Pomeroy, J.W., Westbrook, C.J., 2015. Hydrological regime changes in a Canadian Prairie basin. Hydrological Processes 29, 3893–3904. https://doi.org/10.1002/hyp.10567

Elias, E.H., Rango, A., Steele, C.M., Mejia, J.F., Smith, R., 2015. Assessing climate change impacts on water availability of snowmelt-dominated basins of the Upper Rio Grande basin. Journal of Hydrology: Regional Studies 3, 525–546. https://doi.org/10.1016/j.ejrh.2015.04.004

Faramarzi, M., Abbaspour, K.C., Schulin, R., Yang, H., 2009. Modelling blue and green water resources availability in Iran. Hydrological Processes 26, 1–16. https://doi.org/10.1002/hyp

Faramarzi, M., Srinivasan, R., Iravani, M., Bladon, K.D., Abbaspour, K.C., Zehnder, A.J.B., Goss, G.G., 2015. Setting up a hydrological model of Alberta: Data discrimination analyses prior to calibration. Environmental Modelling and Software 74, 48–65. https://doi.org/10.1016/j.envsoft.2015.09.006

Field, C.B., Barros, V.R., Dokken, D.J., Mach, K.J., Mastrandrea, M.D., Bilir, T.E., Chatterjee, M., Ebi, K.L., Estrada, Y.O., Genova, R.C., Girma, B., Kissel, E.S., Levy, A.N., MacCracken, S., Mastrandrea, P.R., White, L.L., 2014. Climate change 2014 impacts, adaptation and vulnerability: Part A: Global and sectoral aspects: Working group II contribution to the fifth assessment report of the intergovernmental panel on climate change, Climate Change 2014 Impacts, Adaptation and Vulnerability: Part A: Global and Sectoral Aspects. https://doi.org/10.1017/CBO9781107415379

Finger, D., Heinrich, G., Gobiet, A., Bauder, A., 2012. Projections of future water resources and their uncertainty in a glacierized catchment in the Swiss Alps and the subsequent effects on hydropower production during the 21st century. Water Resources Research. https://doi.org/10.1029/2011WR010733

Flerchinger, G.N., Cooley, K.R., Ralston, D.R., 1992. Groundwater response to snowmelt in a mountainous watershed. Journal of Hydrology 133. https://doi.org/10.1016/0022-1694(92)90260-3

Foster, S.B., Allen, D.M., 2015. Groundwater - Surface Water Interactions in a Mountain-to-Coast Watershed: Effects of Climate Change and Human Stressors. Advances in Meteorology 2015. https://doi.org/10.1155/2015/861805

Gao, Z., Wang, Z., Wang, S., Wu, X., An, Y., Wang, W., Liu, J., 2019. Factors that influence the chemical composition and evolution of shallow groundwater in an arid region: a case study from the middle reaches of the Heihe River, China. Environmental Earth Sciences. https://doi.org/10.1007/s12665-019-8391-0

Gleeson, T., Marklund, L., Smith, L., Manning, A.H., 2011. Classifying the water table at

regional to continental scales. Geophysical Research Letters 38, 1–6. https://doi.org/10.1029/2010GL046427

Golder Associates, 2008. Assessment of climate change effects on water yield from the North Saskatchewan River Basin.

Gomez-Velez, J.D., Krause, S., Wilson, J.L., 2014. Effect of low-permeability layers on spatial patterns of hyporheic exchange and groundwater upwelling. Water Resources Research. https://doi.org/10.1002/2013WR015054

Government of Canada, 2019. Historical Climate Data [WWW Document]. URL http://climate.weather.gc.ca/historical_data/search_historic_data_e.html (accessed 8.6.19).

Guevara Ochoa, C., Medina Sierra, A., Vives, L., Zimmermann, E., Bailey, R., 2020. Spatio-temporal patterns of the interaction between groundwater and surface water in plains. Hydrological Processes 34, 1371–1392. https://doi.org/10.1002/hyp.13615

Guzman, J.A., Moriasi, D.N., Gowda, P.H., Steiner, J.L., Starks, P.J., Arnold, J.G., Srinivasan, R., 2015. A model integration framework for linking SWAT and MODFLOW. Environmental Modelling and Software 73, 103–116. https://doi.org/10.1016/j.envsoft.2015.08.011

Haddeland, I., Heinke, J., Biemans, H., Eisner, S., Flörke, M., Hanasaki, N., Konzmann, M., Ludwig, F., Masaki, Y., Schewe, J., Stacke, T., Tessler, Z.D., Wada, Y., Wisser, D., 2014. Global water resources affected by human interventions and climate change. Proceedings of the National Academy of Sciences of the United States of America. https://doi.org/10.1073/pnas.1222475110

Hagemann, S., Chen, C., Clark, D.B., Folwell, S., Gosling, S.N., Haddeland, I., Hanasaki, N., Heinke, J., Ludwig, F., Voss, F., Wiltshire, A.J., 2013. Climate change impact on available water resources obtained using multiple global climate and hydrology models. Earth System Dynamics. https://doi.org/10.5194/esd-4-129-2013

Harding, R., Best, M., Blyth, E., Hagemann, S., kabat, P., Tallaksen, L.M., Warnaars, T., Wiberg, D., Weedon, G.P., Van Lanen, H., Ludwig, F., Haddeland, I., 2011. WATCH: Current knowledge of the terrestrial global water cycle. Journal of Hydrometeorology. https://doi.org/10.1175/JHM-D-11-024.1

Harma, K.J., Johnson, M.S., Cohen, S.J., 2012. Future Water Supply and Demand in the Okanagan Basin, British Columbia: A Scenario-Based Analysis of Multiple, Interacting Stressors. Water Resources Management. https://doi.org/10.1007/s11269-011-9938-3

Hayashi, M., Farrow, C.R., 2014. Watershed-scale response of groundwater recharge to inter-annual and inter-decadal variability in precipitation (Alberta, Canada). Hydrogeology Journal 22, 1825–1839. https://doi.org/10.1007/s10040-014-1176-3

Hayashi, M., van der Kamp, G., Rosenberry, D.O., 2016. Hydrology of Prairie Wetlands: Understanding the Integrated Surface-Water and Groundwater Processes. Wetlands 36,

237–254. https://doi.org/10.1007/s13157-016-0797-9

Huntington, J.L., Niswonger, R.G., 2012. Role of surface-water and groundwater interactions on projected summertime streamflow in snow dominated regions: An integrated modeling approach. Water Resources Research 48, 1–20. https://doi.org/10.1029/2012WR012319

Jutebring Sterte, E., Johansson, E., Sjöberg, Y., Huseby Karlsen, R., Laudon, H., 2018. Groundwater-surface water interactions across scales in a boreal landscape investigated using a numerical modelling approach. Journal of Hydrology. https://doi.org/10.1016/j.jhydrol.2018.03.011

Kobierska, F., Jonas, T., Magnusson, J., Zappa, M., Bavay, M., Bosshard, T., Paul, F., Bernasconi, S.M., 2011. Climate change effects on snow melt and discharge of a partly glacierized watershed in Central Switzerland (SoilTrec Critical Zone Observatory). Applied Geochemistry 26, S60–S62. https://doi.org/10.1016/j.apgeochem.2011.03.029

Kornelsen, K.C., Coulibaly, P., 2014. Synthesis review on groundwater discharge to surface water in the Great Lakes Basin. Journal of Great Lakes Research. https://doi.org/10.1016/j.jglr.2014.03.006

Kult, J., Choi, W., Keuser, A., 2012. Snowmelt runoff modeling: Limitations and potential for mitigating water disputes. Journal of Hydrology. https://doi.org/10.1016/j.jhydrol.2012.01.043

Kundzewicz, Z.W., Döll, P., 2009. Will groundwater ease freshwater stress under climate change? Hydrological Sciences Journal. https://doi.org/10.1623/hysj.54.4.665

Kure, S., Jang, S., Ohara, N., Kavvas, M.L., Chen, Z.Q., 2013. Hydrologic impact of regional climate change for the snowfed and glacierfed river basins in the Republic of Tajikistan: Hydrological response of flow to climate change. Hydrological Processes. https://doi.org/10.1002/hyp.9535

Lewandowski, J., Meinikmann, K., Krause, S., 2020. Groundwater-surface water interactions: Recent advances and interdisciplinary challenges. Water (Switzerland). https://doi.org/10.3390/w12010296

Lucas-Picher, P., Riboust, P., Somot, S., Laprise, R., 2015. Reconstruction of the spring 2011 richelieu river flood by two regional climate models and a hydrological model. Journal of Hydrometeorology. https://doi.org/10.1175/JHM-D-14-0116.1

Lundberg, A., Ala-Aho, P., Eklo, O., Klöve, B., Kværner, J., Stumpp, C., 2016. Snow and frost: Implications for spatiotemporal infiltration patterns - a review. Hydrological Processes. https://doi.org/10.1002/hyp.10703

MacDonald, R.J., Byrne, J.M., Boon, S., Kienzle, S.W., 2012. Modelling the Potential Impacts of Climate Change on Snowpack in the North Saskatchewan River Watershed, Alberta. Water Resources Management 26, 3053–3076. https://doi.org/10.1007/s11269-012-0016-2

Masud, M.B., Ferdous, J., Faramarzi, M., 2018. Projected changes in hydrological variables in the agricultural region of Alberta, Canada. Water (Switzerland) 10. https://doi.org/10.3390/w10121810

Maurya, A.S., Rai, S.P., Joshi, N., Dutt, K.S., Rai, N., 2018. Snowmelt runoff and groundwater discharge in Himalayan rivers: a case study of the Satluj River, NW India. Environmental Earth Sciences. https://doi.org/10.1007/s12665-018-7849-9

McKenney, D.W., Hutchinson, M.F., Papadopol, P., Lawrence, K., Pedlar, J., Campbell, K., Milewska, E., Hopkinson, R.F., Price, D., Owen, T., 2011. Customized Spatial Climate Models for North America. Bulletin of the American Meteorological Society 92, 1611–1622. https://doi.org/10.1175/2011BAMS3132.1

Moore, J.N., Harper, J.T., Greenwood, M.C., 2007. Significance of trends toward earlier snowmelt runoff, Columbia and Missouri Basin headwaters, western United States. Geophysical Research Letters 34, 1–5. https://doi.org/10.1029/2007GL031022

Neitsch, S., Arnold, J., Kiniry, J., Williams, J., 2011. Soil & Water Assessment Tool Theoretical Documentation Version 2009. Texas Water Resources Institute 1–647. https://doi.org/10.1016/j.scitotenv.2015.11.063

North Saskatchewan Watershed Alliance, 2005. The State of the North Sask River Watershed Report.

Orozco, I., Francés, F., Mora, J., 2019. Parsimonious modeling of snow accumulation and snowmelt processes in high mountain basins. Water (Switzerland). https://doi.org/10.3390/w11061288

Park, S., Bailey, R.T., 2017. SWAT-MODFLOW Tutorial—Documentation for Preparing Model Simulations.

Paznekas, A., Hayashi, M., 2016. Groundwater contribution to winter streamflow in the Canadian Rockies. Canadian Water Resources Journal 41, 484–499. https://doi.org/10.1080/07011784.2015.1060870

Qi, J., Li, S., Jamieson, R., Hebb, D., Xing, Z., Meng, F.R., 2017. Modifying SWAT with an energy balance module to simulate snowmelt for maritime regions. Environmental Modelling and Software 93, 146–160. https://doi.org/10.1016/j.envsoft.2017.03.007

Qi, P., Zhang, G., Xu, Y.J., Xia, Z., Wang, M., 2019. Response of water resources to future climate change in a high-latitude river basin. Sustainability (Switzerland) 11. https://doi.org/10.3390/su11205619

Quilbé, R., Rousseau, A.N., Moquet, J.S., Trinh, N.B., Dibike, Y., Gachon, P., Chaumont, D., 2008. Assessing the effect of climate change on river flow using general circulation models and hydrological modelling - Application to the chaudière River, Québec, Canada. Canadian Water Resources Journal 33, 73–94.

Sadro, S., Sickman, J.O., Melack, J.M., Skeen, K., 2018. Effects of Climate Variability on Snowmelt and Implications for Organic Matter in a High-Elevation Lake. Water Resources Research 54, 4563–4578. https://doi.org/10.1029/2017WR022163

Saydi, M., Ding, J. li, Sagan, V., Qin, Y., 2019. Snowmelt modeling using two melt-rate models in the Urumqi River watershed, Xinjiang Uyghur Autonomous Region, China. Journal of Mountain Science. https://doi.org/10.1007/s11629-018-5365-8

Schilling, O.S., Park, Y.J., Therrien, R., Nagare, R.M., 2019. Integrated Surface and Subsurface Hydrological Modeling with Snowmelt and Pore Water Freeze–Thaw. Groundwater 57, 63–74. https://doi.org/10.1111/gwat.12841

Schindler, D.W., Donahue, W.F., 2006. An impending water crisis in Canada's western prairie provinces. Proceedings of the National Academy of Sciences of the United States of America. https://doi.org/10.1073/pnas.0601568103

Shi, H., Fu, X., Chen, J., Wang, G., Li, T., 2014. Spatial distribution of monthly potential evaporation over mountainous regions: case of the Lhasa River basin, China. Hydrological Sciences Journal. https://doi.org/10.1080/02626667.2014.881486

Smerdon, B.D., Hughes, A.T., Jean, G., 2017. Permeability Measurements of Upper Cretaceous and Paleogene Bedrock Cores made from 2004-2015 (tabular data, tab-delimited format, to accompany Open File Report 2016-03).

Smith, R.S., Moore, R.D., Weiler, M., Jost, G., 2014. Spatial controls on groundwater response dynamics in a snowmelt-dominated montane catchment. Hydrology and Earth System Sciences. https://doi.org/10.5194/hess-18-1835-2014

Tanachaichoksirikun, P., Seeboonruang, U., Fogg, G.E., 2020. Improving Groundwater Model in Regional Sedimentary Basin Using Hydraulic Gradients. KSCE Journal of Civil Engineering 24, 1655–1669. https://doi.org/10.1007/s12205-020-1781-8

Taylor, K.E., Stouffer, R.J., Meehl, G.A., 2012. An overview of CMIP5 and the experiment design. Bulletin of the American Meteorological Society 93, 485–498. https://doi.org/10.1175/BAMS-D-11-00094.1

van Vuuren, D.P., Edmonds, J., Kainuma, M., Riahi, K., Thomson, A., Hibbard, K., Hurtt, G.C., Kram, T., Krey, V., Lamarque, J.F., Masui, T., Meinshausen, M., Nakicenovic, N., Smith, S.J., Rose, S.K., 2011. The representative concentration pathways: An overview. Climatic Change 109, 5–31. https://doi.org/10.1007/s10584-011-0148-z

Vogel, M.M., Zscheischler, J., Wartenburger, R., Dee, D., Seneviratne, S.I., 2019. Concurrent 2018 Hot Extremes Across Northern Hemisphere Due to Human-Induced Climate Change. Earth's Future 7, 692–703. https://doi.org/10.1029/2019EF001189

Zhang, Q., Knowles, J.F., Barnes, R.T., Cowie, R.M., Rock, N., Williams, M.W., 2018. Surface and subsurface water contributions to streamflow from a mesoscale watershed in complex mountain terrain. Hydrological Processes. https://doi.org/10.1002/hyp.11469

Zhang, Z., Li, Y., Barlage, M., Chen, F., Miguez-Macho, G., Ireson, A., Li, Z., 2020. Modeling groundwater responses to climate change in the Prairie Pothole Region. Hydrology and Earth System Sciences 24, 655–672. https://doi.org/10.5194/hess-24-655-2020

Zhou, J., Pomeroy, J.W., Zhang, W., Cheng, G., Wang, G., Chen, C., 2014. Simulating cold regions hydrological processes using a modular model in the west of China. Journal of Hydrology 509, 13–24. https://doi.org/10.1016/j.jhydrol.2013.11.013

Zhou, Y., Li, W., 2011. A review of regional groundwater flow modeling. Geoscience Frontiers. https://doi.org/10.1016/j.gsf.2011.03.003

CHAPTER IV – CONCLUSION

4.1 Research Summary

Snowmelt and groundwater dynamics are among the most important hydrological processes in northern latitudes and cold regions that affect dynamics of water quantity and quality of different spatio-temporal scales. Therefore, the primary goal of this study was to develop a framework for assessing the performance and uncertainty associated with different snowmelt modules in hydrological modelling, as well as analysis of regional snow depth, snowmelt and groundwater-surface water (GW-SW) interactions using process-based hydrological modelling. To achieve these goals, the Soil and Water Assessment Tool (SWAT) model was coupled with Energy Balance Modules (EBM) and Temperature-Index Modules (TIM) for assessment of uncertainties in snow depth and snowmelt simulation. The model was also coupled with MODFLOW model for assessment of GW-SW interaction and its response for snowmelt dynamics under changing climate. The models were applied to North Saskatchewan River Basin (NSRB) in central Alberta. The heterogeneity of NSRB in terms of climate, topography and land-use/land-cover allowed us to perform regional analysis of snow and GW-SW interactions in mountainous, foothill, and plain regions in order to assess the effect of regional topography and climate on hydrological responses and their underlying uncertainties in northern latitudes.

First, we analyzed the performance and uncertainty of snow depth and streamflow simulations and projections using different snowmelt modules. We used two generally-used snowmelt approaches including of TIMs and EBMs within SWAT model. We used SWAT default snowmelt approach as one of the widely-used TIMs, and embedded the EBM module into SWAT source code. We also implemented two snow density (SND) approaches in SWAT

source code to account for the effect of snow density functions in performance and uncertainty of snow depth simulations and projections. The two snow density approaches were previously implemented in maritime regions (namely SND1, Qi et al., 2017) and Canadian Prairies (namely SND2, Pomeroy et al., 1998). Results for streamflow simulations, subbasin-scale snow depth simulations, and regional snow depth simulations and projections under climate change scenarios were then analyzed and discussed. The regional analysis of snow depth for 1999-2007 was reported for mountainous, foothill and plain regions of NSRB. For uncertainty assessment of snow depth projections in 2040-2065 time window, we used the Analysis of Variance (ANOVA) approach for quantifying the uncertainty sources related to snow depth projections based on an ensemble of five GCMs, under two future scenarios of RCP2.6 and RCP8.5, and using two downscaling methods.

Results showed that the performance of SWAT-EBM and SWAT-TIM were relatively similar in all three regions of NSRB, while all snowmelt approaches were showing poor performances in mountainous region. However, SWAT-EBM overestimated snow accumulation and spring snowmelt runoff. Also, the choice of SND formulation played a significant role in performance and uncertainty of snow depth analysis, where SND2 resulted in more reliable results of snow depth simulations in all regions of NSRB. The evaluation of cascade of uncertainty for different regions and snowmelt approaches of NSRB showed that the share of uncertainty sources varied among different months and different regions. In general, the share of hydrological model parameter uncertainty (i.e., EBMs and TIMs) was dominant in mountainous region, while the share of GCMs, RCPs, downscaling methods and their interactions was increased in foothill and plain regions. These results provided a better understanding of the performance and uncertainties of using TIMs and EBMs, as well as different snow density

approaches, in regional analysis of snow depth. The results also mark the importance of considering multi-scale spatio-temporal analysis of regional snow depth simulation and projection. Particularly, while some researchers might argue that either GCMs, RCPs, DS or parameter uncertainty could be the main uncertainty source of hydrological projections, this study shows that the dominance of such sources can be substantially different based on spatial and temporal difference of study regions. Another key message from our uncertainty analysis is that in the areas where quality and quantity of input climate data for initial model setup is poor (i.e., mountainous region), the uncertainty of hydrologic model dominates all other uncertainty sources, and both EBMs and TIMs perform equally poor with a high uncertainty range. However, differences between EBMs and TIMs become more apparent in lower elevation regions, where a greater quality and quantity input data were used to initiate model runs and to represent climate variability, a key driver of hydrology and snowmelt, in foothills and plain regions.

Following the snowmelt and snow depth analysis, we focused on regional snowmelt and GW-SW interactions and their changes under future climate conditions. Furthermore, the relations between snowmelt and GW-SW interactions were analyzed in mountainous, foothill and plain regions of NSRB in order to understand how snowmelt governs GW-SW interactions under different spatio-temporal settings. We implemented the integrated SWAT-MODFLOW model for analyzing and projecting snowmelt and GW-SW interactions. For setting up the modelling, we implemented the most suitable snowmelt module from the first part of research (i.e., SWAT-TIM-SND2) to set up, calibrate, and validate the SWAT model based on historical streamflow data (1986-2007) of NSRB. Also, we set up and calibrated the MODFLOW model based on historical hydraulic head data (1983-2007) in various observation wells of the basin.

After model calibration and validation, historical trends of regional snowmelt and GW-SW interactions in different regions of NSRB were outlined, as well as their projected changes under future climate scenarios. The future climate change scenarios were carried out using five GCMs under two emission scenarios of RCP2.6 and RCP8.5. Finally, we evaluated the correlations between snowmelt and GW-SW interactions in different regions, as well as discussing possible drivers of their inter-relations.

The historical simulations of snowmelt and GW-SW interactions and their changes under climate change scenarios revealed the spatio-temporal importance of response of different hydrological processes to climate change. Analysis of snowmelt projections under climate change scenarios predicted earlier snowmelt in mountainous region, with significant decrease of future snowmelt in summer, fall and winter seasons. The shift of snowmelt to early spring has resulted in slower snowmelts in summer to winter, which can be also related to less snow fall and accumulation in mountainous regions. Also, it is predicted that snowmelt will mostly increase in foothill regions, and drop significantly in spring and summer of plain regions. These changes are mostly related to the pattern of precipitation and snowfall in foothill and plain regions, accompanied by temperature increase in such regions. On the other hand, future projections of GW-SW interactions showed that the contribution of groundwater to surface water will increase under future climate scenarios, particularly in warm seasons (i.e., spring and summer). The important effect of earlier snowmelt under future climate scenarios was explained by the results in foothills regions, where it is predicted that groundwater discharge to surface water will increase in spring and summer. As the foothill region is predictably affected by earlier snowmelt, groundwater recharge in this region will increase in the summer, which is the result of soil moisture depletion in that season.

Finally, the relations of regional snowmelt and GW-SW interactions were evaluated through correlation analysis in NSRB regions. High correlation between these two processes was found ($R^2 = 0.494$) in mountainous regions, in contrast to very low correlations ($R^2 < 0.01$) for foothill and plain regions. The low correlation of snowmelt and GW-SW interactions of foothill and plain regions was then attributed to three possible reasons, which are different from those in mountainous regions: (1) high amounts of ET in foothill and plain regions, which could significantly affect groundwater level and GW-SW interactions; (2) the effect of rainfall on GW-SW interactions, particularly in growing seasons where ET and rainfall will alter the dynamics of groundwater recharge and discharge; and (3) the effect of upstream-downstream connection of surface water and groundwater from mountainous regions to foothills and plains regions;

4.2 Study Limitations and Future Directions

The use of hydrological modelling, particularly in regional applications, can always bring about uncertainties and limitations in thoroughly representing the complex interactions of various hydrological processes in a large area. Therefore, the limitations of this study can be summarized as below:

1. The regional study of snowmelt and snow depth modelling requires reliable input data, such as altitudinal representative precipitation, climate, radiation, and other climate data at a high spatial and temporal resolution, and minimal gaps to be existed in datasets. In mountainous regions of NSRB, where the most important hydrological and hydrogeological water processes occur, the number of station data cannot adequately represent the complex climate and topography of that region. Also, the gridded data used for input climate and historical snow depth values had relatively coarse resolutions when compared to the variable

topography and elevation of the west side of NSRB. Therefore, the data availability could play a vital part in representation of hydrological processes through regional modelling, albeit we provided the most reliable data (existed by the date of analysis) for simulation and climate change scenario analysis of all regions within NSRB. Finally, the usage of observed SND data as well as implementing several other SND formulations on snow depth analysis can be beneficial for validating the snow density reproduction results.

2. The setup of MODFLOW model requires various hydrogeological information, properties of geological formations, groundwater storage, groundwater recharge data, constant head, and river data. One of the limitations of this study was the unavailability of geological formation data in mountainous regions of NSRB. The inevitable assumptions related to this gap might have some effects on groundwater simulation and calibrations. Moreover, despite the 10-km grid cell used in MODFLOW and SWAT-MODFLOW analysis, a 25-year simulation of SWAT-MODFLOW lasted more than 8 hours while using a 200-core super-computer. This is mainly because SWAT-MODFLOW is run based on daily runs of MODFLOW in transient mode with daily runs of SWAT. Since the groundwater dynamics are much slower than surface water, the changes in groundwater system can be reported in weekly, bi-weekly or monthly time-steps, while still representing groundwater dynamics properly. Therefore, linking daily-basis simulation runs of SWAT with weekly- or monthly-basis simulations of MODFLOW can greatly reduce the SWAT-MODFLOW simulation time, without degrading the simulation quality in terms of results and dynamics.
3. Various factors and processes have potentially great impact on sub-surface flow and its interaction with surface water. The effects of wetlands, potholes and water bodies can be significant in GW-SW interactions since they attenuate water flow and provide the base for

GW-SW interactions. However, at a large regional scale such effect might be critical only in specific sub-basins, where these water bodies are dominant landscape features in them. If the majority of sub-basins are governed with such water bodies in entire study watershed, then a significant effect can been found in regional GW-SW interactions. Furthermore, improvements in the representation of (1) low permeability lenses, (2) geospatial features related to prehistoric and contemporary times, and (3) frozen soil as well as their effect on and water infiltration and surface-sub surface connectivity of water can be a subject for future studies of regional analysis of snowmelt and groundwater. In the end, we acknowledge that land-use/land-cover and hydraulic conductivity (K) values were assumed to be constant throughout the historical and future analysis, while it is shown that changes in soil type, vegetation cover, and K values can directly affect snowmelt and its relation with GW-SW interactions.

This study provided the basis for understanding the performance and uncertainty associated with simulation and projection of snow depth and streamflow using multiple snowmelt and snow density approaches. We also presented the projected future of regional snowmelt and GW-SW dynamics, as well as how they can be correlated and dependent on one another. It is clear that model parameterization under lack of data can result in noticeable uncertainty in future projections of streamflow and snow depth. While the improvements in providing more reliable input data are yet in demand, simulations and projections of snow, streamflow, and groundwater dynamics in regional scale can provide the fundamental understanding of most important and critical elements of hydrological processes in northern latitudes. As a result, comprehensive studies such as this research effort may help policy-makers in facing possible adversaries under the uncertain future of climate and water resources.

BIBLIOGRAPHY

Abbas, T., Hussain, F., Nabi, G., Boota, M.W., Wu, R.-S., 2019. Uncertainty evaluation of SWAT model for snowmelt runoff in a Himalayan watershed. Terrestrial, Atmospheric and Oceanic Sciences 30, df. https://doi.org/10.3319/tao.2018.10.08.01

Abbaspour, K.C., 2015. SWAT-CUP: SWAT Calibration and Uncertainty Programs- A User Manual, Department of Systems Analysis, Intergrated Assessment and Modelling (SIAM),EAWAG. Swiss Federal Institute of Aqualtic Science and Technology, Duebendorf, Switzerland. https://doi.org/10.1007/s00402-009-1032-4

Adams, J.J., Rostron, B.J., Mendoza, C.A., 2004. Coupled fluid flow, heat and mass transport, and erosion in the Alberta basin: Implications for the origin of the Athabasca oil sands. Canadian Journal of Earth Sciences 41, 1077–1095. https://doi.org/10.1139/E04-052

Aggarwal, S.P., Thakur, P.K., Nikam, B.R., Garg, V., 2014. Integrated approach for snowmelt run-off estimation using temperature index model, remote sensing and GIS. Current Science 106, 397–407.

Akiyama Sakai, A., Yamazaki, Y., Wang, G., Fujita, K., Nakawo, M., Kubota, J., and Konagaya, Y., T., 2007. Surfacewater-groundwater interaction in the Heihe River basin, Northwestern China. Bull Glaciol Res.

Alberta Environment and Parks, 2019. Alberta river basins [WWW Document]. URL https://web.archive.org/web/20160409210242/http://www.environment.alberta.ca/apps/basins/default.aspx (accessed 7.30.19).

Alberta Geological Survey, 2019. 3D provincial geological framework model of Alberta, version 2.

Aliyari, F., Bailey, R.T., Tasdighi, A., Dozier, A., Arabi, M., Zeiler, K., 2019. Coupled SWAT-MODFLOW model for large-scale mixed agro-urban river basins. Environmental Modelling and Software 115, 200–210. https://doi.org/10.1016/j.envsoft.2019.02.014

Allen, D.M., Whitfield, P.H., Werner, A., 2010. Groundwater level responses in temperate mountainous terrain: Regime classification, and linkages to climate and streamflow. Hydrological Processes 24, 3392–3412. https://doi.org/10.1002/hyp.7757

Ammar, M.E., Gharib, A., Islam, Z., Davies, E.G.R., Seneka, M., Faramarzi, M., 2020. Future floods using hydroclimatic simulations and peaks over threshold: An alternative to nonstationary analysis inferred from trend tests. Advances in Water Resources 136, 103463. https://doi.org/10.1016/j.advwatres.2019.103463

Anand, J., Gosain, A.K., Khosa, R., Srinivasan, R., 2018. Regional scale hydrologic modeling for prediction of water balance, analysis of trends in streamflow and variations in streamflow: The case study of the Ganga River basin. Journal of Hydrology: Regional Studies 16, 32–53. https://doi.org/10.1016/j.ejrh.2018.02.007

Arnold, J., Moriasi, D., Gassman, P., Abbaspour, K., White, M., Srinivasan, R., Santhi, C.,

Harmel, R., van Griensven, A., Van Liew, M., Kannan, N., Jha, M., 2012. SWAT: Model Use, Calibration, and Validation. Transactions of the ASABE 55, 1317–1335. https://doi.org/10.13031/2013.42244

Arnold, J., Srinivasan, R., Muttiah, R., Williams, J., 1998. Large Area Hydrologic Modeling and Assessment; Part I: Model Development. Journal of the American Water Resources Association 17, 73. https://doi.org/10.1016/S0899-9007(00)00483-4

Ashraf Vaghefi, S., Iravani, M., Sauchyn, D., Andreichuk, Y., Goss, G., Faramarzi, M., 2019. Regionalization and parameterization of a hydrologic model significantly affect the cascade of uncertainty in climate-impact projections. Climate Dynamics 0, 0. https://doi.org/10.1007/s00382-019-04664-w

Assani, A.A., Landry, R., Laurencelle, M., 2012. Comparison of interannual variability modes and trends of seasonal precipitation and streamflow in southern quebec (canada). River Research and Applications. https://doi.org/10.1002/rra.1544

Avanzi, F., De Michele, C., Ghezzi, A., 2015. On the performances of empirical regressions for the estimation of bulk snow density. Geogr. Fis. Dinam. Quat. 38, 105–112. https://doi.org/10.4461/GFDQ.2015.38.10

Aygün, O., Kinnard, C., Campeau, S., 2020. Impacts of climate change on the hydrology of northern midlatitude cold regions, Progress in Physical Geography. https://doi.org/10.1177/0309133319878123

Bai, Y., Fernald, A., Tidwell, V., Gunda, T., 2019. Reduced and Earlier Snowmelt Runoff Impacts Traditional Irrigation Systems. Journal of Contemporary Water Research & Education. https://doi.org/10.1111/j.1936-704x.2019.03318.x

Bailey, R.T., Wible, T.C., Arabi, M., Records, R.M., Ditty, J., 2016. Assessing regional-scale spatio-temporal patterns of groundwater–surface water interactions using a coupled SWAT-MODFLOW model. Hydrological Processes 30, 4420–4433. https://doi.org/10.1002/hyp.10933

Barthel, R., Banzhaf, S., 2016. Groundwater and Surface Water Interaction at the Regional-scale – A Review with Focus on Regional Integrated Models. Water Resources Management. https://doi.org/10.1007/s11269-015-1163-z

Bavera, D., Bavay, M., Jonas, T., Lehning, M., De Michele, C., 2014. A comparison between two statistical and a physically-based model in snow water equivalent mapping. Advances in Water Resources 63, 167–178. https://doi.org/10.1016/j.advwatres.2013.11.011

Bekele, E.B., Rostron, B.J., Person, M.A., 2003. Fluid pressure implications of erosional unloading, basin hydrodynamics and glaciation in the Alberta Basin, Western Canada. Journal of Geochemical Exploration 78–79, 143–147. https://doi.org/10.1016/S0375-6742(03)00148-1

Beven, K., Freer, J., 2001. Equifinality, data assimilation, and uncertainty estimation in mechanistic modelling of complex environmental systems using the GLUE methodology.

Journal of Hydrology 249, 11–29. https://doi.org/https://doi.org/10.1016/S0022-1694(01)00421-8

Bocchiola, D., Groppelli, B., 2010. Spatial estimation of snow water equivalent at different dates within the Adamello Park of Italy. Cold Regions Science and Technology 63, 97–109. https://doi.org/10.1016/j.coldregions.2010.06.001

Bormann, K.J., Westra, S., Evans, J.P., McCabe, M.F., 2013. Spatial and temporal variability in seasonal snow density. Journal of Hydrology 484, 63–73. https://doi.org/10.1016/j.jhydrol.2013.01.032

Bosshard, T., Carambia, M., Georgen, K., Kotlarski, S., Krahe, P., Zappa, M., Schar, C., 2013. Quantifying uncertainty sources in an emsemble of hydrological climate-impact projections. Water Resources Research 49, 1523–1536. https://doi.org/10.1007/s00704-017-2359-3

Brannen, R., Spence, C., Ireson, A., 2015. Influence of shallow groundwater-surface water interactions on the hydrological connectivity and water budget of a wetland complex. Hydrological Processes 29, 3862–3877. https://doi.org/10.1002/hyp.10563

Brimelow, J., Stewart, R., Hanesiak, J., Kochtubajda, B., Szeto, K., Bonsal, B., 2014. Characterization and assessment of the devastating natural hazards across the Canadian Prairie Provinces from 2009 to 2011. Natural Hazards 73, 761–785. https://doi.org/10.1007/s11069-014-1107-6

Brown, R.D., B.Bransnett, 2010. Canadian Meteorological Centre (CMC) Daily Snow Depth Analysis Data, Version 1. [WWW Document]. Boulder, Colorado USA. NASA National Snow and Ice Data Center Distributed Active Archive Center. https://doi.org/10.5067/W9FOYWH0EQZ3

Bürger, G., Sobie, S.R., Cannon, A.J., Werner, A.T., Murdock, T.Q., 2013. Downscaling extremes: An intercomparison of multiple methods for future climate. Journal of Climate 26, 3429–3449. https://doi.org/10.1175/JCLI-D-12-00249.1

Candela, L., Elorza, F.J., Tamoh, K., Jiménez-Martínez, J., Aureli, A., 2014. Groundwater modelling with limited data sets: The Chari-Logone area (Lake Chad Basin, Chad). Hydrological Processes. https://doi.org/10.1002/hyp.9901

Cannon, A.J., 2015. Selecting GCM scenarios that span the range of changes in a multimodel ensemble: Application to CMIP5 climate extremes indices. Journal of Climate 28, 1260–1267. https://doi.org/10.1175/JCLI-D-14-00636.1

Carroll, R.W.H., Bearup, L.A., Brown, W., Dong, W., Bill, M., Willlams, K.H., 2018. Factors controlling seasonal groundwater and solute flux from snow-dominated basins. Hydrological Processes 32, 2187–2202. https://doi.org/10.1002/hyp.13151

Carroll, R.W.H., Deems, J.S., Niswonger, R., Schumer, R., Williams, K.H., 2019. The Importance of Interflow to Groundwater Recharge in a Snowmelt-Dominated Headwater Basin. Geophysical Research Letters 46, 5899–5908. https://doi.org/10.1029/2019GL082447

Chauvin, G.M., Flerchinger, G.N., Link, T.E., Marks, D., Winstral, A.H., Seyfried, M.S., 2011. Long-term water balance and conceptual model of a semi-arid mountainous catchment. Journal of Hydrology 400, 133–143. https://doi.org/10.1016/j.jhydrol.2011.01.031

Chawla, I., Mujumdar, P.P., 2018. Partitioning uncertainty in streamflow projections under nonstationary model conditions. Advances in Water Resources 112, 266–282. https://doi.org/10.1016/j.advwatres.2017.10.013

Chen, J., Brissette, F.P., Leconte, R., 2011a. Uncertainty of downscaling method in quantifying the impact of climate change on hydrology. Journal of Hydrology 401, 190–202. https://doi.org/10.1016/j.jhydrol.2011.02.020

Chen, J., Brissette, F.P., Poulin, A., Leconte, R., 2011b. Overall uncertainty study of the hydrological impacts of climate change for a Canadian watershed. Water Resources Research 47, 1–16. https://doi.org/10.1029/2011WR010602

Chen, M., Izady, A., Abdalla, O.A., 2017. An efficient surrogate-based simulation-optimization method for calibrating a regional MODFLOW model. Journal of Hydrology 544, 591–603. https://doi.org/10.1016/j.jhydrol.2016.12.011

Chunn, D., Faramarzi, M., Smerdon, B., Alessi, D.S., 2019. Application of an integrated SWAT-MODFLOW model to evaluate potential impacts of climate change and water withdrawals on groundwater-surface water interactions in west-central Alberta. Water (Switzerland) 11. https://doi.org/10.3390/w11010110

Clilverd, H.M., White, D.M., Tidwell, A.C., Rawlins, M.A., 2011. The sensitivity of northern groundwater recharge to climate change: A case study in Northwest Alaska. Journal of the American Water Resources Association 47, 1228–1240. https://doi.org/10.1111/j.1752-1688.2011.00569.x

Clow, D.W., Nanus, L., Verdin, K.L., Schmidt, J., 2012. Evaluation of SNODAS snow depth and snow water equivalent estimates for the Colorado Rocky Mountains, USA. Hydrological Processes 26, 2583–2591. https://doi.org/10.1002/hyp.9385

Cochand, F., Therrien, R., Lemieux, J.M., 2019. Integrated Hydrological Modeling of Climate Change Impacts in a Snow-Influenced Catchment. Groundwater. https://doi.org/10.1111/gwat.12848

Cochand, M., Christe, P., Ornstein, P., Hunkeler, D., 2019. Groundwater Storage in High Alpine Catchments and Its Contribution to Streamflow. Water Resources Research 55, 2613–2630. https://doi.org/10.1029/2018WR022989

Comola, F., Schaefli, B., Ronco, P. Da, Botter, G., Bavay, M., Rinaldo, A., Lehning, M., 2015. Scale-dependent effects of solar radiation patterns on the snow-dominated hydrologic response. Geophysical Research Letters 42, 3895–3902. https://doi.org/10.1002/2015GL064075

Condon, L.E., Atchley, A.L., Maxwell, R.M., 2020. Evapotranspiration depletes groundwater under warming over the contiguous United States. Nature communications 11, 873.

https://doi.org/10.1038/s41467-020-14688-0

DeBeer, C.M., Pomeroy, J.W., 2017. Influence of snowpack and melt energy heterogeneity on snow cover depletion and snowmelt runoff simulation in a cold mountain environment. Journal of Hydrology 553, 199–213. https://doi.org/10.1016/j.jhydrol.2017.07.051

Debele, B., Srinivasan, R., Gosain, A.K., 2010. Comparison of process-based and temperature-index snowmelt modeling in SWAT. Water Resources Management 24, 1065–1088. https://doi.org/10.1007/s11269-009-9486-2

Deng, Y., Flerchinger, G.N., Cooley, K.R., 1994. Impacts of spatially and temporally varying snowmelt on subsurface flow in a mountainous watershed: 2. Subsurface processes. Hydrological Sciences Journal. https://doi.org/10.1080/02626669409492772

Déqué, M., Rowell, D.P., Lüthi, D., Giorgi, F., Christensen, J.H., Rockel, B., Jacob, D., Kjellström, E., De Castro, M., Van Den Hurk, B., 2007. An intercomparison of regional climate simulations for Europe: Assessing uncertainties in model projections. Climatic Change 81, 53–70. https://doi.org/10.1007/s10584-006-9228-x

Devito, K.J., Hill, A.R., Roulet, N., 1996. Groundwater-surface water interactions in headwater forested wetlands of the Canadian Shield. Journal of Hydrology. https://doi.org/10.1016/0022-1694(95)02912-5

Dingman, L., 2015. Physical Hydrology. Waveland Press.

Du, X., Loiselle, D., Alessi, D.S., Faramarzi, M., 2020. Hydro-climate and biogeochemical processes control watershed organic carbon inflows: Development of an in-stream organic carbon module coupled with a process-based hydrologic model. Science of the Total Environment 718, 137281. https://doi.org/10.1016/j.scitotenv.2020.137281

Dumanski, S., Pomeroy, J.W., Westbrook, C.J., 2015. Hydrological regime changes in a Canadian Prairie basin. Hydrological Processes 29, 3893–3904. https://doi.org/10.1002/hyp.10567

Elias, E.H., Rango, A., Steele, C.M., Mejia, J.F., Smith, R., 2015. Assessing climate change impacts on water availability of snowmelt-dominated basins of the Upper Rio Grande basin. Journal of Hydrology: Regional Studies 3, 525–546. https://doi.org/10.1016/j.ejrh.2015.04.004

FAO, 2003. Digital soil map of the world and derived soil properties. Rome, Italy: FAO.

Faramarzi, M., Abbaspour, K.C., Adamowicz, W.L.V., Lu, W., Fennell, J., Zehnder, A.J.B., Goss, G.G., 2017. Uncertainty based assessment of dynamic freshwater scarcity in semi-arid watersheds of Alberta, Canada. Journal of Hydrology: Regional Studies 9, 48–68. https://doi.org/10.1016/j.ejrh.2016.11.003

Faramarzi, M., Abbaspour, K.C., Schulin, R., Yang, H., 2009. Modelling blue and green water resources availability in Iran. Hydrological Processes 26, 1–16. https://doi.org/10.1002/hyp

Faramarzi, M., Srinivasan, R., Iravani, M., Bladon, K.D., Abbaspour, K.C., Zehnder, A.J.B.,

Goss, G.G., 2015. Setting up a hydrological model of Alberta: Data discrimination analyses prior to calibration. Environmental Modelling and Software 74, 48–65. https://doi.org/10.1016/j.envsoft.2015.09.006

Ficklin, D.L., Barnhart, B.L., 2014. SWAT hydrologic model parameter uncertainty and its implications for hydroclimatic projections in snowmelt-dependent watersheds. Journal of Hydrology 519, 2081–2090. https://doi.org/10.1016/j.jhydrol.2014.09.082

Field, C.B., Barros, V.R., Dokken, D.J., Mach, K.J., Mastrandrea, M.D., Bilir, T.E., Chatterjee, M., Ebi, K.L., Estrada, Y.O., Genova, R.C., Girma, B., Kissel, E.S., Levy, A.N., MacCracken, S., Mastrandrea, P.R., White, L.L., 2014. Climate change 2014 impacts, adaptation and vulnerability: Part A: Global and sectoral aspects: Working group II contribution to the fifth assessment report of the intergovernmental panel on climate change, Climate Change 2014 Impacts, Adaptation and Vulnerability: Part A: Global and Sectoral Aspects. https://doi.org/10.1017/CBO9781107415379

Finger, D., Heinrich, G., Gobiet, A., Bauder, A., 2012. Projections of future water resources and their uncertainty in a glacierized catchment in the Swiss Alps and the subsequent effects on hydropower production during the 21st century. Water Resources Research. https://doi.org/10.1029/2011WR010733

Flerchinger, G.N., Cooley, K.R., Ralston, D.R., 1992. Groundwater response to snowmelt in a mountainous watershed. Journal of Hydrology 133. https://doi.org/10.1016/0022-1694(92)90260-3

Foster, S.B., Allen, D.M., 2015. Groundwater - Surface Water Interactions in a Mountain-to-Coast Watershed: Effects of Climate Change and Human Stressors. Advances in Meteorology 2015. https://doi.org/10.1155/2015/861805

Franz, K.J., Hogue, T.S., Sorooshian, S., 2008. Operational snow modeling: Addressing the challenges of an energy balance model for National Weather Service forecasts. Journal of Hydrology 360, 48–66. https://doi.org/10.1016/j.jhydrol.2008.07.013

Fu, C., James, A.L., Yao, H., 2015. Investigations of uncertainty in SWAT hydrologic simulations: A case study of a Canadian Shield catchment. Hydrological Processes 29, 4000–4017. https://doi.org/10.1002/hyp.10477

Fuka, D.R., Easton, Z.M., Brooks, E.S., Boll, J., Steenhuis, T.S., Walter, M.T., 2012. A Simple Process-Based Snowmelt Routine to Model Spatially Distributed Snow Depth and Snowmelt in the SWAT Model. Journal of the American Water Resources Association 48, 1151–1161. https://doi.org/10.1111/j.1752-1688.2012.00680.x

Gao, Z., Wang, Z., Wang, S., Wu, X., An, Y., Wang, W., Liu, J., 2019. Factors that influence the chemical composition and evolution of shallow groundwater in an arid region: a case study from the middle reaches of the Heihe River, China. Environmental Earth Sciences. https://doi.org/10.1007/s12665-019-8391-0

Gleeson, T., Marklund, L., Smith, L., Manning, A.H., 2011. Classifying the water table at regional to continental scales. Geophysical Research Letters 38, 1–6.

https://doi.org/10.1029/2010GL046427

Golder Associates, 2008. Assessment of climate change effects on water yield from the North Saskatchewan River Basin.

Gomez-Velez, J.D., Krause, S., Wilson, J.L., 2014. Effect of low-permeability layers on spatial patterns of hyporheic exchange and groundwater upwelling. Water Resources Research. https://doi.org/10.1002/2013WR015054

Government of Canada, 2019. Historical Climate Data [WWW Document]. URL http://climate.weather.gc.ca/historical_data/search_historic_data_e.html (accessed 8.6.19).

Government of Canada, 2017. Canadian Land Cover, Circa 2000 (Vector) - GeoBase Series, 1996-2005 [WWW Document]. URL https://open.canada.ca/data/en/dataset/97126362-5a85-4fe0-9dc2-915464cfdbb7 (accessed 4.15.20).

Gray, D.M., Landine, P.G., 1988. An energy-budget snowmelt model for the Canadian Prairies. Canadian Journal of Earth Sciences 25, 1292–1303. https://doi.org/10.1139/e88-124

Guevara Ochoa, C., Medina Sierra, A., Vives, L., Zimmermann, E., Bailey, R., 2020. Spatio-temporal patterns of the interaction between groundwater and surface water in plains. Hydrological Processes 34, 1371–1392. https://doi.org/10.1002/hyp.13615

Guillaume, J.H.A., Jakeman, J.D., Marsili-Libelli, S., Asher, M., Brunner, P., Croke, B., Hill, M.C., Jakeman, A.J., Keesman, K.J., Razavi, S., Stigter, J.D., 2019. Introductory overview of identifiability analysis: A guide to evaluating whether you have the right type of data for your modeling purpose. Environmental Modelling and Software 119, 418–432. https://doi.org/10.1016/j.envsoft.2019.07.007

Guzman, J.A., Moriasi, D.N., Gowda, P.H., Steiner, J.L., Starks, P.J., Arnold, J.G., Srinivasan, R., 2015. A model integration framework for linking SWAT and MODFLOW. Environmental Modelling and Software 73, 103–116. https://doi.org/10.1016/j.envsoft.2015.08.011

Haddeland, I., Heinke, J., Biemans, H., Eisner, S., Flörke, M., Hanasaki, N., Konzmann, M., Ludwig, F., Masaki, Y., Schewe, J., Stacke, T., Tessler, Z.D., Wada, Y., Wisser, D., 2014. Global water resources affected by human interventions and climate change. Proceedings of the National Academy of Sciences of the United States of America. https://doi.org/10.1073/pnas.1222475110

Hagemann, S., Chen, C., Clark, D.B., Folwell, S., Gosling, S.N., Haddeland, I., Hanasaki, N., Heinke, J., Ludwig, F., Voss, F., Wiltshire, A.J., 2013. Climate change impact on available water resources obtained using multiple global climate and hydrology models. Earth System Dynamics. https://doi.org/10.5194/esd-4-129-2013

Haghnegahdar, A., Razavi, S., Yassin, F., Wheater, H., 2017. Multicriteria sensitivity analysis as a diagnostic tool for understanding model behaviour and characterizing model uncertainty. Hydrological Processes 31, 4462–4476. https://doi.org/10.1002/hyp.11358

Harder, P., Helgason, W.D., Pomeroy, J.W., 2018. Modeling the Snowpack Energy Balance

during Melt under Exposed Crop Stubble. Journal of Hydrometeorology 19, 1191–1214. https://doi.org/10.1175/jhm-d-18-0039.1

Harding, R., Best, M., Blyth, E., Hagemann, S., kabat, P., Tallaksen, L.M., Warnaars, T., Wiberg, D., Weedon, G.P., Van Lanen, H., Ludwig, F., Haddeland, I., 2011. WATCH: Current knowledge of the terrestrial global water cycle. Journal of Hydrometeorology. https://doi.org/10.1175/JHM-D-11-024.1

Harma, K.J., Johnson, M.S., Cohen, S.J., 2012. Future Water Supply and Demand in the Okanagan Basin, British Columbia: A Scenario-Based Analysis of Multiple, Interacting Stressors. Water Resources Management. https://doi.org/10.1007/s11269-011-9938-3

Hayashi, M., Farrow, C.R., 2014. Watershed-scale response of groundwater recharge to inter-annual and inter-decadal variability in precipitation (Alberta, Canada). Hydrogeology Journal 22, 1825–1839. https://doi.org/10.1007/s10040-014-1176-3

Hayashi, M., van der Kamp, G., Rosenberry, D.O., 2016. Hydrology of Prairie Wetlands: Understanding the Integrated Surface-Water and Groundwater Processes. Wetlands 36, 237–254. https://doi.org/10.1007/s13157-016-0797-9

Helbig, N., Van Herwijnen, A., Magnusson, J., Jonas, T., 2015. Fractional snow-covered area parameterization over complex topography. Hydrology and Earth System Sciences 19, 1339–1351. https://doi.org/10.5194/hess-19-1339-2015

Hock, R., 2003. Temperature index melt modelling in mountain areas. Journal of Hydrology 282, 104–115. https://doi.org/10.1016/S0022-1694(03)00257-9

Huntington, J.L., Niswonger, R.G., 2012. Role of surface-water and groundwater interactions on projected summertime streamflow in snow dominated regions: An integrated modeling approach. Water Resources Research 48, 1–20. https://doi.org/10.1029/2012WR012319

Intergovernamental Panel on Climate Change, 2013. Climate Change 2013.

Jamieson, B., Schirmer, M., 2016. Measuring snow surface temperature: why, why not, and how?

Jarvis, A., Guevara, E., Reuter, H.I., Nelson, A.D., 2008. Hole-filled SRTM for the globe : version 4 : data grid.

Jencso, K.G., McGlynn, B.L., Gooseff, M.N., Wondzell, S.M., Bencala, K.E., Marshall, L.A., 2009. Hydrologic connectivity between landscapes and streams: Transferring reach- and plot-scale understanding to the catchment scale. Water Resources Research. https://doi.org/10.1029/2008WR007225

Jost, G., Weiler, M., Gluns, D.R., Alila, Y., 2007. The influence of forest and topography on snow accumulation and melt at the watershed-scale. Journal of Hydrology 347, 101–115. https://doi.org/10.1016/j.jhydrol.2007.09.006

Jutebring Sterte, E., Johansson, E., Sjöberg, Y., Huseby Karlsen, R., Laudon, H., 2018. Groundwater-surface water interactions across scales in a boreal landscape investigated

using a numerical modelling approach. Journal of Hydrology. https://doi.org/10.1016/j.jhydrol.2018.03.011

Kim, Y., Ohn, I., Lee, J.K., Kim, Y.O., 2019. Generalizing uncertainty decomposition theory in climate change impact assessments. Journal of Hydrology X 3, 100024. https://doi.org/10.1016/j.hydroa.2019.100024

Kobierska, F., Jonas, T., Magnusson, J., Zappa, M., Bavay, M., Bosshard, T., Paul, F., Bernasconi, S.M., 2011. Climate change effects on snow melt and discharge of a partly glacierized watershed in Central Switzerland (SoilTrec Critical Zone Observatory). Applied Geochemistry 26, S60–S62. https://doi.org/10.1016/j.apgeochem.2011.03.029

Kornelsen, K.C., Coulibaly, P., 2014. Synthesis review on groundwater discharge to surface water in the Great Lakes Basin. Journal of Great Lakes Research. https://doi.org/10.1016/j.jglr.2014.03.006

Krause, P., Boyle, D.P., Bäse, F., 2005. Comparison of different efficiency criteria for hydrological model assessment. Advances in Geosciences 5, 89–97. https://doi.org/10.5194/adgeo-5-89-2005

Kult, J., Choi, W., Keuser, A., 2012. Snowmelt runoff modeling: Limitations and potential for mitigating water disputes. Journal of Hydrology. https://doi.org/10.1016/j.jhydrol.2012.01.043

Kundzewicz, Z.W., Döll, P., 2009. Will groundwater ease freshwater stress under climate change? Hydrological Sciences Journal. https://doi.org/10.1623/hysj.54.4.665

Kure, S., Jang, S., Ohara, N., Kavvas, M.L., Chen, Z.Q., 2013. Hydrologic impact of regional climate change for the snowfed and glacierfed river basins in the Republic of Tajikistan: Hydrological response of flow to climate change. Hydrological Processes. https://doi.org/10.1002/hyp.9535

Lewandowski, J., Meinikmann, K., Krause, S., 2020. Groundwater-surface water interactions: Recent advances and interdisciplinary challenges. Water (Switzerland). https://doi.org/10.3390/w12010296

Li, H., Wang, Z., He, G., Man, W., 2017. Estimating snow depth and snow water equivalence using repeat-pass interferometric SAR in the northern piedmont region of the Tianshan Mountains. Journal of Sensors 2017. https://doi.org/10.1155/2017/8739598

Liu, W., Wang, L., Sun, F., Li, Z., Wang, H., Liu, J., Yang, T., Zhou, J., Qi, J., 2018. Snow Hydrology in the Upper Yellow River Basin Under Climate Change: A Land Surface Modeling Perspective. Journal of Geophysical Research: Atmospheres 123, 12,676-12,691. https://doi.org/10.1029/2018JD028984

Liu, Y., Yang, W., Shao, H., Yu, Z., Lindsay, J., 2018. Development of an integrated modelling system for evaluating water quantity and quality effects of individual wetlands in an agriculturalwatershed. Water (Switzerland) 10. https://doi.org/10.3390/w10060774

Lucas-Picher, P., Riboust, P., Somot, S., Laprise, R., 2015. Reconstruction of the spring 2011

richelieu river flood by two regional climate models and a hydrological model. Journal of Hydrometeorology. https://doi.org/10.1175/JHM-D-14-0116.1

Lundberg, A., Ala-Aho, P., Eklo, O., Klöve, B., Kværner, J., Stumpp, C., 2016. Snow and frost: Implications for spatiotemporal infiltration patterns - a review. Hydrological Processes. https://doi.org/10.1002/hyp.10703

MacDonald, R.J., Byrne, J.M., Boon, S., Kienzle, S.W., 2012. Modelling the Potential Impacts of Climate Change on Snowpack in the North Saskatchewan River Watershed, Alberta. Water Resources Management 26, 3053–3076. https://doi.org/10.1007/s11269-012-0016-2

Mahmood, T.H., Pomeroy, J.W., Wheater, H.S., Baulch, H.M., 2017. Hydrological responses to climatic variability in a cold agricultural region. Hydrological Processes 31, 854–870. https://doi.org/10.1002/hyp.11064

Mantua, N., Tohver, I., Hamlet, A., 2010. Climate change impacts on streamflow extremes and summertime stream temperature and their possible consequences for freshwater salmon habitat in Washington State. Climatic Change. https://doi.org/10.1007/s10584-010-9845-2

Mas, A., Baraer, M., Arsenault, R., Poulin, A., Préfontaine, J., 2018. Targeting high robustness in snowpack modeling for Nordic hydrological applications in limited data conditions. Journal of Hydrology 564, 1008–1021. https://doi.org/10.1016/j.jhydrol.2018.07.071

Massmann, C., 2019. Modelling snowmelt in ungauged catchments. Water (Switzerland) 11. https://doi.org/10.3390/w11020301

Masud, M.B., Ferdous, J., Faramarzi, M., 2018. Projected changes in hydrological variables in the agricultural region of Alberta, Canada. Water (Switzerland) 10. https://doi.org/10.3390/w10121810

Maurer, E.P., Brekke, L.D., Pruitt, T., 2010. Contrasting lumped and distributed hydrology models for estimating climate change impacts on California watersheds. Journal of the American Water Resources Association. https://doi.org/10.1111/j.1752-1688.2010.00473.x

Maurya, A.S., Rai, S.P., Joshi, N., Dutt, K.S., Rai, N., 2018. Snowmelt runoff and groundwater discharge in Himalayan rivers: a case study of the Satluj River, NW India. Environmental Earth Sciences. https://doi.org/10.1007/s12665-018-7849-9

McKenney, D.W., Hutchinson, M.F., Papadopol, P., Lawrence, K., Pedlar, J., Campbell, K., Milewska, E., Hopkinson, R.F., Price, D., Owen, T., 2011. Customized Spatial Climate Models for North America. Bulletin of the American Meteorological Society 92, 1611–1622. https://doi.org/10.1175/2011BAMS3132.1

Meloysund, V., Leira, B., Hoiseth, K. V., Liso, K.R., 2007. Review: Predicting snow density using meteorological data. Meteorological Applications 14, 413–423. https://doi.org/10.1002/met

Meng, T., Carewa, R., Florkowski, W.J., Klepacka, A.M., 2017. Analyzing temperature and precipitation influences on yield distributions of canola and spring wheat in Saskatchewan. Journal of Applied Meteorology and Climatology 56, 897–913.

https://doi.org/10.1175/JAMC-D-16-0258.1

Mizukami, N., Clark, M.P., Slater, A.G., Brekke, L.D., Elsner, M.M., Arnold, J.R., Gangopadhyay, S., 2014. Hydrologic implications of different large-scale meteorological model forcing datasets in mountainous regions. Journal of Hydrometeorology 15, 474–488. https://doi.org/10.1175/JHM-D-13-036.1

Moore, J.N., Harper, J.T., Greenwood, M.C., 2007. Significance of trends toward earlier snowmelt runoff, Columbia and Missouri Basin headwaters, western United States. Geophysical Research Letters 34, 1–5. https://doi.org/10.1029/2007GL031022

Negi, H.S., Thakur, N.K., Mishra, V.D., 2007. Estimation and validation of snow surface temperature using modis data for snow-avalanche studies in NW-Himalaya. Journal of the Indian Society of Remote Sensing 35, 287. https://doi.org/10.1007/BF02990785

Neitsch, S., Arnold, J., Kiniry, J., Williams, J., 2011. Soil & Water Assessment Tool Theoretical Documentation Version 2009. Texas Water Resources Institute 1–647. https://doi.org/10.1016/j.scitotenv.2015.11.063

North Saskatchewan Watershed Alliance, 2005. The State of the North Sask River Watershed Report.

Orozco, I., Francés, F., Mora, J., 2019. Parsimonious modeling of snow accumulation and snowmelt processes in high mountain basins. Water (Switzerland). https://doi.org/10.3390/w11061288

Park, S., Bailey, R.T., 2017. SWAT-MODFLOW Tutorial—Documentation for Preparing Model Simulations.

Paznekas, A., Hayashi, M., 2016. Groundwater contribution to winter streamflow in the Canadian Rockies. Canadian Water Resources Journal 41, 484–499. https://doi.org/10.1080/07011784.2015.1060870

Pomeroy, J.W., Gray, D.M., Shook, K.R., Toth, B., Essery, R.L.H., Pietroniro, A., Hedstrom, N., 1998. An evaluation of snow accumulation and ablation processes for land surface modelling. Hydrological Processes 12, 2339–2367. https://doi.org/10.1002/(SICI)1099-1085(199812)12:15<2339::AID-HYP800>3.0.CO;2-L

Poulin, A., Brissette, F., Leconte, R., Arsenault, R., Malo, J.S., 2011. Uncertainty of hydrological modelling in climate change impact studies in a Canadian, snow-dominated river basin. Journal of Hydrology 409, 626–636. https://doi.org/10.1016/j.jhydrol.2011.08.057

Pradhanang, S.M., Anandhi, A., Mukundan, R., Zion, M.S., Pierson, D.C., Schneiderman, E.M., Matonse, A., Frei, A., 2011. Application of SWAT model to assess snowpack development and streamflow in the Cannonsville watershed, New York, USA. Hydrological Processes 25, 3268–3277. https://doi.org/10.1002/hyp.8171

Prudhomme, C., Davies, H., 2009. Assessing uncertainties in climate change impact analyses on the river flow regimes in the UK. Part 2: Future climate. Climatic Change 93, 197–222. https://doi.org/10.1007/s10584-008-9461-6

Qi, J., Li, S., Jamieson, R., Hebb, D., Xing, Z., Meng, F.R., 2017. Modifying SWAT with an energy balance module to simulate snowmelt for maritime regions. Environmental Modelling and Software 93, 146–160. https://doi.org/10.1016/j.envsoft.2017.03.007

Qi, P., Zhang, G., Xu, Y.J., Xia, Z., Wang, M., 2019. Response of water resources to future climate change in a high-latitude river basin. Sustainability (Switzerland) 11. https://doi.org/10.3390/su11205619

Quilbé, R., Rousseau, A.N., Moquet, J.S., Trinh, N.B., Dibike, Y., Gachon, P., Chaumont, D., 2008. Assessing the effect of climate change on river flow using general circulation models and hydrological modelling - Application to the chaudière River, Québec, Canada. Canadian Water Resources Journal 33, 73–94.

Rahman, K., Maringanti, C., Beniston, M., Widmer, F., Abbaspour, K., Lehmann, A., 2013. Streamflow Modeling in a Highly Managed Mountainous Glacier Watershed Using SWAT: The Upper Rhone River Watershed Case in Switzerland. Water Resources Management 27, 323–339. https://doi.org/10.1007/s11269-012-0188-9

Raleigh, M.S., Clark, M.P., 2014. Are temperature-index models appropriate for assessing climate change impacts on snowmelt? Proc. 82nd Western Snow Conference 45–51.

Raleigh, M.S., Livneh, B., Lapo, K., Lundquist, J.D., 2016. How does availability of meteorological forcing data impact physically based snowpack simulations? Journal of Hydrometeorology 17, 99–120. https://doi.org/10.1175/JHM-D-14-0235.1

Razavi, S., Gupta, H. V., 2019. A multi-method Generalized Global Sensitivity Matrix approach to accounting for the dynamical nature of earth and environmental systems models. Environmental Modelling and Software 114, 1–11. https://doi.org/10.1016/j.envsoft.2018.12.002

Razavi, S., Tolson, B.A., Matott, L.S., Thomson, N.R., MacLean, A., Seglenieks, F.R., 2010. Reducing the computational cost of automatic calibration through model preemption. Water Resources Research 46, 1–17. https://doi.org/10.1029/2009WR008957

Renard, B., Kavetski, D., Kuczera, G., Thyer, M., Franks, S.W., 2010. Understanding predictive uncertainty in hydrologic modeling: The challenge of identifying input and structural errors. Water Resources Research 46, 1–22. https://doi.org/10.1029/2009WR008328

Reshmidevi, T. V., Nagesh Kumar, D., Mehrotra, R., Sharma, A., 2018. Estimation of the climate change impact on a catchment water balance using an ensemble of GCMs. Journal of Hydrology 556, 1192–1204. https://doi.org/10.1016/j.jhydrol.2017.02.016

Sadro, S., Sickman, J.O., Melack, J.M., Skeen, K., 2018. Effects of Climate Variability on Snowmelt and Implications for Organic Matter in a High-Elevation Lake. Water Resources Research 54, 4563–4578. https://doi.org/10.1029/2017WR022163

Saydi, M., Ding, J. li, Sagan, V., Qin, Y., 2019. Snowmelt modeling using two melt-rate models in the Urumqi River watershed, Xinjiang Uyghur Autonomous Region, China. Journal of Mountain Science. https://doi.org/10.1007/s11629-018-5365-8

Schaner, N., Voisin, N., Nijssen, B., Lettenmaier, D.P., 2012. The contribution of glacier melt to streamflow. Environmental Research Letters 7. https://doi.org/10.1088/1748-9326/7/3/034029

Schilling, O.S., Park, Y.J., Therrien, R., Nagare, R.M., 2019. Integrated Surface and Subsurface Hydrological Modeling with Snowmelt and Pore Water Freeze–Thaw. Groundwater 57, 63–74. https://doi.org/10.1111/gwat.12841

Schindler, D.W., Donahue, W.F., 2006. An impending water crisis in Canada's western prairie provinces. Proceedings of the National Academy of Sciences of the United States of America. https://doi.org/10.1073/pnas.0601568103

Scibek, J., Allen, D.M., Cannon, A.J., Whitfield, P.H., 2007. Groundwater-surface water interaction under scenarios of climate change using a high-resolution transient groundwater model. Journal of Hydrology 333, 165–181. https://doi.org/10.1016/j.jhydrol.2006.08.005

Seiller, G., Anctil, F., 2014. Climate change impacts on the hydrologic regime of a Canadian river: Comparing uncertainties arising from climate natural variability and lumped hydrological model structures. Hydrology and Earth System Sciences 18, 2033–2047. https://doi.org/10.5194/hess-18-2033-2014

Shaw, D.A., Vanderkamp, G., Conly, F.M., Pietroniro, A., Martz, L., 2012. The Fill-Spill Hydrology of Prairie Wetland Complexes during Drought and Deluge. Hydrological Processes 26, 3147–3156. https://doi.org/10.1002/hyp.8390

Shi, H., Fu, X., Chen, J., Wang, G., Li, T., 2014. Spatial distribution of monthly potential evaporation over mountainous regions: case of the Lhasa River basin, China. Hydrological Sciences Journal. https://doi.org/10.1080/02626667.2014.881486

Shrestha, R.R., Dibike, Y.B., Prowse, T.D., 2012. Modelling of climate-induced hydrologic changes in the Lake Winnipeg watershed. Journal of Great Lakes Research 38, 83–94. https://doi.org/10.1016/j.jglr.2011.02.004

Singh, K.K., Mishra, V.D., Singh, D.K., Ganju, A., 2013. Estimation of snow surface temperature for NW Himalayan regions using passive microwave satellite data. Indian Journal of Radio and Space Physics 42, 27–33.

Singh, V.P., Frevert, D.K., 2002. Mathematical Models of Large Watershed Hydrology. Water Resources Publications.

Smerdon, B.D., Hughes, A.T., Jean, G., 2017. Permeability Measurements of Upper Cretaceous and Paleogene Bedrock Cores made from 2004-2015 (tabular data, tab-delimited format, to accompany Open File Report 2016-03).

Smith, R.S., Moore, R.D., Weiler, M., Jost, G., 2014. Spatial controls on groundwater response dynamics in a snowmelt-dominated montane catchment. Hydrology and Earth System Sciences. https://doi.org/10.5194/hess-18-1835-2014

Stoll, S., Hendricks Franssen, H.J., Butts, M., Kinzelbach, W., 2011. Analysis of the impact of climate change on groundwater related hydrological fluxes: A multi-model approach

including different downscaling methods. Hydrology and Earth System Sciences 15, 21–38. https://doi.org/10.5194/hess-15-21-2011

Sturm, M., Taras, B., Liston, G.E., Derksen, C., Jonas, T., Lea, J., 2010. Estimating snow water equivalent using snow depth data and climate classes. Journal of Hydrometeorology 11, 1380–1394. https://doi.org/10.1175/2010JHM1202.1

Sun, N., Yan, H., Wigmosta, M.S., Leung, L.R., Skaggs, R., Hou, Z., 2019. Regional Snow Parameters Estimation for Large-Domain Hydrological Applications in the Western United States. Journal of Geophysical Research: Atmospheres 124, 5296–5313. https://doi.org/10.1029/2018JD030140

Tanachaichoksirikun, P., Seeboonruang, U., Fogg, G.E., 2020. Improving Groundwater Model in Regional Sedimentary Basin Using Hydraulic Gradients. KSCE Journal of Civil Engineering 24, 1655–1669. https://doi.org/10.1007/s12205-020-1781-8

Taylor, K.E., Stouffer, R.J., Meehl, G.A., 2012. An overview of CMIP5 and the experiment design. Bulletin of the American Meteorological Society 93, 485–498. https://doi.org/10.1175/BAMS-D-11-00094.1

Tobin, C., Schaefli, B., Nicótina, L., Simoni, S., Barrenetxea, G., Smith, R., Parlange, M., Rinaldo, A., 2013. Improving the degree-day method for sub-daily melt simulations with physically-based diurnal variations. Advances in Water Resources 55, 149–164. https://doi.org/10.1016/j.advwatres.2012.08.008

Todd Walter, M., Brooks, E.S., McCool, D.K., King, L.G., Molnau, M., Boll, J., 2005. Process-based snowmelt modeling: Does it require more input data than temperature-index modeling? Journal of Hydrology 300, 65–75. https://doi.org/10.1016/j.jhydrol.2004.05.002

Troin, M., Arsenault, R., Brissette, F., 2015. Performance and Uncertainty Evaluation of Snow Models on Snowmelt Flow Simulations over a Nordic Catchment (Mistassibi, Canada). Hydrology 2, 289–317. https://doi.org/10.3390/hydrology2040289

Troin, M., Poulin, A., Baraer, M., Brissette, F., 2016. Comparing snow models under current and future climates: Uncertainties and implications for hydrological impact studies. Journal of Hydrology 540, 588–602. https://doi.org/10.1016/j.jhydrol.2016.06.055

Ul Islam, S., Déry, S.J., 2017. Evaluating uncertainties in modelling the snow hydrology of the Fraser River Basin, British Columbia, Canada. Hydrology and Earth System Sciences 21, 1827–1847. https://doi.org/10.5194/hess-21-1827-2017

USACE, 1998. Runoff From Snowmelt. Engineering and Design 142.

Valeo, C., Ho, C.L.I., 2004. Modeling urban snowmelt runoff. Journal of Hydrology 299, 237–251. https://doi.org/10.1016/j.jhydrol.2004.08.007

van der Kamp, G., Hayashi, M., Gallén, D., 2003. Comparing the hydrology of grassed and cultivated catchments in the semi-arid Canadian prairies. Hydrological Processes 17, 559–575. https://doi.org/10.1002/hyp.1157

van Vuuren, D.P., Edmonds, J., Kainuma, M., Riahi, K., Thomson, A., Hibbard, K., Hurtt, G.C., Kram, T., Krey, V., Lamarque, J.F., Masui, T., Meinshausen, M., Nakicenovic, N., Smith, S.J., Rose, S.K., 2011. The representative concentration pathways: An overview. Climatic Change 109, 5–31. https://doi.org/10.1007/s10584-011-0148-z

Verdhen, A., Chahar, B.R., Sharma, O.P., 2014. Springtime snowmelt and streamflow predictions in the Himalayan Mountains. Journal of Hydrologic Engineering 19, 1452–1461. https://doi.org/10.1061/(ASCE)HE.1943-5584.0000816

Vetter, T., Huang, S., Aich, V., Yang, T., Wang, X., Krysanova, V., Hattermann, F., 2015. Multi-model climate impact assessment and intercomparison for three large-scale river basins on three continents. Earth System Dynamics 6, 17–43. https://doi.org/10.5194/esd-6-17-2015

Vetter, T., Reinhardt, J., Flörke, M., van Griensven, A., Hattermann, F., Huang, S., Koch, H., Pechlivanidis, I.G., Plötner, S., Seidou, O., Su, B., Vervoort, R.W., Krysanova, V., 2017. Evaluation of sources of uncertainty in projected hydrological changes under climate change in 12 large-scale river basins. Climatic Change 141, 419–433. https://doi.org/10.1007/s10584-016-1794-y

Vogel, M.M., Zscheischler, J., Wartenburger, R., Dee, D., Seneviratne, S.I., 2019. Concurrent 2018 Hot Extremes Across Northern Hemisphere Due to Human-Induced Climate Change. Earth's Future 7, 692–703. https://doi.org/10.1029/2019EF001189

Wang, B., Liu, D.L., Waters, C., Yu, Q., 2018. Quantifying sources of uncertainty in projected wheat yield changes under climate change in eastern Australia. Climatic Change 151, 259–273. https://doi.org/10.1007/s10584-018-2306-z

Wilby, R.L., Harris, I., 2006. A framework for assessing uncertainties in climate change impacts: Low-flow scenarios for the River Thames, UK. Water Resources Research 42, 1–10. https://doi.org/10.1029/2005WR004065

Wu, Q., Liu, S., Cai, Y., Li, X., Jiang, Y., 2017. Improvement of hydrological model calibration by selecting multiple parameter ranges. Hydrology and Earth System Sciences 21, 393–407. https://doi.org/10.5194/hess-21-393-2017

Yip, S., Ferro, C.A.T., Stephenson, D.B., Hawkins, E., 2011. A Simple, Coherent Framework for Partitioning Uncertainty in Climate Predictions. Journal of Climate 4634–4643. https://doi.org/10.1175/2011JCLI4085.1

Young, K.L., Assini, J., Abnizova, A., Miller, E.A., 2013. Snowcover and melt characteristics of upland/lowland terrain: Polar bear pass, bathurst island, nunavut, Canada. Hydrology Research 44, 2–20. https://doi.org/10.2166/nh.2012.083

Zeinivand, H., de Smedt, F., 2010. Prediction of snowmelt floods with a distributed hydrological model using a physical snow mass and energy balance approach. Natural Hazards 54, 451–468. https://doi.org/10.1007/s11069-009-9478-9

Zeinivand, H., Smedt, F., 2009. Hydrological modeling of snow accumulation and melting on

river basin scale. Water Resources Management 23, 2271–2287. https://doi.org/10.1007/s11269-008-9381-2

Zhang, Q., Knowles, J.F., Barnes, R.T., Cowie, R.M., Rock, N., Williams, M.W., 2018. Surface and subsurface water contributions to streamflow from a mesoscale watershed in complex mountain terrain. Hydrological Processes. https://doi.org/10.1002/hyp.11469

Zhang, X., Srinivasan, R., Debele, B., Hao, F., 2008. Runoff simulation of the headwaters of the yellow river using the SWAT model with three snowmelt algorithms. Journal of the American Water Resources Association 44, 48–61. https://doi.org/10.1111/j.1752-1688.2007.00137.x

Zhang, Y., Carey, S.K., Quinton, W.L., Janowicz, J.R., Pomeroy, J.W., Flerchinger, G.N., 2010. Comparison of algorithms and parameterisations for infiltration into organic-covered permafrost soils. Hydrology and Earth System Sciences 14, 729–750. https://doi.org/10.5194/hess-14-729-2010

Zhang, Z., Li, Y., Barlage, M., Chen, F., Miguez-Macho, G., Ireson, A., Li, Z., 2020. Modeling groundwater responses to climate change in the Prairie Pothole Region. Hydrology and Earth System Sciences 24, 655–672. https://doi.org/10.5194/hess-24-655-2020

Zhou, J., Pomeroy, J.W., Zhang, W., Cheng, G., Wang, G., Chen, C., 2014. Simulating cold regions hydrological processes using a modular model in the west of China. Journal of Hydrology 509, 13–24. https://doi.org/10.1016/j.jhydrol.2013.11.013

Zhou, Y., Li, W., 2011. A review of regional groundwater flow modeling. Geoscience Frontiers. https://doi.org/10.1016/j.gsf.2011.03.003

APPENDICES

Table A.1. Data sources for SWAT model setup, uncertainty assessment and future projections

	Scenarios/dataset	Time span	Spatial Resolution	Time step	Reference
Input climate data	Meteorological stations	1983-2007	-	Daily	Government of Canada: http://climate.weather.gc.ca
	CFSR	1983-2007	0.3° grid	Daily	SWAT weather generator: http://globalweather.tamu.edu
GIS Layers	Land-use/Land cover map	2000	30 m × 30 m	-	Geobase Land Cover Data (Government of Canada, 2017)
	Soil map	2003	10 km × 10 km	-	Food and Agriculture Organization of the United Nations (FAO, 2003)
	Digital Elevation Maps (DEM)	2008	90 m × 90 m 10 m × 10 m	-	SRTM (Jarvis et al., 2008) http://www.altalis.com/
Model conceptual data	Glacier melt	1985-2005	River basin	Monthly	Faramarzi *et al.* (2015, 2017)
	Reservoirs	Since compilation	River basin	Monthly	AESRD, Alberta Environment Sustainable Resources Development: measured data at hydrometric stations.
Observed data	Hydrometric station data	1986-2007	River basin	Monthly	Environment Canada: https://wateroffice.ec.gc.ca/
	Snow depth data	1999-2007	24 km × 24 km	Monthly	Brown and B.Bransnett (2010)

Table A.2. Properties of hydrometric stations across NSRB; station IDs are based on Figure 2.1 (data source: https://wateroffice.ec.gc.ca/)

Region	Station ID	Station Name	Operation Schedule	Data Availability
Mountainous	1	North Saskatchewan River at Whirpool Point	Continuous	1983-2007
	2	Brazeau River Below Cardinal River	Seasonal (May to October)	
Foothill	3	Clearwater River near Dovercourt	Continuous	1983-2007
	4	North Saskatchewan River Near Rocky Mountain House	Seasonal (April to October)	
Plain	5	North Saskatchewan River at Edmonton	Continuous	1983-2007
	6	North Saskatchewan River Near Deer Creek		

Table A.3. Equations used in SWAT-EBM for total daily snowmelt for rain-on-snow and rain-free conditions with different vegetation levels (USACE, 1998).

Rain-on-snow conditions	
$LAI > 0.8$	$LAI \leq 0.8$
$M = 1.27 + 1.3259 \cdot T_a + 2.0574 \cdot (T_a - T_{ss})$ $+0.0126 \cdot R \cdot (T_a - T_{ss})/B + 0.00625 \cdot SNO \cdot T_s$	$M = 1.016 + 1.3259 \cdot T_a + 0.8591 \cdot k_v \cdot v$ $\cdot (T_a - T_{ss}) + 0.0126 \cdot R \cdot (T_a - T_{ss})/B$ $+0.00625 \cdot SNO \cdot T_s$
Rain-free conditions	
$LAI > 0.8$	$0.6 < LAI \leq 0.8$
$M = 1.3259 \cdot T_a + 2.1031 \cdot (T_a - T_{ss}) + 0.00625$ $\cdot SNO \cdot T_s$	$M = 1.3259 \cdot T_a + 0.8591 \cdot k_v \cdot v \cdot (T_a - T_{ss})$ $+0.00625 \cdot SNO \cdot T_s$
$0.1 < LAI \leq 0.6$	$LAI \leq 0.1$
$M = 2.4282 \cdot (1 - LAI) \cdot k_s \cdot R_s \cdot (1 - \alpha)$ $+1.3259 \cdot LAI \cdot T_a + 0.8591 \cdot k_v \cdot v \cdot (T_a - T_{ss})$ $+0.00625 \cdot SNO \cdot T_s$	$M = 3.084 \cdot k_s \cdot R_s \cdot (1 - \alpha) + (1 - C_c) \cdot (0.9694$ $\cdot T_a - 21.336 \cdot \varepsilon \cdot \left(\frac{T_{ss} + 273.15}{273.15}\right)^4 + 1.3259 \cdot C_c \cdot T_c$ $+0.8591 \cdot k_v \cdot v \cdot (T_a - T_{ss}) + 0.00625 \cdot SNO \cdot T_s$

Table A.4. List of the ensemble GCMs and scenarios available from PCIC, where downscaled and bias corrected data were used in this study

GCM Name	Country	Institution	Spatial Resolution (Lon x Lat)	Scenario
CanESM2	Canada	Canadian Centre for Climate Modelling and Analysis	2.7906 x 2.8125	RCP 2.6, 8.5
CCSM4	United States	National Center for Atmospheric Research	0.9424 x 1.25	RCP 2.6, 8.5
CNRM-CM5	France	Centre National de Recherches Meteorologiques/Centre Europeen de Recherche et Formation Avancees en Calcul Scientifiqu	1.4008 x 1.40625	RCP 2.6, 8.5
CSIRO-MK3.6.0	Australia	Commonwealth Scientific and Industrial Research Organization in collaboration with the Queensland Climate Change Centre of Excellence	1.8653 x 1.875	RCP 2.6, 8.5
MIROC5	Japan	Meteorological Research Institute	1.4008 x 1.40625	RCP 2.6, 8.5

Table A.5. The three criteria of efficiency used for SWAT-EBM and SWAT-TIM model performance assessment in this study.

Formula	Description of the variables	References
$R^2 = \frac{[\sum_{i=1}^{n}(O_i - \bar{O})(S_i - \bar{S})]^2}{\sum_{i=1}^{n}(O_i - \bar{O})^2 \sum_{i=1}^{n}(S_i - \bar{S})^2}$	O_i and S_i are observed and simulated value for the day i, respectively; $\bar{O}$ and $\bar{S}$ are average values for observed and simulated values, respectively; n is the total number of simulated values, and b is the coefficient of the regression line between measured and simulated data (Abbaspour, 2015).	Abbaspour et al., 2015; Krause et al., 2005
$NS = 1 - \frac{\sum_{i=i}^{n}(O_i - S_i)^2}{\sum_{i=1}^{n}(O_i - \bar{O})^2}$		
$bR^2 = \begin{cases} \lvert b\rvert R^2 & \text{if } \lvert b\rvert \leq 1 \\ \lvert b\rvert^{-1} R^2 & \text{if } \lvert b\rvert > 1 \end{cases}$		

Table A.6. Regional analysis of performance of SWAT-EBM and SWAT-TIM in snow depth simulations.

	EBM-SND1	TIM-SND1	EBM-SND2	TIM-SND2
Mountain NS	0.51	0.45	0.25	0.79
Mountain bR^2	0.23	0.19	0.69	0.58
Mountain R^2	0.66	0.65	0.78	0.8
Foothill NS	0.73	0.76	0.23	0.8
Foothill bR^2	0.46	0.51	0.63	0.65
Foothill R^2	0.76	0.8	0.8	0.81
Plain NS	0.73	0.78	0.2	0.74
Plain bR^2	0.48	0.55	0.62	0.57
Plain R^2	0.75	0.79	0.77	0.74

Table A.7. Annual average contributions of different sources to the cascade of uncertainty in snow depth projections for 2040-2064 period.

	Mountain				Foothill				Plain			
Uncertainty Source	SND1		SND2		SND1		SND2		SND1		SND2	
	EBM	TIM	EBM	TIM	EBM	TIM	EBM	TIM	EBM	TIM	EBM	TIM
PPU (%)	58.0	56.8	75.4	57.0	23.9	39.4	57.8	42.1	31.0	27.2	59.0	27.5
RCP (%)	10.6	13.2	5.4	13.2	9.5	4.8	6.7	5.4	4.1	4.0	2.5	4.0
DS (%)	1.9	1.7	1.6	2.6	6.6	6.1	2.2	4.7	6.3	9.8	2.5	9.5
GCM (%)	5.1	6.5	2.6	6.1	24.4	15.9	8.1	14.7	27.2	20.7	10.6	19.6
Interactions (%)	24.4	21.8	15.0	21.1	35.7	33.8	25.3	33.0	31.3	38.2	25.5	39.4